PERFORMANCE OF AN INDOOR MOBILE RADIO COMMUNICATION SYSTEM USING DIRECT-SEQUENCE SPREAD SPECTRUM WITH DMSK MODULATION AND DIVERSITY

A Thesis

Submitted to the College of Graduate Studies and Research

in Partial Fulfillment of the Requirements

for the Degree of

Master of Science

in the

Department of Electrical Engineering

University of Saskatchewan

by

Songlei Hu

Saskatoon, Saskatchewan

March 1992

COPYRIGHT

ACKNOWLEDGEMENTS

The author would like to express her gratitude and appreciation to Dr. Surinder Kumar for his guidance throughout the course of this work.

Special appreciations are extended to her parents for their encouragement and moral support during the study.

Financial assistance provided by the Natural Science and Engineering Research Council of Canada is gratefully acknowledged.

Finally, the author would like to thank her friends for their much needed support.

UNIVERSITY OF SASKATCHEWAN
Electrical Engineering Abstract 92A357

Performance of an Indoor Mobile Radio Communication System Using Direct-Sequence Spread Spectrum with DMSK Modulation and Diversity

Student: Songlei Hu Supervisor: Dr. Surinder Kumar

M.Sc. Thesis Presented to the
College of Graduate Studies and Research

March 1992

ABSTRACT

Radio communication in an indoor mobile environment requires that the mobile units be simple in construction, low in cost, efficient in bandwidth usage and somewhat immune to multipath propagation. This presents a difficult problem. Direct-sequence spread spectrum multiple access (DS-SSMA) with differential minimum shift keying (DMSK) carrier modulation is proposed and analyzed for use in indoor mobile radio digital communication systems.

An analysis for computing the bit error rate (BER) performance of the proposed system is developed. The analysis takes into account multiple order diversity that is commonly required for such systems. Performance results are numerically computed using the analysis method developed in the thesis. These results are compared with the results reported before in literature for DS-SSMA with differential phase shift keying (DPSK) carrier modulation.

DPSK was found to outperform DMSK modulation. This can be attributed to higher bandwidth efficiency of DMSK. In spite of this poorer performance DMSK may be chosen because of this higher spectral efficiency and other benefits such as simplicity and better prime power efficiency of the mobile.

TABLE OF CONTENTS

Copyright i

Acknowledgements ii

Abstract iii

Table of Contents iv

List of Figures vii

List of Symbols ix

Chapter 1 Introduction **1**

1.1 Background 1

1.2 Thesis objectives 3

1.3 Thesis organization 4

Chapter 2 Spread Spectrum System **6**

2.1 Spread spectrum 6
- 2.1.1 Definition 6
- 2.1.2 Direct-sequence spread spectrum 7
- 2.1.3 Spread spectrum properties 13

2.2 Codes for spread spectrum 15
- 2.2.1 M-sequence 16
- 2.2.2 Gold code 19

2.2.3 Kasami code 20

2.3 Spread spectrum multiple access 21

2.4 Summary 23

Chapter 3 Digital Modulation/Demodulation Technique 24

3.1 The necessity for modulation 24

3.2 Phase shift keying 25

3.3 Quadrature-multiplexed signalling 27
3.3.1 Quadrature-multiplexing 27
3.3.2 Quadrature phase shift keying 29
3.3.3 Offset-quadrature phase shift keying 30
3.3.4 Minimum shift keying 31

3.4 DMSK modulation and noncoherent detection at the receiver 34
3.4.1 Noncoherent detection 34
3.4.2 DMSK modulation 35

3.5 Spectral properties for MSK 36
3.5.1 The derivation of power spectral density 36
3.5.2 Bandwidth efficiency of MSK 39

3.6 Summary 39

Chapter 4 Indoor Mobile Radio Channel Model 40

4.1 Communication environment for an indoor mobile radio 40
4.1.1 Multipath effect 40
4.1.2 Rayleigh fading 44
4.1.3 The effect of multiple users 45

4.2 Diversity technique for fading multipath channel 46
4.2.1 Diversity transmission methods 46
4.2.2 Combining methods 50

4.3 Summary 52

Chapter 5 Bit Error Rate Performance 53

5.1 System model, definitions and assumptions 53
5.1.1 Transmitter model 55
5.1.2 Channel model 58
5.1.3 Receiver model 59

5.2 System performance analysis 62
5.2.1 Selection diversity 70
5.2.2 Predetection combining diversity 76

5.3 Monte Carlo approximation method 77
5.3.1 Sample-mean Monte Carlo method 77
5.3.2 Sample-mean method approximation for the system performance 78

Chapter 6 Bit-Error-Rate Computed Performance 79

6.1 Error performance with selection diversity 79
6.1.1 Gold code as the spreading code 83
6.1.2 Kasami code as the spreading code 85
6.1.3 Comparison of results with Gold code and Kasami code 86

6.2 BER with predetection combining diversity 87

6.3 Comparison between selection diversity and predetection combining diversity 88

6.4 Performance comparison between DMSK and DPSK modulations 89

6.4 Summary 93

Chapter 7 Conclusions and Discussions 94

References 95

Appendix A 97

Appendix B 99

LIST OF FIGURES

Figure		
2.1	Direct-sequence spread spectrum transmitter	8
2.2	Direct-sequence spread spectrum receiver	9
2.3	Direct-sequence spreading and despreading waveforms	10
2.4	Power spectra of signal and interference spread and despread	12
2.5	Power spectra of jamming and signal in spread spectrum system	14
2.6	An example of 4-stage m-sequence	17
2.7	SSMA system model	23
3.1	Polar plot for BPSK	26
3.2	Quadrature multiplexing method	28
3.3	(a) I and Q data stream for QPSK, (b) Signal-space diagram for QPSK	29
3.4	(a) I and Q data stream for OQPSK, (b) Signal-space diagram for OQPSK	30
3.5	MSK waveform	33
3.6	Differential detection of DMSK signal	36
3.7	Baseband equivalent power spectra for MSK, BPSK, QPSK or OQPSK	38
4.1	Multipath model	41
4.2	Discrete-time model	43
4.3	Cumulative probability distribution of received signal strength	45
4.4	Antenna diversity	48
4.5	Signals from different channels	49
4.6	Spread spectrum diversity	49
4.7	Block diagram of antenna diversity	50

5.1	A star- connected indoor mobile radio system	54
5.2	Block diagram of a DMSK modulator with direct-sequence spread spectrum	56
5.3	Base station receiver with DSSS and selection diversity	59
5,4	Base station receiver with DSSS and predetection combining diversity	60
5.5	Receiver block diagram with differential detection	63
6.1	The performance of DMSK with selection diversity for K=2, L=1	83
6.2	The performance of DMSK with selection diversity for K=15, L=4, N=255 and Gold code	84
6.3	The performance of DMSK with selection diversity for K=15, L=4, N=255 and Kasami code	85
6.4	The comparison of the performance of DMSK with selection diversity for Kasami and Gold codes	86
6.5	The performance of DMSK with predetection combining diversity for K=15, L=4, and N=255	88
6.6	The comparison of selection and predetection combining diversity for DMSK (K=15, L=4, and N=255)	89
6.7	The comparison of the performance of DMSK and DPSK with selection diversity for K=15, L=4, and N=255	90
6.8	The comparison of the performance of DMSK and DPSK with predetection combining diversity for K=15, L=4, and N=255	91
6.9	Block diagram of transmitters for (a) DPSK (b) DMSK	92
A.1	Diagram for computing the correlation coefficient	98

LIST OF SYMBOLS

Symbol	
BER	Bit Error Rate
BPF	Band Pass Filter
BPSK	Binary Phase Shift Keying
CDMA	Code Division Multiple Access
CPFSK	Continuous Phase Frequency Shift Keying
DMSK	Differential Minimum Shift Keying
DPSK	Differential Phase Shift Keying
EM	Electromagnetic
FDMA	Frequency Division Multiple Access
FSK	Frequency Shift Keying
IF	Inter-Frequency
LPF	Low Pass Filter
MSK	Minimum Shift Keying
OQPSK	Offset-Quadrature Phase Shift Keying
PBX	Private Branch Exchange
PSK	Phase Shift Keying
QPSK	Quadrature Phase Shift Keying
RF	Radio Frequency
RHS	Right Hand Side
SSMA	Spread Spectrum Multiple Access
SS	Spread Spectrum
TDMA	Time Division Multiple Access

Chapter 1

Introduction

1.1 Background

In a large number of radio communication systems thermal noise generated by receiver front end stages is the major obstacle. This noise is generated by the random motion of the electrons in devices. Such communication systems are designed to be power and bandwidth efficient, i.e., minimum signal power and bandwidth necessary to achieve the desired performance is employed.

In spread spectrum (SS) communication systems, on the other hand, the signal is spread over a bandwidth much wider than that required to achieve communications when thermal noise is the main obstacle. This is obviously done to overcome other impairments. Consider, for example, a situation where someone is deliberately trying to disrupt the communications by transmitting a jamming signal in the frequency band being used. By spreading the signal spectrum, it is ensured that only a small portion of the spectrum is destroyed by the jammer. To jam the whole band the jammer signal will have to have very large power. This feature of spread spectrum is referred to as the antijamming property. Also the spreading results in a signal looking like wideband thermal noise. This results in a low probability of detection or interception by an undesired user. The antijamming and low detection properties of spread spectrum are very attractive for military communication systems.

Transmission of signals using noise like waveforms was experimented by Mortimer Rogoff [9] in late nineteen forties and early fifties. The early spread spectrum

communication systems were developed in mid-nineteen fifties. Most of these systems were for military communications and were very expensive. Because of defence applications, there was a considerable amount of secrecy involved and spread spectrum technology was not made widely available.

Recently, some of the potential of spread spectrum in commercial applications has been realized. Interest in these applications has been spurred by the spectrum regulatory agency ruling that permits the use of spread spectrum in the 900 MHz and other frequency bands without a formal licence. As the spread spectrum signal is spread over a wide bandwidth, it has low power. Also different users use different codes to spread the signal. Thus the signals from two users with different codes can co-exist in the same bandwidth. The signals are resolved at the receiver by using the corresponding codes to despread the signal and recover the information.

There are a number of radio channels where the electromagnetic waves travel from the transmitter to the receiver through different paths. This happens when there are a number of reflectors and scatterers present in the channel. Such channels are known as multipath channels. As the signals travel using these multiple paths over different distances, their phase at the receiver is random. This results in wide fluctuation of the received signal. For example, if two paths with equal attenuation and lengths differing by one half wavelength are present, the result will be a complete cancellation of the signals. An indoor mobile radio channel is particularly susceptible to multipath effect.

A multipath channel is in effect a self jamming channel. The desired signal from a strong path is jammed by reflections of itself. Multipath effect causes severe performance degradation. Because of this, the indoor mobile radio environment is a difficult environment for communications. A spread spectrum signal being a wideband signal the effect of multipath can be overcome when this signal is used for indoor mobile radios. In

fact, because of the wide bandwidth used in spread spectrum, the individual signal paths can be resolved. A diversity system which selects the best path or combines the signals from different paths after proper phasing can be implemented. A number of commercial spread spectrum indoor mobile radio systems are currently in various stages of development.

A more formal definition of the spread spectrum and a more detailed explanation of the theoretical basis resulting in the above properties of spread spectrum is presented in the next chapter. The signal spreading can be realized using a number of different methods. These methods are discussed in the next chapter as well. The most common method is to use a high rate pseudonoise code (or code with noise like spectrum called PN code). The information data is multiplied by this code. Such a system is called a direct-sequence spread spectrum (DS-SS) system. However the multiplied signal is still at baseband frequencies. For radio communication a high frequency carrier has to be modulated with this PN code multiplied data. As the mobile radio system uses portable receivers, the carrier modulation method should be such that it can be demodulated using simple receiver structures. Noncoherent detection methods which can recover the modulation without requiring the precise phase recovery of the carrier are suitable because of their simplicity. One such carrier modulation method is the differential minimum shift keying (DMSK) modulation [2]. A definition and properties of differential minimum shift keying modulation are presented in Chapter 2.

The performance analysis of a direct-sequence spread spectrum indoor mobile radio communication system with differential minimum shift keying modulation is not available in literature. This problem is addressed in this thesis. The thesis objectives are discussed in the next section.

1.2 Thesis objectives

The bit-error-rate (BER) performance of a direct-sequence spread spectrum has been analyzed [8] before using differential phase shift keying (DPSK) modulation. Differential minimum shift keying is another noncoherent carrier modulation method well suited for the indoor mobile direct-sequence spread spectrum radio. Differential minimum shift keying has certain desirable features such as battery power efficient direct radio frequency (RF) generation [18] which make this method advantageous over differential phase shift keying. An analytical study of differential minimum shift keying bit-error-rate performance is not available. The objectives of the thesis may be laid down as:

1) Develop an analytical method for obtaining differential minimum shift keying bit-error-rate performance in an indoor mobile direct-sequence spread spectrum radio system. The system model should include multiuser operation and a diversity scheme.

2) Using the above method compute the bit-error-rate performance with different system parameters. Compare these results with previously reported results for differential phase shift keying.

1.3 Thesis organization

In addition to this introductory chapter, the thesis is organized in six other chapters and two appendices.

A formal definition of spread spectrum modulation as well as a description of its properties is presented in Chapter 2.

Chapter 3 includes a discussion of various carrier modulation methods. Non-coherent demodulation methods such as differential minimum shift keying are introduced. Features of differential minimum shift keying which make it an attractive modulation method for the indoor mobile radio application are briefly discussed.

A description of the indoor mobile radio channel is the subject of Chapter 4. A channel model for use in the performance analysis is included.

An analytical method for the performance analysis of a direct-sequence spread spectrum multiple access (DS-SSMA) system with differential minimum shift keying modulation in an indoor multipath environment is developed in Chapter 5.

Using the method developed in Chapter 5, the bit-error-rate results are computed for different system parameters in Chapter 6. A comparison with differential phase shift keying performance is also presented.

Conclusions are presented in Chapter 7.

Appendix A presents the derivation of the correlation coefficient equation.

The computer programs used for carrying out the bit-error-rate computations are given in Appendix B.

Chapter 2

Spread Spectrum System

In this chapter the definition and properties of spread spectrum are presented. In particular the direct-sequence spread spectrum method is discussed in some detail.

2.1 Spread spectrum

2.1.1 Definition

As stated in Chapter 1, spread spectrum (SS) signal is spread over a bandwidth much larger than that of the baseband signal. A formal definition that reflects this basic characteristic of SS is given below [1].

"Spread spectrum is a means of transmission in which a signal occupies a bandwidth in excess of the minimum necessary to send the information; the spreading is accomplished by means of a code which is independent of the data. Synchronized reception with the code at the receiver is used for despreading and subsequent data recovery."

In practice, bandwidth expansion may be done for different purposes. Not all these bandwidth expansion methods can be classified as spread spectrum. Low-rate coding, for example, results in wider transmission bandwidth. It does not satisfy the definition of SS signal above and is not classified as such.

Three methods are commonly used in generating SS. These are direct-sequence modulation, frequency hopping and time hopping [1]. Only the first method is used in this thesis. This method is discussed in some detail below.

2.1.2 Direct-sequence spread spectrum

In this method the signal is spread using a wideband spreading code. The spreading code is used to directly modulate the phase of a carrier that has been previously modulated by a data signal.

Consider a data-modulated carrier expressed as

$$S_d(t) = d(t)\sqrt{2P}\cos\omega_0 t \quad , \tag{2.1}$$

where P is an average power of the signal, ω_0 is the radian frequency, and d(t) is the data information.

The bandwidth occupied by this signal is between one-half and twice the data rate and depends on the details of the data-modulation method used.

The signal spreading is achieved by multiplying the above signal by a high rate code c(t). So that the spread signal may be expressed as

$$S_t(t) = d(t)\,c(t)\sqrt{2P}\cos\omega_0 t \quad . \tag{2.2}$$

This process is illustrated in Fig.2.1. The bandwidth of the transmitted signal is much larger than the minimum bandwidth needed to transmit the information data. This assumes that the bandwidth of c(t) is much larger than that of d(t).

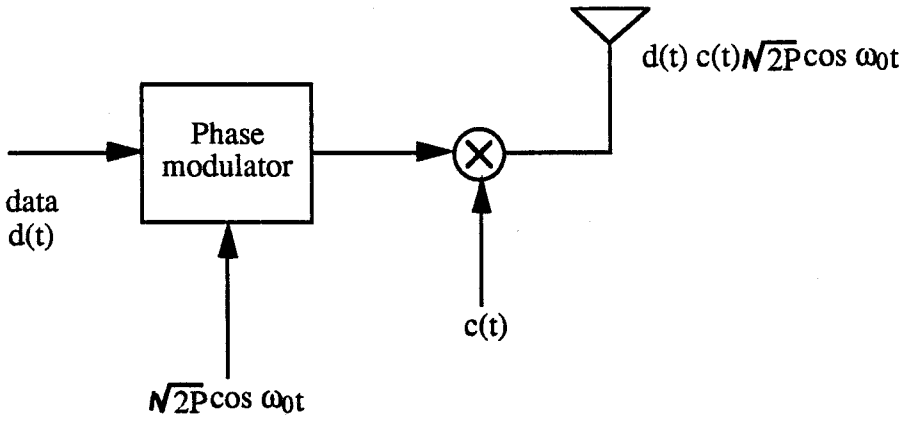

Fig.2.1 Direct-sequence spread spectrum transmitter

The received signal contains the required signal, the interference caused by SS signals from other users, and white Gaussian noise. To demodulate this received signal, a corresponding despreading code is employed by the receiver. Considering a transmission time delay of T_d, and assuming the random phase φ in transmission to be zero, the received signal may be written as

$$r(t) = d(t - T_d)\, c(t - T_d) \sqrt{2P} \cos \omega_0 (t - T_d) + \text{interference} + \text{white Gaussian noise} \quad (2.3)$$

Fig.2.2 illustrates the demodulation process. As shown in this figure, the received signal is multiplied by the same spreading code as in the transmitter with an estimated time delay of $\hat{T}_d$. The purpose of $c(t - \hat{T}_d)$ is to remove the spreading code from the received signal. This also results in resolution of the desired signal from those of the other users. The signal component of the output after despreading, (point A in the Fig. 2.2), is

$$c(t - T_d)\, c(t - \hat{T}_d)\, d(t - T_d) \sqrt{2P} \cos \omega_0 (t - T_d).$$

If the estimation, $\hat{T}_d$ in the receiver is perfect, i.e., $\hat{T}_d = T_d$, $c(t-T_d)\, c(t-\hat{T}_d) = 1$ for $c(t) = \pm 1$. This results in the spectrum of the required signal being despread. At the same time the spectrum of any interference signal from other users will not be despread as $c(t-\hat{T}_d)$ does not match the interfering signal spreading code. The despread signal is then passed through a bandpass filter. A major portion of the output power of the filter, (point B in the Fig.2.2), is the signal, $S_d(t-T_d)$. Once the signal is despread and filtered, it can be demodulated using the conventional demodulation methods.

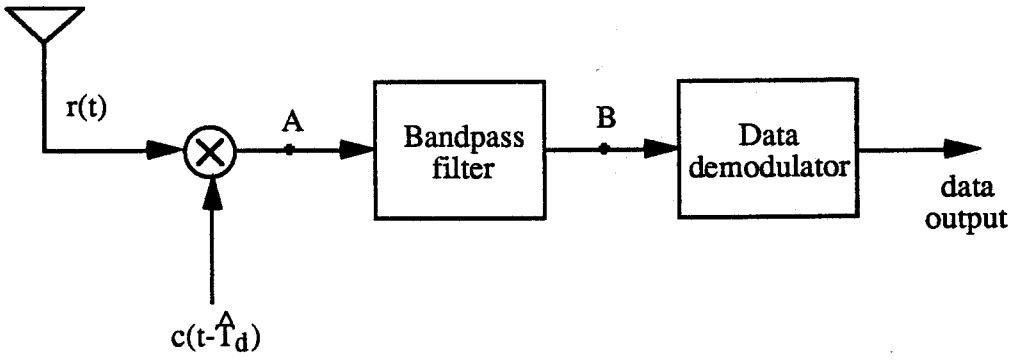

Fig.2.2 Direct-sequence spread spectrum receiver

The importance of correct delay estimation is illustrated by showing the waveforms in the despreading process in Fig.2.3.

Waveforms (a), (b), (c), and (d) show the spreading process. Waveforms (a) and (b) are the data and spreading code respectively, (c) is the data-modulated carrier waveform and (d) is the data and the spreading code-modulated carrier waveform. Waveforms (e), (f) and (g) illustrate the despreading process. (e) is a replica of (b) (spreading code) with a time delay of $\frac{1}{2}T_c$; (f) is the result of waveform (d) multiplied by waveform (e). Because of incorrect delay estimation the waveform in (f) is not equivalent to the data-modulated carrier

$S_d(t)$. In (g) the despread waveform with correct delay estimation is shown. As may be seen this is same as the data modulated signal $S_d(t)$ in (c).

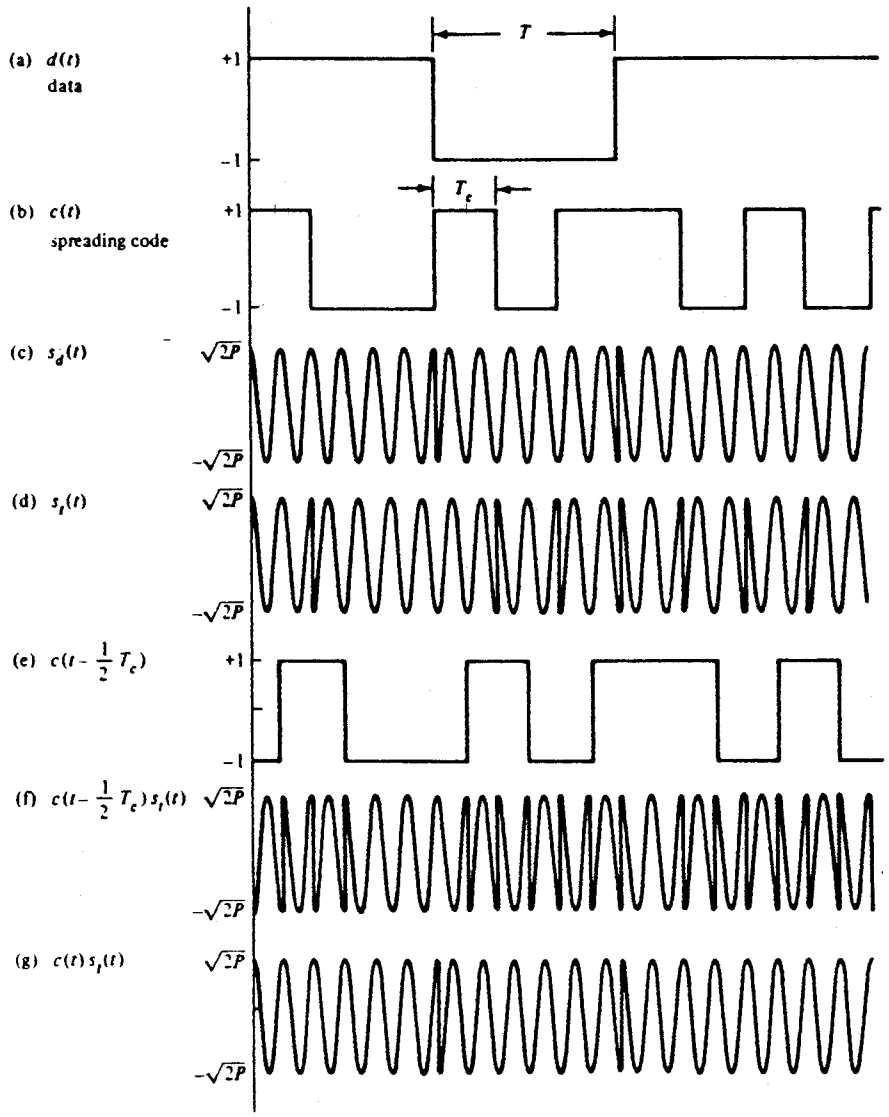

Fig. 2.3 Direct-sequence spreading and despreading waveforms [from ref. 2]

The signal spectra in Fig.2.4 provide further insight into spreading and despreading process.

As may be seen from Fig.2.4 (a), the bandwidth of the spread signal is much larger than the information bandwidth. The spectrum of the signal is despread into a small bandwidth, as shown in Fig.2.4 (b). The interference signal is spread over a very wide frequency band. A small amount of interference energy is present in the information bandwidth. It is thus easy to recover the signal from the interference.

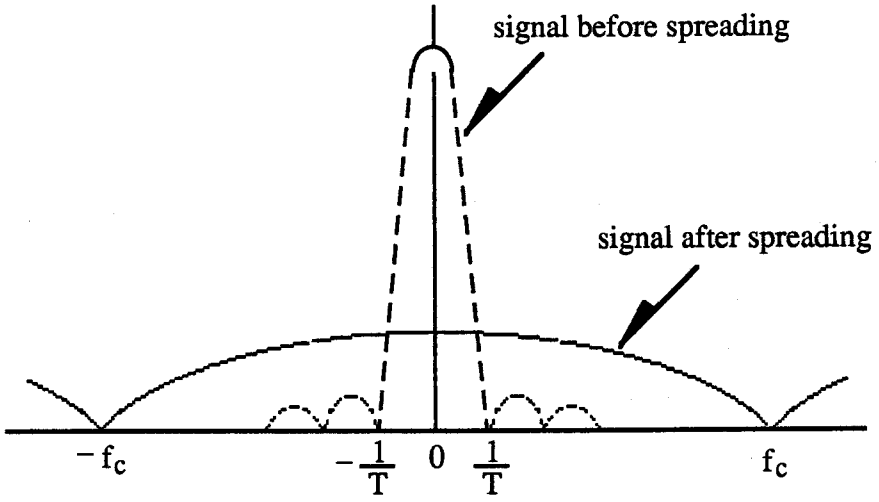

(a)

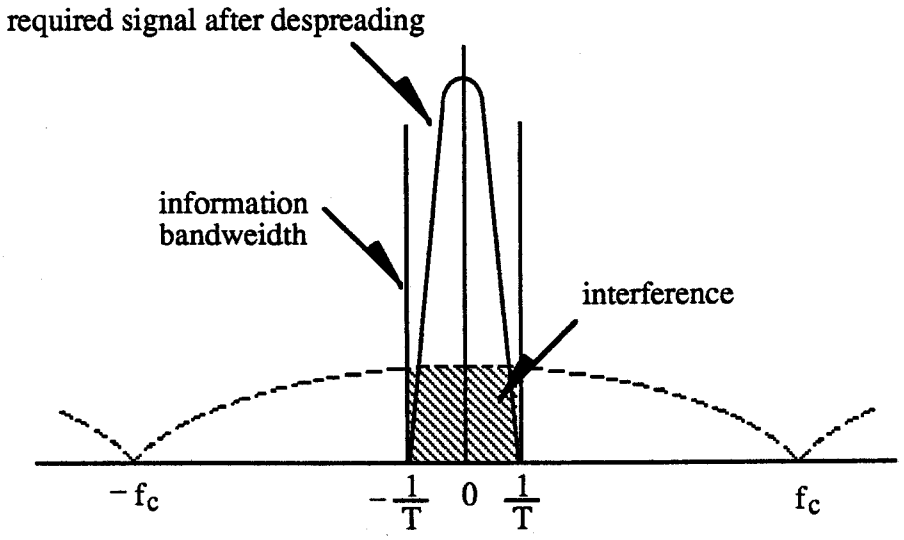

(b)

Fig. 2.4 Power spectra of signal and interference spread and despread
(a) Signal power spectra
(b) Signal and interference power spectra after despreading

The spreading of the signal results in many useful properties. These are discussed in the next section.

2.1.3 Spread spectrum properties

A) Antijamming and antiinterference

In this thesis intentional interference is referred to as jamming. Unintentional interference, such as self-interference caused by multipath propagation and cross-interference caused by other users, is referred to as interference. Antijamming and antiinterference properties of spread spectrum are the result of spreading and despreading processes.

A jamming signal is normally a high power narrow bandwidth radio frequency signal. As shown in Fig.2.5.(a), it can jam only a few components of a wide bandwidth spread signal. When the received signal containing the jammer signal is multiplied by the despreading code in the receiver, the spectrum of the required signal will be collapsed. Simultaneously, the spectrum of the jamming signal will be spread. This results in the energy of the required signal being concentrated in a narrow information band and the energy of the jamming signal being dispersed in a relatively wide bandwidth. Consequently, in the information bandwidth the despread jamming signal has little energy remaining as shown in Fig.2.5(b). In this case, the influence of the jamming signal can be removed by the detection process.

In contrast to jamming, interference is a wide band signal having the same bandwidth as the required signal. The interference signal will not be despread to a narrow bandwidth unless a synchronized corresponding spreading code is used in the despreading process at the receiver. This results in a major portion of the energy in the information bandwidth being due to the signal, and only a small portion being due to the interference. Obviously the majority of the interference energy is outside of the information bandwidth as shown in Fig.2.4. This situation is similar to that in the antijamming case.

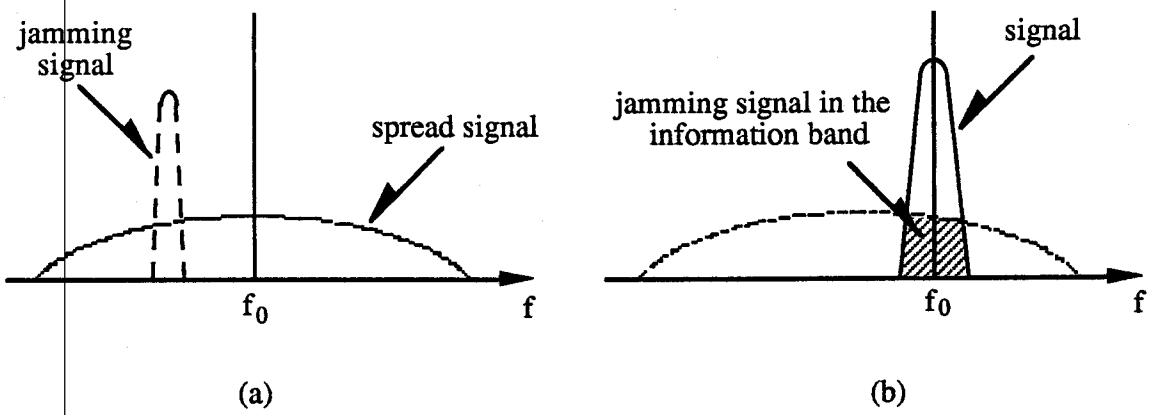

Fig.2.5 Power spectra of jamming and signal
in spread spectrum system
(a) Received signal spectrum (b) Spectrum after despreading

B) Inherent frequency diversity

A spread spectrum signal is a wide band signal. Usually, the bandwidth is larger than the reciprocal of the difference between path time delays. This means that the paths in multipath channels can be resolved [11] [12]. This resolution of multiple path can be used to implement a diversity reception technique. Path resolution and diversity improvement are presented in Chapter 4.

C) Code-division multiple access

Spread spectrum modulation can be used to implement a multiple access technique termed code-division multiple access (CDMA). This technique will be described in detail in a later section. In a spread spectrum multiple user system, every user has a unique spreading code to spread their own signal in the transmitter. All of the users share the same frequency band at the same time. At any receiver, a corresponding spreading code for each user is set to select the desired signal from the received signal containing interference from other users.

To spread a signal's spectrum, a spreading code is necessary. The spreading code is an important issue in the design of SS systems. This subject is the topic of the next section.

2.2 Codes for spectrum spreading

The spreading code used to spread and despread a data-modulated carrier is a binary sequence generated using shift registers. During each time interval the contents of these registers are the modulo-2 sum of the contents of the registers during the preceding time interval. For the spread spectrum system to operate efficiently, this binary sequence is selected to possess certain desirable properties. In CDMA communication system, a set or a group of the binary sequences or spreading codes is needed. In this case, the binary sequence is required to have the following properties:

1) Easy to generate.

2) The sequence repeats after a certain time period. The period depends on the system requirements.

3) Each spreading code in the set is easy to distinguish from a time shifted version of itself.

4) Each spreading code in the set is easy to distinguish from every other spreading code in the set.

In practice, property 3) is identical with small auto-correlation requirement and property 4) is identical with small cross-correlation requirement .

The basic maximal-length binary sequence called m-sequence is discussed first in the next section. The Gold code and Kasami code which can be constructed using the m-

sequence are discussed in Sections 2.2.2 and 2.2.3. The mathematical background on this subject is available in references [2],[3] and [4].

2.2.1 M-sequence

A maximal-length sequence has a maximal possible period for an n-stage shift register used to generate the code. For example, a 4-stage linear feedback shift register generator with a generating polynomial [2] $g(D) = D^4 + D + 1$ is shown in Fig. 2.6. D is the time shift operator and it represents one bit delay. The generating polynomial specifies the feedback connections in the code generator circuit. It generates a sequence with a maximal period of $N = 2^n - 1 = 2^4 - 1 = 15$.

In Fig. 2.6, rectangles represent the shift register stages. The output sequence is denoted by b(D). Any one of the initial states, except the all-zero state, results in the same state cycle sequence as that shown in Fig.2.6. The first column from the right in this figure represents the output sequence of the generator. Because all possible states, except the all-zero state, appear once in the state cycle, the period of the output sequence is the maximum possible.

The output sequence, or spreading code, consists of ones and zeroes and has a period N. This can be expressed by

$$b(D) = \cdots + b_{-2}D^{-2} + b_{-1}D^{-1} + b_0 + b_1D^1 + b_2D^2 + \cdots,$$

where b_i is binary symbol and D is time shift operator. The binary symbol multiplied by D^j implies that the binary symbol occurs during the jth time interval of the sequence.

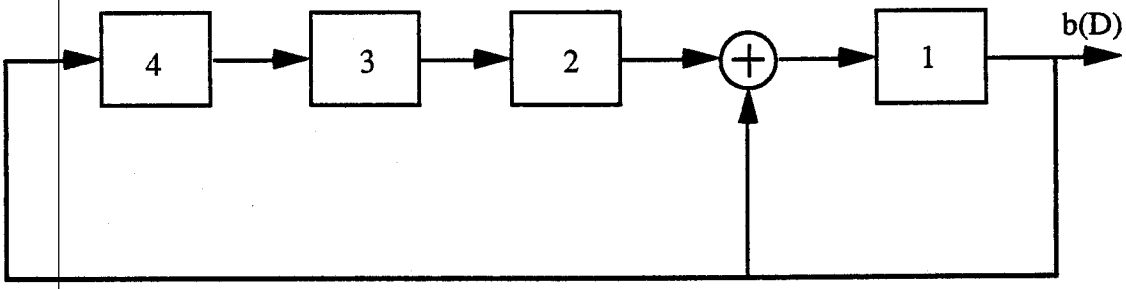

(a)

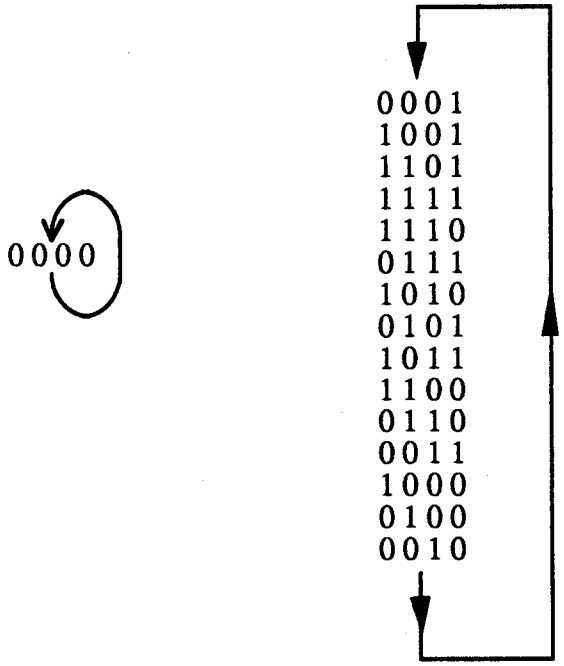

(b)

Fig.2.6 An example of 4-stage m-sequence
(a) Generator circuit (b) Shift register sequence

The periodicity of the spreading code, may be expressed by $b_i = b_{N+i}$ for any i. The spreading waveform, c(t), derived from the spreading code is periodic with period $T = NT_c$, and is specified by

$$c(t) = \sum_{i=-\infty}^{\infty} a_i \, P(t - iT_c) \quad , \tag{2.4}$$

where

$$a_i = (-1)^{b_i} \quad ,$$

P(t) = shaping signal over time 0 to T_c.

An m-sequence possesses the following properties [2]:

1) For an m-sequence constructed with the primitive polynomial of degree n (n stage shift register) the period is equal to $N=2^n -1$.

2) In m-sequence digit "one" appears once more than the digit "zero". The number of ones in this sequence is (N+1)/2.

3) The modulo-2 sum of an m-sequence and any phase shift of the same sequence is another phase of the same sequence.

4) If a window of width n is slid along the sequence N times, each n-tuple except the all zero n-tuple appears exactly once.

5) The auto-correlation function of the sequence can be defined as

$$\theta_b(k) = \sum_{i=-\infty}^{\infty} a_i \, a_{i+k} \tag{2.5}$$

$$\theta_b(k) = \begin{cases} N & k = iN \\ -1 & k \neq iN \end{cases} \qquad \text{for m-sequence}$$

where i is any integer and N is the sequence period.

Although an m-sequence is simple to generate, only one sequence can be generated using one generator. Because of this an m-sequence is not suitable for use in practical CDMA systems.

2.2.2 Gold code

A Gold code [2],[5] is a code family or code set constructed from appropriately selected m-sequences. The method used to generate a set of Gold codes is described below [2],[5].

Consider an m-sequence b of length N , and a second sequence b' obtained by sampling every qth symbol of b. The second sequence is said to be a decimation of the first, and the notation b'=b[q] is used to indicate that b' is obtained by sampling every qth symbol of b. The decimation of m-sequence may or may not yield another m-sequence. When the decimation, b', yields m-sequence with period N , the decimation is said to be a proper decimation. The pair, b and b' in this case are known as a preferred pair of m-sequences.

Let b(D) and b'(D) represent a preferred pair of m-sequences having period $N = 2^n-1$. A set of Gold codes is defined by

$$G(b,b') = \{b(D),\ b'(D),\ b(D)\oplus b'(D),\ b(D)\oplus Db'(D),\ b(D)\oplus D^2b'(D),$$
$$\cdots,\ b(D)\oplus D^{N-1}b'(D)\} \qquad (2.6)$$

Note that G(b,b') contains $N + 2 = 2^n + 1$ sequences of period N. It can be shown that for two sequences, denoted by y and z, in G(b,b'), the cross-correlation (which is defined to be similar to auto-correlation in eq.(2.5) with a_{i+k} from another code) denoted

by $\theta_{y,z}(i)$, and auto-correlation, denoted by $\theta_y(i)$, can only take one of the following three values [6], [7]

$$\begin{cases} -1 \\ -(1+2^{[(n+2)/2]}) \\ 2^{[(n+2)/2]} - 1 \end{cases}$$

The cross correlation may be defined as

$$\theta_{y,z}(i) \in \{-1, -(1+2^{[(n+2)/2]}), 2^{[(n+2)/2]} - 1\} \quad , \quad \text{for all integer } i$$

the auto-correlation $\theta_y(i)$ for a Gold code is similarly given by

$$\theta_y(i) \in \{-1, -(1+2^{[(n+2)/2]}), 2^{[(n+2)/2]} - 1\} \quad , \quad \text{for all } i \neq 0 \bmod N$$

It is seen, from the above, that to construct a set of Gold codes, a preferred pair of m-sequences is necessary. A preferred pair of m-sequences is obtained when the following conditions are satisfied:

1) $n \neq 0 \bmod 4$; that is n is odd or $n = 2 \bmod 4$

2) $b' = b[q]$ where $q = 2^k + 1$, or $q = 2^{2k} - 2^k + 1$

3) $\gcd(n, k) = \begin{cases} 1 & \text{for n odd} \\ 2 & \text{for } n=2 \bmod 4 \end{cases}$

where "gcd" denotes the greatest common divisor.

2.2.3 Kasami code

A small set of codes called Kasami codes [5] can also be constructed from m-sequences. Kasami codes have desirable correlation properties [19, 20 from 5]. Let n be an even number and b an m-sequence of period $N = 2^n - 1$, generated by the primitive polynomial of degree n. Consider the sequence $b'=b[2^{n/2}+1]$. Therefore this sequence , b'

, can be generated by the primitive polynomial of degree n/2. So b' is m-sequence with period $2^{n/2}-1$. The small set of Kasami codes is defined by

$$K_s(b) = \{b(D), b(D)\oplus b'(D), b(D)\oplus Db'(D), b(D)\oplus D^2b'(D), \cdots, b(D)\oplus D^{2^{n/2}-2}b'(D)\} \tag{2.7}$$

This set contains only $2^{n/2}$ sequences, with the cross-correlation function:

$$\theta_{y,z}(i) \in \{-1, -(2^{n/2}+1), (2^{n/2}+1)-2\} \ , \quad \text{for all integer } i$$

and auto-correlation function:

$$\theta_y(i) \in \{-1, -(2^{n/2}+1), (2^{n/2}+1)-2\} \ , \quad \text{for all } i\neq 0 \bmod N$$

For a period $N = 2^n - 1$, the set of Gold codes contains $2^n + 1$ sequences and the set of Kasami codes contains $2^{n/2}$ sequences. The maximum cross correlation for the set of Kasami codes is approximately one half that for the set of Gold codes.

2.3 Spread spectrum multiple access

There are a number of communication systems where a communication channel has to be shared by a number of different users. The process of multiplexing the channel between the users is called multiple access. The basic methods of multiple access are: Frequency Division Multiple Access (FDMA), Time Division Multiple Access (TDMA), and Code Division Multiple Access (CDMA). In FDMA different users employ different frequency bands to transmit signals at the same time. To avoid interference these frequency bands must not overlap. Any one of the signals can be recovered by filtering. In TDMA, users are allocated different non-overlapping time slots to transmit their signals. In this case they share the full channel bandwidth at different time slots. Precise time synchronization is

required at the receiver to recover the signals for TDMA. In CDMA system, every user is assigned unique spread code sequence and all users transmit signals simultaneously in the full channel bandwidth. The recovery of the signals is achieved by correlation using the corresponding user's spreading code at the receiver.

FDMA and TDMA techniques require precise frequency or time coordination among the transmitters and receivers. The CDMA does not have these requirements. Its multiple access capability is due primarily to the coding that allows all users to transmit signals simultaneously using the same frequency band. This makes CDMA an attractive technique for a variety of communication and satellite systems. For a multiple user mobile communication system a CDMA technique can be designed to provide multiple access capability. This type of system is also known as a spread spectrum multiple access (SSMA) system.

In SSMA system the bandwidth of spreading code is much larger than the information bandwidth. Fig.2.7 illustrates a SSMA or CDMA system. The spreading code $c_k(t)$ belongs to a user k, $d_k(t)$ is the data information signal for user k, $c(t - \hat{T}_d)$is the estimation of $c_k(t)$ with a time delay T_d in the receiver. As mentioned in section 1 when $\hat{T}_d = T_d$, the signal can be demodulated from received signal r(t) easily.

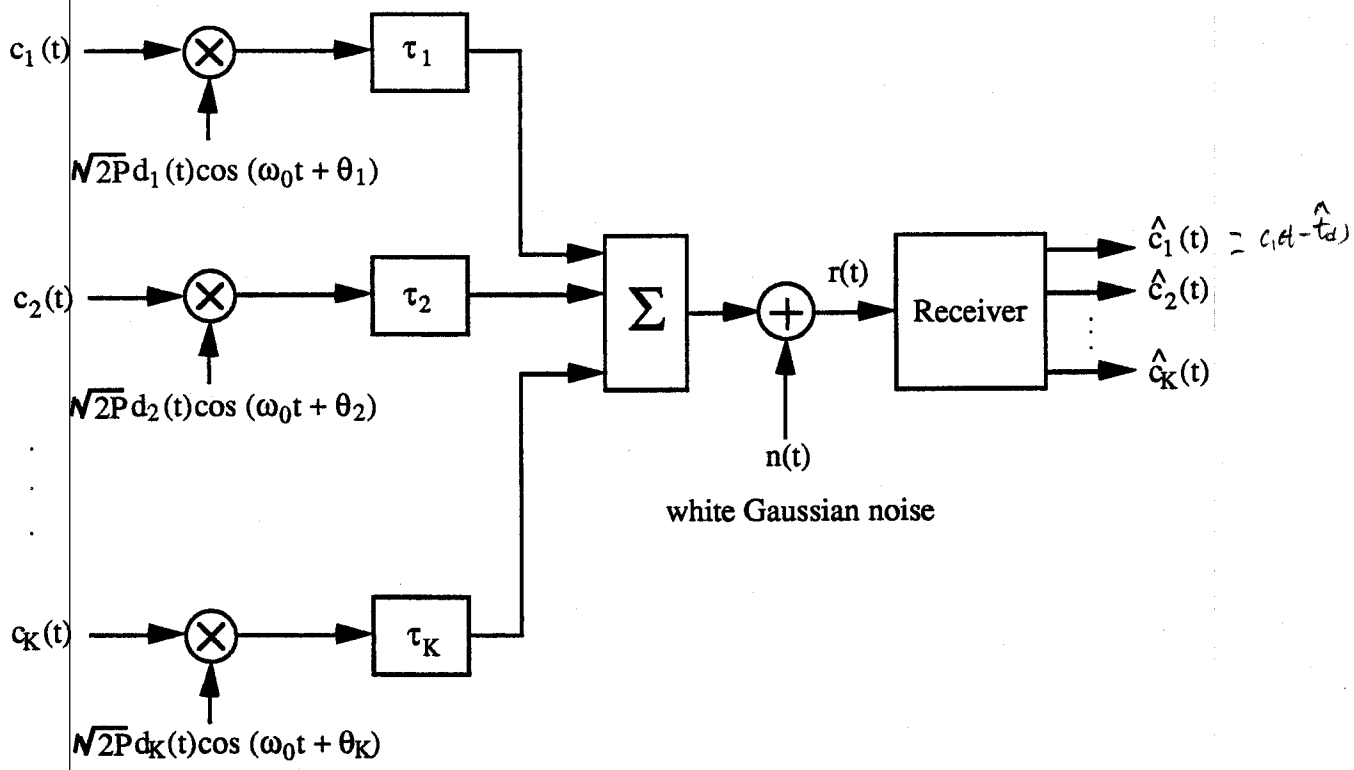

Fig. 2.7 SSMA system model

2.4 Summary

A spread spectrum system is suitable for a multipath, multiple user radio communication environment. Such a system has antiinterference, inherent frequency diversity properties. Also multiple accessing can be implemented using CDMA technique. Choice of a spreading code influences the performance of a spread spectrum system. Low auto-correlation and cross-correlation properties of a spreading code result in an improved system performance. Time delay estimation is an important problem in spread spectrum systems.

In the next chapter various digital modulation methods that can be used in a spread spectrum system are introduced.

Chapter 3

Digital Modulation/Demodulation Technique

To implement radio communication systems using practically realizable antennas, it is necessary that the information signal be modulated on a high frequency signal. In this chapter commonly used digital modulation schemes are introduced. In particular differential minimum shift keying (DMSK) is discussed in detail. Also differential detection of a DMSK signal which is a simpler detection method, is presented.

3.1 The necessity for modulation

Modulation is a process whereby some aspect of a waveform is controlled by some aspect of another waveform. The waveform that is controlled is called the carrier and the controlling waveform is called the modulating signal. In practice various types of modulation are used. Each is generally identified by the parameter of the carrier that is controlled. Some of the more common types include amplitude, frequency, phase, and pulse modulation or any combination of these.

Modulations can also be classified as either analog or digital. In analog modulation the set of modulated waveforms consists of an infinite number of elements that form a continuum. Digital modulation, on the other hand, consists of a finite number of unique carrier waveforms. The set of waveforms in a digital modulation scheme typically consists of 2^n elements. Digital modulation can be considered to be either baseband or bandpass modulation. In baseband modulation the "carrier signal" is a zero Hertz or DC signal and the resulting "modulated carrier" is a set of pulse waveforms. In bandpass modulation the carrier is a sinusoidal waveform that is modulated in some form by the modulation signal.

Modulation results in a number of benefits in a practical communication system. In radio communication, bandpass modulation is an important step needed to realize a practical system. In such systems the signal is converted to an electromagnetic (EM) wave by using an antenna. If the carrier signal is modulated by an information signal, the EM field will propagate outward from the antenna, and carry the information with it. In order to efficiently convert the carrier signal power into the EM field, the antenna size should be of the order of one wavelength of the signal to be transmitted. Choice of a high frequency carrier results in an antenna of realizable size. For example if the signal frequency, f, to be transmitted is 3000 Hz, and the speed of EM wave propagation, c, is 3×10^8 m/s, the wavelength of this signal and the size of the antenna will be of the order of $c/f = 10^5$ meters or 100 kilometers. It is not practical to make such a huge antenna. If the signal frequency is increased to 300 MHz the antenna will be reduced to 1 meter. Other benefits of modulation in radio communication include the capability to have different information signals modulate different frequency carriers. This allows the signals to be transmitted at the same time and still be separable. This technique is known as frequency division multiplexing. Thus the modulation allows the system designer to make the modulated signal compatible with the channel used for communication.

A number of digital modulation schemes, such as BPSK, QPSK, OQPSK, MSK and FSK are used in practice. Some of these are discussed in the next section.

3.2 Phase shift keying

When the phase of the carrier is controlled by the modulating signal, the modulation method is referred to as phase shift keying (PSK). PSK is a commonly used modulation method in digital communication systems. It can be easily implemented and has a number of desirable properties.

The general expression for a PSK signal is

$$S_i(t) = \sqrt{2P}\cos[\omega_0 t + \phi_i(t)] \qquad 0 \le t \le T_b \qquad i = 1, 2, \cdots, M, \qquad (3.1)$$

where P is the signal power, ω_0 is the radian frequency, and T_b is the time duration of the information data bit. The phase term, $\phi_i(t)$, will have M discrete values given by

$$\phi_i(t) = \frac{2\pi i}{M}, \qquad i = 1, 2, \cdots, M$$

The signal waveforms can be represented as vectors where the vector length is the signal amplitude, and the vector direction is the signal phase.

When M is 2, the PSK is a binary PSK (BPSK), which is the simplest form of PSK modulation. In BPSK modulation, the information signal modulates the phase of the waveform, $S_i(t)$, into two states, zero or π (180°). The phase changes abruptly, from 0 to π, or from π to 0, at the interbit switching instants.

The vector representation of a BPSK signal is shown in Fig. 3.1.

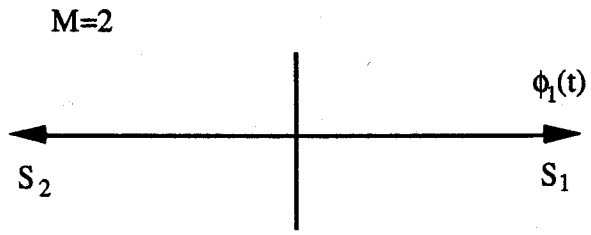

Fig. 3.1 Phasor diagram of BPSK

In this Fig. $\phi_1(t) = \cos\omega_0 t$, $S_1 = \sqrt{2P}\,\phi_1(t)$, and $S_2 = -\sqrt{2P}\,\phi_1(t)$. A signal set with vectors which are negative of each other is called an antipodal set.

3.3 Quadrature-multiplexed signalling

Constant envelope modulation is preferred when a nonlinear transmitter is used to transmit the radio signals. A nonlinear transmitter will put signal power into extraneous sidebands when transmitting a signal with amplitude fluctuation. These sidebands can interfere with the signals in adjacent channel, as well as reduce the power of the main signal.

Quadrature-multiplexed signalling schemes result in a constant envelope of the modulated signal. The general technique consists of two different data streams which modulate two carriers in phase quadrature. Each data stream modulates the carrier using BPSK modulation. This modulation method is further discussed in the next section.

3.3.1 Quadrature multiplexing

Let $d_I(t)$ and $d_Q(t)$ express two data streams, called an I stream and a Q stream. These streams are formed by dividing the original bit stream, d(t), into two streams consisting of even and odd bit streams. Each stream has half the bit rate of the original stream, i.e., the bit duration is $2T_b$. Each stream modulates a carrier of the same frequency but in phase quadrature. At the receiver $d_I(t)$ and $d_Q(t)$ can be separated by using for demodulation the carriers that are in phase quadrature. The block diagram of this system is shown in Fig.3.2. The transmitted signal is given by

$$S_t(t) = A_1 d_I(t) \cos(2\pi f_0 t + \alpha) + A_2 d_Q(t) \sin(2\pi f_0 t + \alpha) , \qquad (3.2)$$

where A_1 and A_2 are amplitudes of the inphase and quadrature carriers respectively. α represents a constant phase shift.

Considering that the two data streams $d_I(t)$ and $d_Q(t)$ have a bit duration of $2T_b$ and assuming each to be either +1 or -1, the modulated signal may be written as

$$S_t(t) = A\cos(2\pi f_0 t - \theta(t) + \alpha), \qquad (3.3\ a)$$

where

$$A = \sqrt{A_1^2 + A_2^2}$$

$$\theta(t) = \arctan\frac{A_2 d_Q(t)}{A_1 d_I(t)}. \qquad (3.3\ b)$$

Because the values of $d_I(t)$ and $d_Q(t)$ are limited to ± 1, $\theta(t) \in \{\tan^{-1}\frac{A_2}{A_1}, \tan^{-1}\frac{A_2}{A_1} + \pi, -\tan^{-1}\frac{A_2}{A_1}, -\tan^{-1}\frac{A_2}{A_1} + \pi\}$

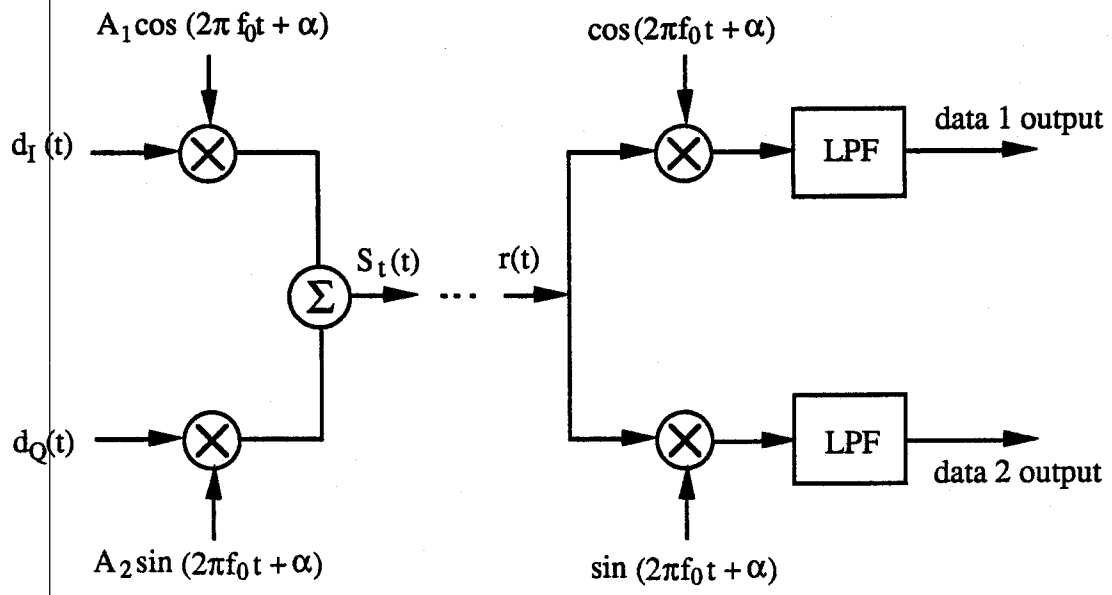

Fig. 3.2 Quadrature multiplexing method

3.3.2 Quadrature phase shift keying

If in equation (3.3) $A_1 = A_2 = \frac{A}{\sqrt{2}}$, and $d_I(t)$ and $d_Q(t)$ change signs at the same instants as shown in Fig. 3.3.a, the resulting modulated signal is called quadrature phase shift keying (QPSK). QPSK modulation changes the phase of the carrier by 0, ± 90, or 180 degree at the interbit switching instants. The signal-space (phasor) diagram is shown in Fig.3.3.b. The dashed lines with arrows represent the phase transitions. The four dots represent the four QPSK vectors. As may be seen the phase transitions can be 0°, ±90°, ±180°.

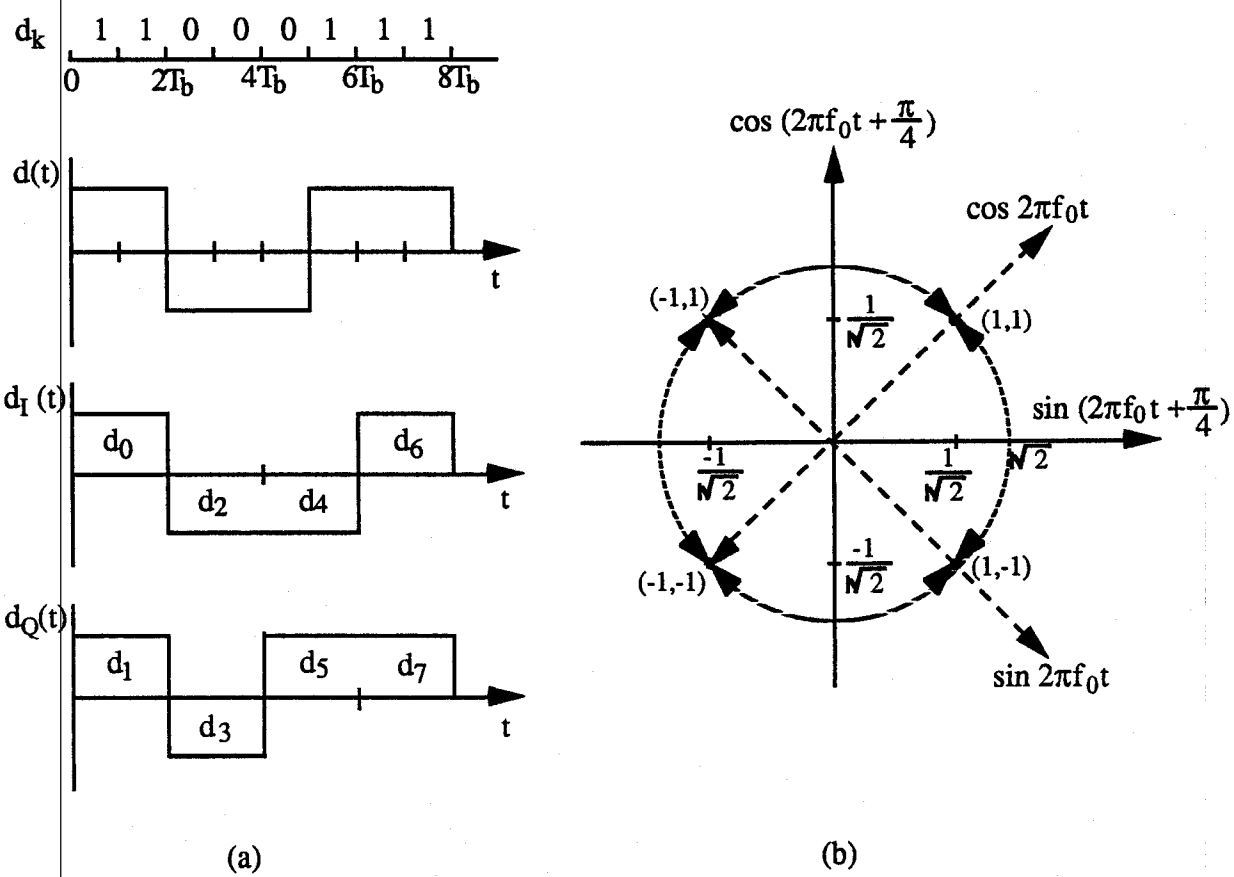

Fig. 3.3 (a) I and Q data stream for QPSK
(b) Signal-space (phasor) diagram for QPSK

3.3.3 Offset-quadrature phase shift keying

If in the equation (3.3), $A_1 = A_2 = \frac{A}{\sqrt{2}}$, and the instant that $d_I(t)$ changes sign is staggered by T_b seconds with respect to the instant that $d_Q(t)$ changes sign, (as shown in Fig.3.4.a), the phase modulated signal is called offset-quadrature phase-shift keying (OQPSK). As $d_I(t)$ and $d_Q(t)$ cannot change signs at the same instant, the set of phase shifts for OQPSK is limited to 0 or ± 90 degrees. The signal-space (phasor) diagram for OQPSK is shown in Fig.3.4.b.

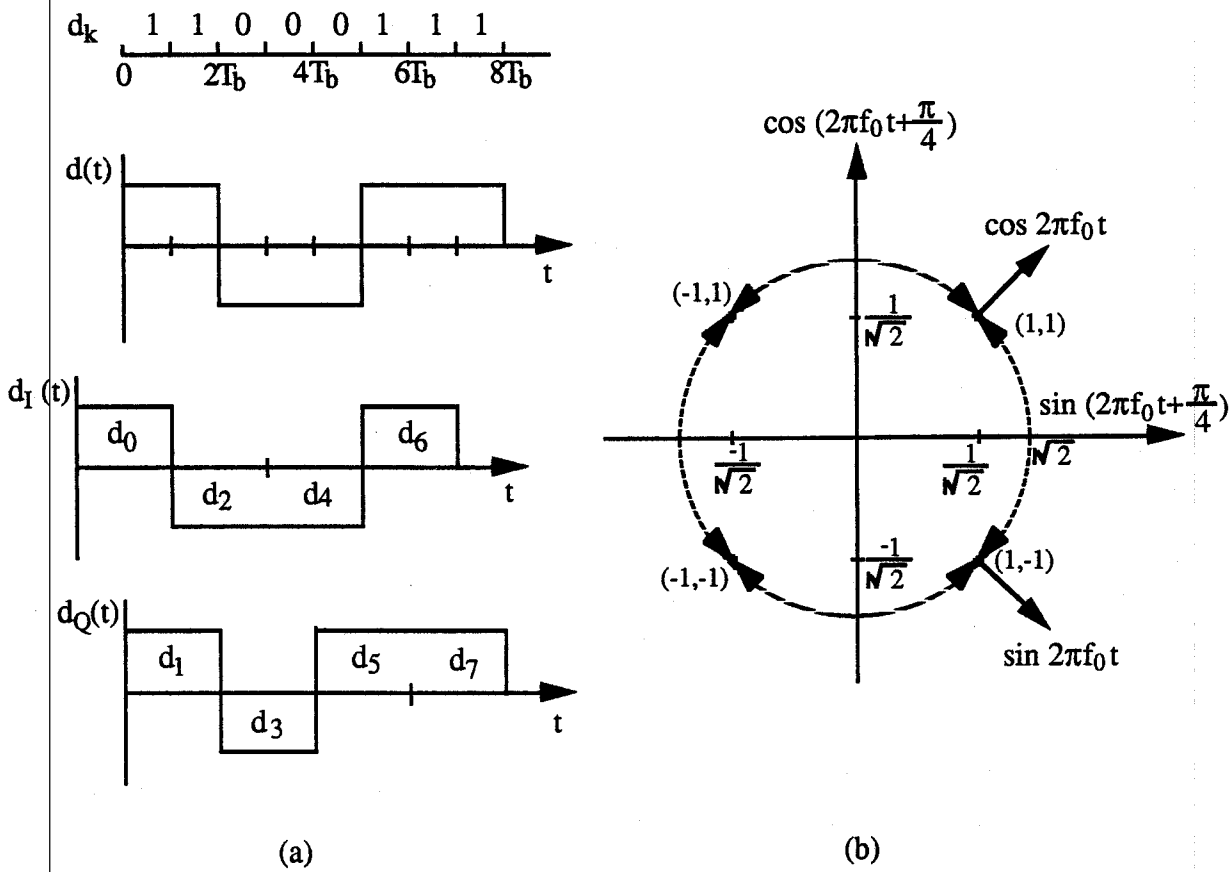

Fig.3.4 (a) I and Q data stream for OQPSK
(b) Signal-space (phasor) diagram for OQPSK

The OQPSK modulation method avoids carrier phase jumps of 180°. Because of this the OQPSK signal has lower amplitude variation than the QPSK signal when the modulated signals are filtered. For this reason OQPSK is preferred over QPSK when the system requires significant bandlimiting and nonlinear amplification [2] [9].

3.3.4 Minimum shift keying

The elimination of 180° phase transients in OQPSK results in lower spectrum spreading. Further improvement is possible if any abrupt carrier phase transitions are also avoided. In such a modulation method phase transition is realized by a continuous phase change over the bit interval.

If the modulation signal streams, I and Q, are sinusoidally weighted as $d_I(t)\cos\frac{\pi}{2T_b}t$ and $d_Q(t)\sin\frac{\pi}{2T_b}t$, instead of $d_I(t)$ and $d_Q(t)$ in OQPSK, such a continuous phase change is realized. This modulation method is called minimum shift keying (MSK) [2] [9]. MSK can be viewed as a special case of OQPSK, and the resulting waveform can be expressed as

$$S_t(t) = A\left[d_I(t)\cos\left(\frac{\pi}{2T_b}t\right)\cos 2\pi f_0 t + d_Q(t)\sin\left(\frac{\pi}{2T_b}t\right)\sin 2\pi f_0 t \right], \qquad (3.4)$$

An MSK signal waveform is shown in Fig.3.5

MSK can also be viewed as a type of continuous-phase frequency shift keying (CPFSK) [2], [9]. The MSK signal can be expressed as

$$S_t(t) = A\cos\left[2\pi\left(f_0 + \frac{d_k}{4T_b}\right)t + x_k \right] \qquad kT_b \le t < (k+1)T_b, \qquad (3.5)$$

where $d_k = \pm 1$ represents the bipolar data being transmitted at a rate $R_b = \frac{1}{T_b}$. From (3.5), $\Delta f = \frac{1}{2T_b}$; this is the minimum tone spacing for orthogonal frequency shift keying (FSK) [9]. Because of this the modulation scheme is named as minimum shift keying. The phase

term x_k is constant over the kth interval $kT_b < t < (k + 1)T_b$, and is selected to maintain phase continuity. For each data interval, the value of x_k is determined by the requirement that the phase of the waveform must be continuous at the bit transitions occurring at the times $t = kT_b$. To satisfy the phase continuity, requirement x_k is given by

$$x_k = \left[x_{k-1} + \frac{\pi k}{2}(d_{k-1} + d_k) \right] \text{ modulo } 2\pi \quad , \tag{3.6}$$

x_k has values of 0 or π.

Equation (3.5) can be expressed in a quadrature representation as

$$S_t(t) = A \left[a_k \cos\left(\frac{\pi}{2T_b}t\right) \cos 2\pi f_0 t + b_k \sin\left(\frac{\pi}{2T_b}t\right) \sin 2\pi f_0 t \right] , \tag{3.7}$$

where $a_k = \cos x_k = \pm 1$, $b_k = d_k \cos x_k = \pm 1$

Equation (3.7) is identical in form to (3.4).and thus MSK can be classified as a form of OQPSK with sinusoidal symbol weighting.

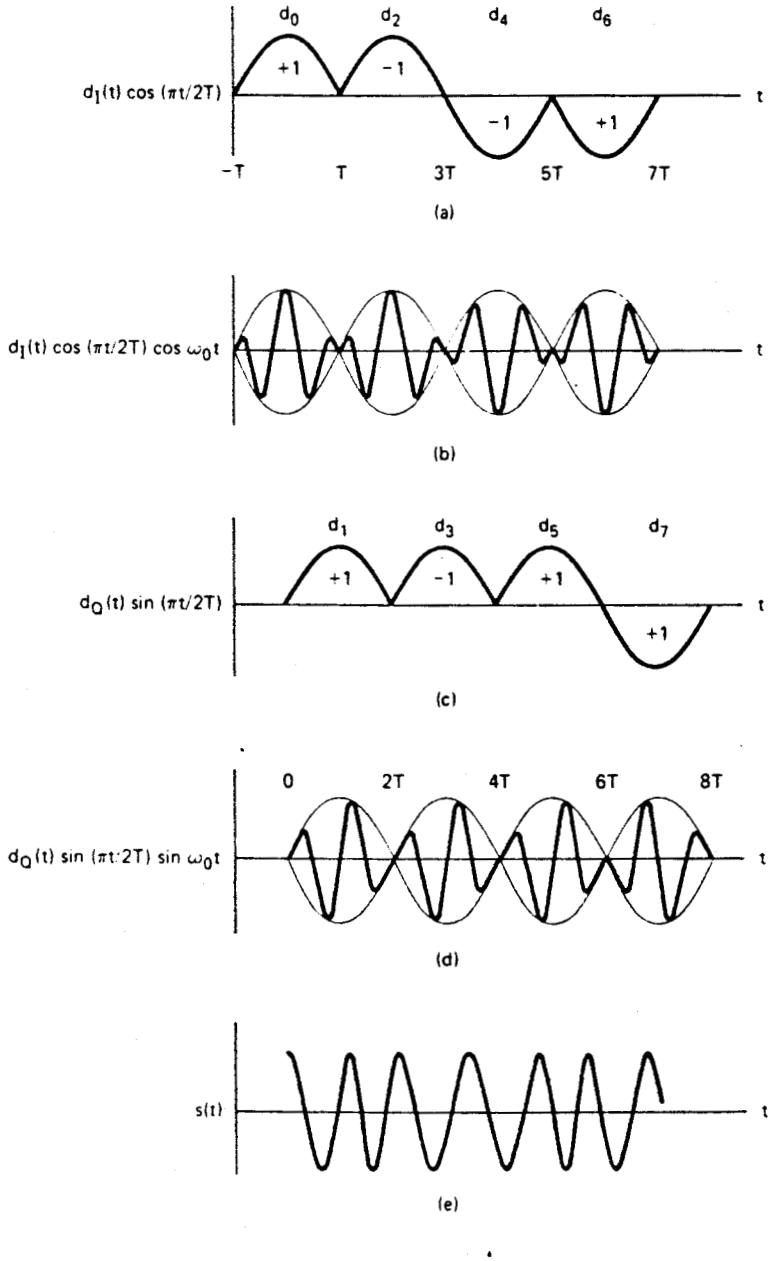

Fig. 3.5 MSK waveforms [from ref. 9]

3.4 DMSK modulation and noncoherent detection at the receiver

3.4.1 Noncoherent detection

For coherent detection the phase of the received signal must be available to the receiver. However recovery of the carrier's phase at the receiver is a difficult task. For example, in a fading multipath environment, several versions of the signal exist at the same time. The interference among these versions results in phase changing rapidly. This makes the phase tracking very hard. In such a case, a coherent receiver design becomes very complex. Coherent detection is therefore not an efficient and economic demodulation method in a fading multipath environment. For noncoherent detection the recovery of carrier's phase is not required at the receiver. Because of this a noncoherent receiver detection is much simpler. The price to be paid for this advantage is an increased probability of error.

Differential coherent detection utilizes the phase information of the previous symbol as the phase reference for detecting the current symbol. It is classified as a noncoherent detection as this method does not require the recovery of carrier phase from the received signal. This detection method can be implemented when the following conditions are met.

1) The unknown relative phase shift of the received signal due to the channel characteristics is either constant or varies slowly over at least two symbol intervals.

2) A known relationship exists between two successive symbol phases which depends on the input data sequence.

Differential coherent detection is an effective detection method. Several modulation schemes can be differentially detected. Differential PSK (DPSK), differential MSK (DMSK) are two well known examples. Note that for the differential detection to be

feasible the modulator has to incorporate differential encoding. When differential encoding is used the data information is sent as the change in phase rather than the absolute phase of the carrier .

3.4.2. DMSK modulation

DMSK modulation is the process where the original data sequence is differentially encoded, and is then modulated on the carrier using MSK modulation. At the receiver the signal is detected using noncoherent differential detection. This is followed by differential decoding of the data.

The equation for generating a differentially encoded sequence $\{C_n\}$ is given by

$$C_n = D_n \oplus C_{n-1} , \tag{3.7}$$

where C_n is the nth differentially encoded data bit which has a value of 0 or 1. D_n is the nth data bit from the source sequence $\{D_n\}$, and assumes values of 0 or 1. Note that $\oplus$ denotes binary addition without a carry.

Differentially coherent detection compares the phase of the current symbol with the phase of the preceding symbol, as shown in Fig.3.6. A differentially decoded sequence, denoted by $\{\hat{D}_n\}$, can be formed using the following equation

$$\hat{D}_n = C_n \oplus C_{n-1} , \tag{3.8}$$

where $\hat{D}_n$ is the nth differentially decoded data.

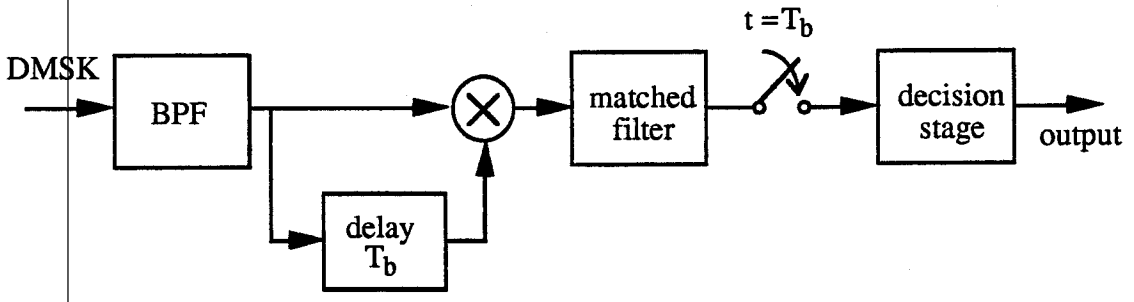

Fig. 3.6 Differential detection of DMSK signal

As stated before, the DMSK receiver with differential detection is considerably simpler than a coherent detection receiver. However, a poor system performance will result when the channel does not satisfy the two conditions specified in Section 3.4.1.

3.5 Spectral properties of MSK

3.5.1 The derivation of power spectral density

The power spectrum of a modulated signal is an upconverted version of the baseband spectrum. It is therefore only necessary to consider the baseband power spectrum.

Equation (3.4) may be written in exponential form as

$$S_t(t) = \mathrm{Re}\left[(x(t) - jy(t))\, e^{j2\pi f_0 t} \right], \qquad (3.8)$$

where $x(t) - jy(t) = z(t)$ is the low-frequency complex envelope of $S_t(t)$, and $x(t)=Ad_I(t)\cos\frac{\pi}{2T_b}t$, $y(t)=Ad_Q(t)\sin\frac{\pi}{2T_b}t$.

The power spectral density of the equivalent baseband signal is the Fourier transform of the auto-correlation function of z(t) [9].

As $d_I(t)$ and $d_Q(t)$ are two rectangular pulse streams, these can be expressed as,

$$d_I(t) = \sum_{n=-\infty}^{\infty} d_{2n} P(t - 2nT_b + \Delta t)$$

$$d_Q(t) = \sum_{n=-\infty}^{\infty} d_{2n+1} P(t - (2n+1)T_b + \Delta t) \quad ,$$

where $P(t)=\prod(\frac{t}{2T_b})$, is a rectangular function with a duration $2T_b$. The symbol denotes the nth bit of an independent identically distributed (iid) random sequence with zero mean and variance 1. The time delay, Δt, is a random variable uniformly distributed over $(0, T_b)$.

Let $G_z(f) \Leftrightarrow E\{z(t)z(t+\tau)^*\}$, $I(f) \Leftrightarrow \cos(\frac{\pi}{2T_b}t)\prod(\frac{t}{2T_b})$, and $Q(f) \Leftrightarrow \sin(\frac{\pi}{2T_b}t)\prod(\frac{t-T_b}{2T_b})$; where '$\Leftrightarrow$' represents Fourier transform relationship and E denotes expectation. The MSK power spectral density is given by [2] [9],

$$G_z(f) = \frac{A^2[\,|I(f)|^2 + |Q(f)|^2]}{2T_b}$$

$$= \frac{8AT_b^2(1 + \cos 4\pi T_b f)}{\pi^2(1 - 16T_b f^2)^2} \quad . \qquad (3.9)$$

Equation (3.9) is the power spectral density function of MSK. Using the same method, the power spectral densities for BPSK, QPSK and OQPSK can be derived [2],[9]. The spectrum of MSK is shown in Fig. 3.7. For comparison purposes, the spectra of BPSK, QPSK and OQPSK are also shown in this figure.

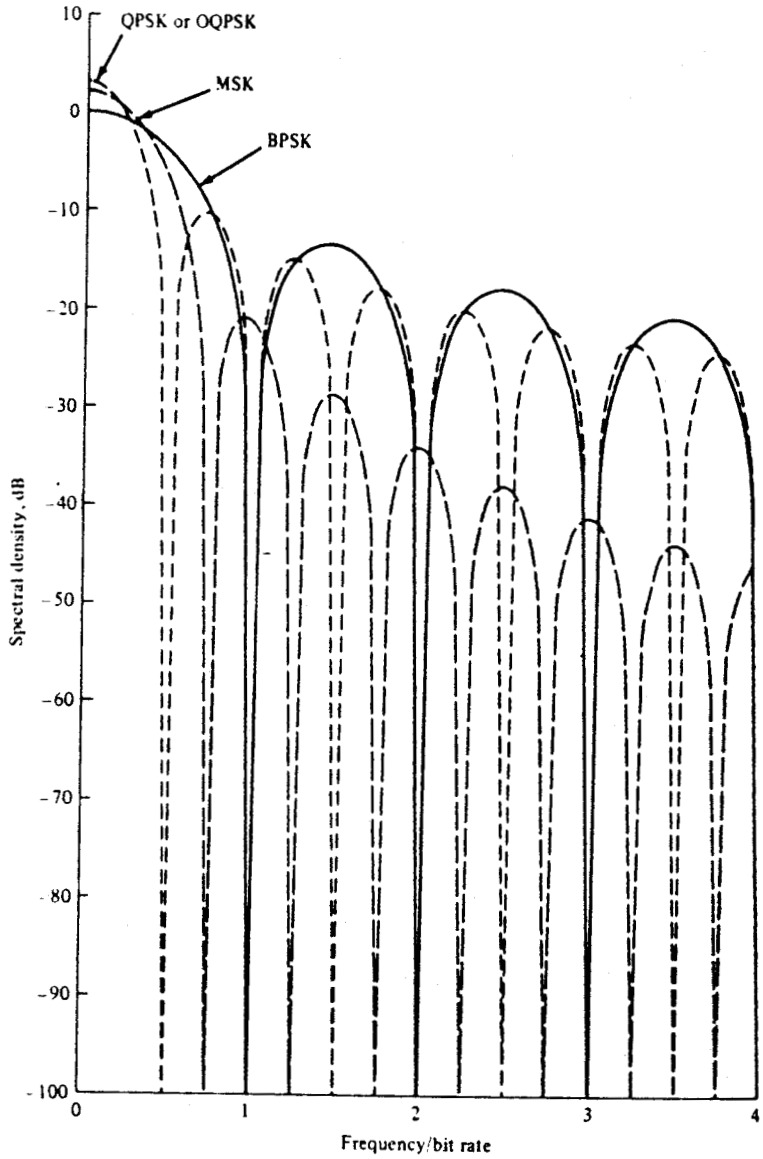

Fig. 3.7 Baseband equivalent power spectra for MSK, BPSK, QPSK or OQPSK [from ref. 2]

3.5.2 Bandwidth efficiency of MSK

From Fig.3.7, it is seen that the first null is at a frequency of $0.5R_b$ Hz for OQPSK and QPSK, $0.75R_b$ Hz for MSK, and R_b Hz for BPSK, where R_b is the bit rate. The MSK spectrum falls off at a faster rate than other modulation methods. As compared to the other modulations the MSK signal has more power in the main lobe. The MSK signal causes lower interference to signals in the adjacent frequency band.

Bandwidth efficiency is defined as the ratio of the bit rate R_b to the required channel bandwidth W. It has units of bits/second/Hz. MSK has better bandwidth efficiency than BPSK. Its bandwidth efficiency is comparable to that of QPSK and OQPSK.

3.6 Summary

Radio communication systems require that the information be modulated on a high frequency carrier. Phase shift keying is the most common method employed in digital radio systems. Minimum shift keying is a form of offset quadrature phase shift keying. It uses a continuous phase change over the bit interval, thereby resulting in a compact spectrum. It is a preferred method for systems with bandlimiting and nonlinear amplification. DMSK is a form of MSK which can be detected using simple noncoherent receiver structure. This modulation method is proposed for the indoor mobile SS radio system. Before the performance of DMSK in such a system is analyzed, a channel model for the indoor mobile radio is required. This is the subject of the next chapter.

Chapter 4

Indoor Mobile Radio Channel Model

Mobile radio communication can provide voice and data links between two or more points without the constraints of a fixed length wireline. This freedom from wirelines has generated interest and demand for indoor mobile radio telephone communication. To investigate indoor mobile radio systems it is important to develop a channel model that represents the communication environment. In this chapter such a model is developed. It is shown that the multipath effect is the dominant feature that degrades communications. This effect and a solution known as diversity are discussed in detail.

4.1 Communication environment for an indoor mobile radio

In an indoor mobile radio communication system, the locations of the transmitters and receivers can change. If the transmitters and receivers are within a building, walls, ceilings and other objects will reflect and absorb (attenuate) radio waves. As the transmitters and receivers move randomly, a very complex and difficult radio propagation channel is formed. This channel will have more than one transmission path between any pair of transmitter and receiver. Each path would in general have a different time delay and path gain.

4.1.1 Multipath effect

When a signal passes through the channel described above, different versions of the transmitted signal can be received. Each version will have different amplitude, phase, and time delays. At the receiver the combination of these different signals results in a distorted

received signal. Each nondirect path is referred to as a multipath as shown in Fig.4.1, and the overall effect is referred to as the multipath effect.

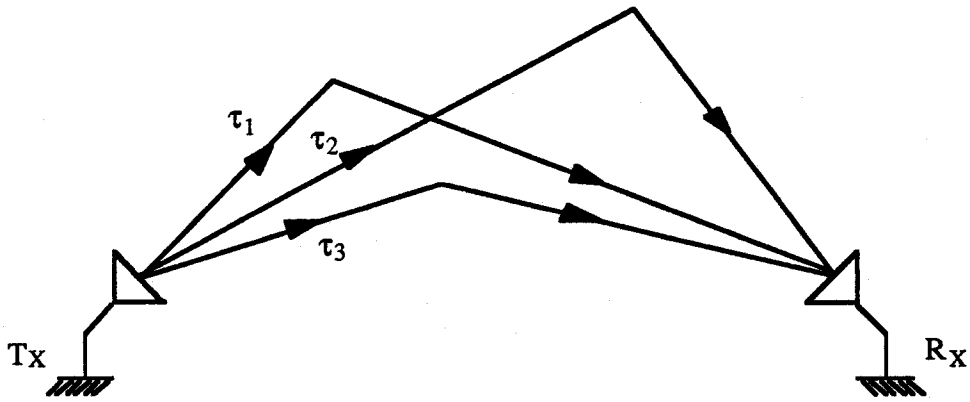

Fig.4.1 Multipath model

Each path in a multipath channel is separated from every other paths by some time delay. The overall delay structure is referred to as the multipath time-delay structure. If each multipath signal can be separated at the receiver, it is possible to reconstruct an undistorted received signal. However, not all paths can be resolved. The time delay and frequency bandwidth of the signal will determine if the multipaths can be resolved or not. Hence, multipath effect can be classified as unresolved multipath and resolved multipath.

A) Unresolved multipath model

An unresolved multipath transmission occurs when the transmitting signal's bandwidth is less than the reciprocal of the difference between any two path delays [11], [12]. Only signal amplitude fluctuations can be measured in this channel. Although the fluctuation of this amplitude depends on the multiple paths, the paths can not be resolved by measurement. This type of channel occurs in buildings where the transmission distance

between the transmitter and the receiver is short, and the spectrum of signal is narrow or is not spread.

B) Resolved multipath model

To resolve any two paths, the transmitted signal's bandwidth must be larger than the reciprocal of the difference between the path delays, i.e.,

$$| t_k - t_j | > \frac{1}{W}, \tag{4.1}$$

where W is the transmission bandwidth, and t_k and t_j are the two path delays. In resolved multipath channel, three variables, time delay τ_j, path gain β_j, and path phase γ_j, are determined for each "resolvable" path. This type of channel occurs when the transmission distance between the transmitter and the receiver is large, and the signal's spectrum is wide or is spread. This is the case for an indoor multipath channel where spread spectrum is used. Such a channel is referred to as a resolved multipath channel.

C) Discrete-time approximation to the resolved multipath model

Consider a discrete delay axis divided into bins of width Δ numbered beginning with 1. The delay width Δ is defined as the delay resolution. This is determined by the signal bandwidth, i.e., $\Delta = \frac{1}{W}$. Each multipath can be placed in a bin according to the value of the path delay. Any two paths, say k_1 and k_2 that have $| t_{k1} - t_{k2} | < \frac{1}{W}$, are considered a single path with a common delay $t_k \cong t_{k1} \cong t_{k2}$. Each such path will occupy one bin and will be considered to be centered in one bin. The delay of any physical path lying in bin j is then quantized to $\Delta(j - \frac{1}{2})$ seconds. This process results in a discrete time approximation to the resolved multipaths and is called a discrete-time multipath model. This model is shown in Fig.4.2 [11].

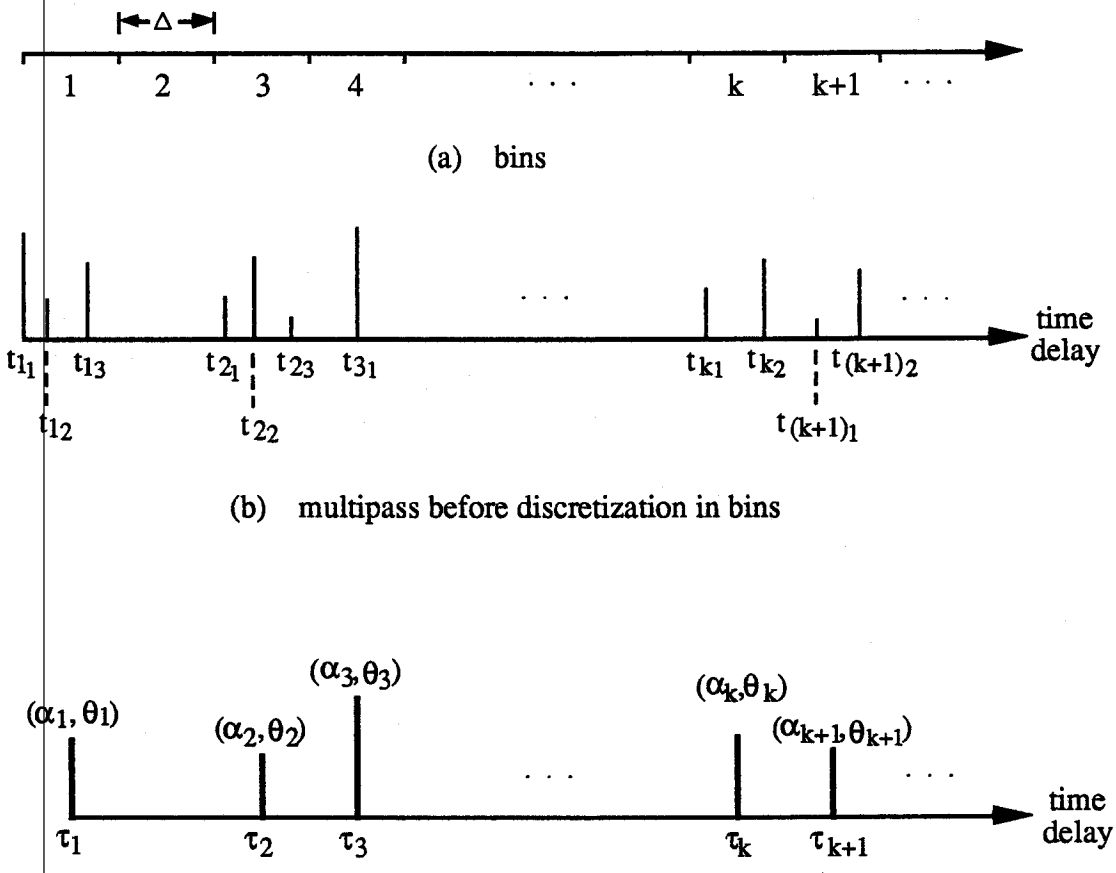

(a) bins

(b) multipass before discretization in bins

(c) multipath after discretization in bins

Fig.4.2 Discrete-time model

In Fig.4.2(b), the paths in the same bin k are unresolved. The paths located in same bin are denoted by $\{\tau_k, \alpha_k, \theta_k\}$, as shown in Fig.4.2(c).

The mathematical model for such a multipath communication environment is used to determine the effect on the signal being transmitted. In general, four parameters can describe the multipath channel illustrated in Fig.4.2. These are the number of paths, the time delay, the attenuation, and the phase. Usually, these are all random variables. If the multipath is considered discrete in time, and h(t) denotes the lowpass equivalent of the channel impulse response, h(t) may be expressed as [8] [10] [13]:

$$h(t) = \sum_{j=1}^{L} \beta_j \, \delta(t - \tau_j) \, e^{j\gamma_j} \quad , \tag{4.2}$$

where L is the number of multipaths, β_j is the jth path gain, τ_j is the time delay of the jth path, and γ_j is the phase of the jth path.

If the maximum multipath delay spread is known, the maximum possible number of the resolved paths is given by [13]

$$L_m = \left[\frac{T_m}{\Delta} \right] + 1 \, , \tag{4.3}$$

where T_m is the maximum multipath time delay spread, Δ is as previously defined, and [x] denotes to take the largest integer less than x.

4.1.2 Rayleigh fading

In a multipath propagation channel the amplitude of the signal can change randomly. Both the experimental and theoretical results show that the distribution of signal amplitude approximately follows a Rayleigh distribution [12], [14]. That is, the path gain of a multipath channel resembles a Rayleigh distribution. In Fig.4.3, a typical amplitude distribution is plotted as a cumulative probability distribution in 1 dB increments of signal strength [14]. As shown in Fig.4.3 it is close to the Rayleigh characteristic. The Rayleigh distribution is a good approximation for the signal amplitude in a multipath channel.

The lth path gain is denoted by β_j and the Rayleigh probability density function $f_{\beta_j}(x)$ is given by

$$f_{\beta_j}(x) = \begin{cases} \dfrac{x}{\rho_j} e^{-\dfrac{x^2}{2\rho_j}} & x \geq 0 \\ 0 & x < 0 \end{cases} \tag{4.4}$$

where ρ_j is equal to half the average path power, i.e., $\rho_j = \frac{1}{2} E\{\beta_j^2\}$, and ρ_j may be different for each path.

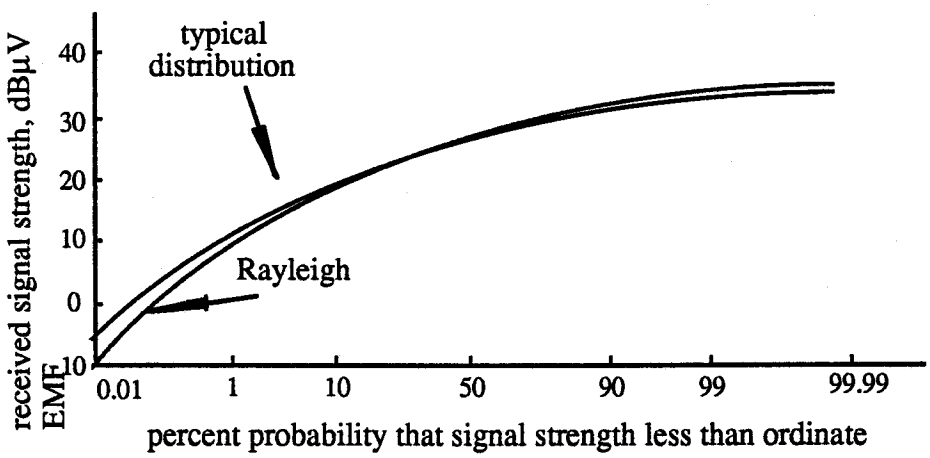

Fig.4.3 Cumulative probability distribution of the received signal strength

4.1.3 The effect of multiple users

As stated before "multiple users" refers to a situation when there are a number of users in the same transmission channel. Each user has its own transmitter and receiver. In this case, regardless of the multiple access method used there will be a cross-interference from other users. In a SSMA system users share the same frequency band and all users can receive all signals. To distinguish the signals a spreading code, unique to each user, is given to the corresponding receiver. Because of different time delay of the signal and the non-orthogonality of the spreading codes, the receiver can't remove other users' signals completely. The signal at the output of the bandpass filter shown in Fig.2.2 contains not only the required signal, but also the remainder of other users' signals. This remainder signal is called cross-interference, and it affects the demodulation or detection of the

required signal resulting in an increase in the probability of error. As the cross-interference increases so does the error probability. This effect is referred to as the multiple user effect.

A reduction in the number of multiple users will result in an improvement in the bit error performance. An improvement in this performance can also be obtained by selecting codes with low cross-correlation properties.

4.2 Diversity technique for fading multipath channel

The indoor mobile radio communication channel is a multipath fading channel. When the channel experiences a deep fade the attenuation can be quite large. Obviously, when a signal is transmitted during this time the communication system will have a very high error rate. However, if receiver is supplied with several replicas or versions of the same signal information transmitted over independently fading channels, it can combine the replicas or select the largest one among the replicas. In this case the signal fading can be overcome. This results from the fact that the probability of all channels experiencing a deep fade is very small for independent fading channels. This forms the basis of diversity techniques used for fading channels. The objective of diversity is to mitigate the effect of deep fades. Usually, there are several methods that will produce several independently fading replicas of the same information signal. With any one of the methods, different types of combining or decision procedures can be used at the receiver.

4.2.1 Diversity transmission methods

One method is called frequency diversity. In this method the same information signal is modulated on L carriers separated by $1/T_m$ [16], where T_m is the maximum delay spread.

A second method is time diversity. To achieve L independently fading versions of the same information signal by time diversity, the signal is transmitted in L different time slots. The difference between successive time slots has to be equal to or exceed the coherence time of the channel [16].

A third method is antenna diversity or space diversity [16]. In this method L independently fading versions of the same information are obtained by spacing L antennas a certain distance apart. The distance is chosen to produce multipath components that have significantly different propagation delays for different antennas.

A fourth method is spread spectrum diversity [16]. In multipath channel, spread spectrum technique can make the multipath resolvable. The spread spectrum diversity can be obtained by a bank of the matched filters with same reference code, but different time delay. This is equivalent to receiving different versions of the transmitted signal from different paths. These versions are independent of each other, and can be combined in different ways.

For an indoor multipath fading environment, spread spectrum diversity and antenna diversity are attractive. For example, one transmitter antenna and three receiver antennas form a three-channel transmission system, shown in Fig.4.4. The receiver antennas are spaced so that every antenna can receive different versions of the same signal simultaneously. Fig.4.4 shows only the direct paths for each channel. If the fluctuations of the signal in the three transmission channels, denoted by $\beta(\tau_i, t_j)$, are independent and follow a Rayleigh distribution, (where τ_i represents a different channel, and t_j stands for a different instant of time), then the probability that each channel is in a deep fade is small. Fig.4.5 illustrates this. Antenna diversity is suitable for the reverse channel, i.e., for receiving signals at the base station in a mobile radio communication system. For portable receiver spread spectrum diversity is more practical. For example, there are three matched

filters in one mobile receiver shown in Fig.4.6. Three matched filters have same code with the different time delays τ_1, τ_2, and τ_3 respectively. The samplers following the matched filters have different sampling time. Delayed clocks are used to obtain the synchronized signals at the output. In Fig.4.6, $\tau_1<\tau_2<\tau_3$, and the three paths are assumed to be independent of each other. The signal versions received from different paths are same as those in Fig.4.5.

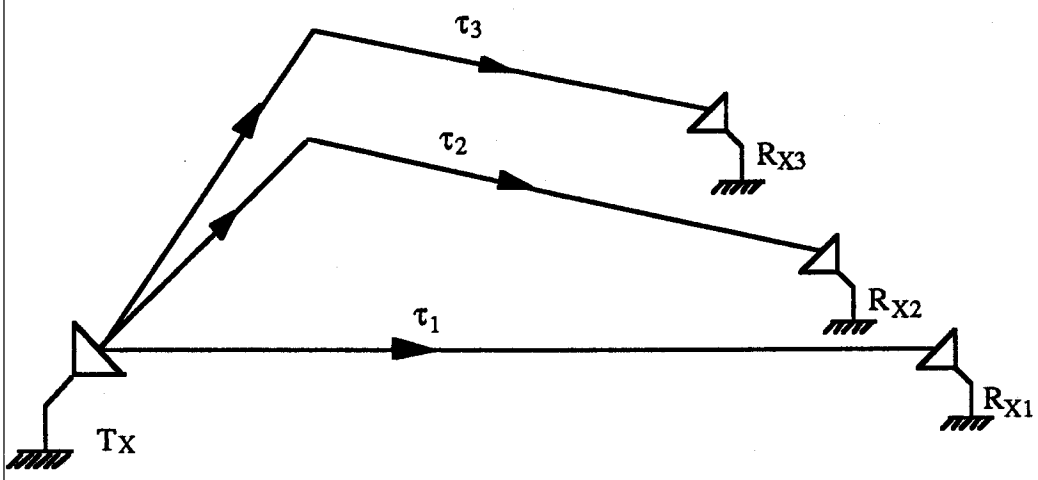

Fig.4.4 Antenna diversity

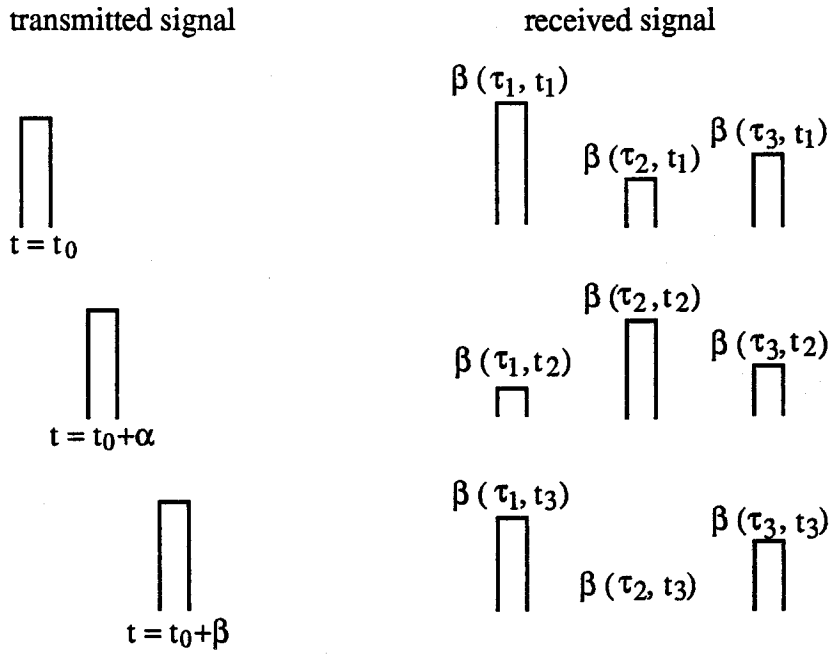

Fig.4.5 Signals from different channels

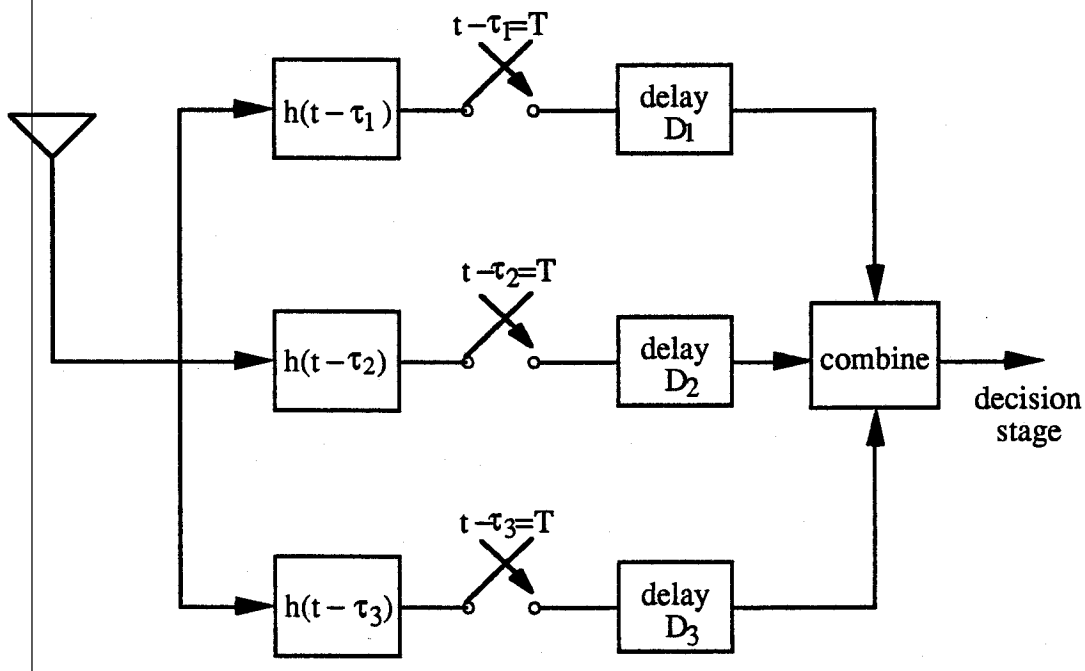

Fig. 4.6 Spread spectrum diversity

4.2.2 Combining methods

Diversity methods are also classified by the combining techniques employed in implementing the diversity system [21]. Two commonly used combining methods are discussed below.

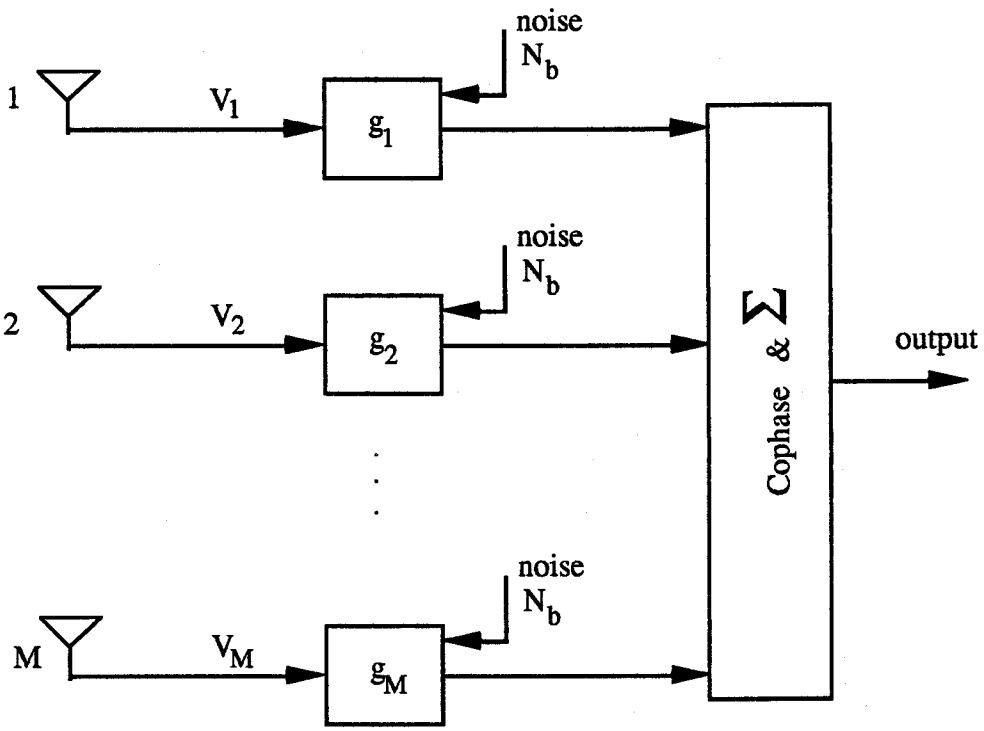

Fig.4.7 Block diagram of antenna diversity

a) Predetection combining diversity

In predetection combining diversity, different versions of the same signal are combined before the detection stage. As shown in Fig.4.7, in antenna diversity the signals received from different antennas are amplified, cophased, and added. Each antenna with its associated amplifier and cophasing circuit makes up a single diversity branch. In this figure V_i denotes the ith version of the signal voltage from the ith antenna. Signal magnitude $|V_i|$

follows a Rayleigh distribution; g_i is the amplifier gain in the ith branch, and it is assumed that the input noise power N_b is same for all amplifiers.

Usually the signal-to-noise ratio, denoted by S/N, is an important parameter used to evaluate system performance. The S/N of the system with diversity is briefly discussed below.

The output signal voltage V_0 is

$$V_0 = \sum_{i=1}^{M} g_i V_i \quad . \tag{4.5}$$

The noise output power N_0 is

$$N_0 = N_b \sum_{i=1}^{M} g_i^2 \quad . \tag{4.6}$$

Hence the resulting signal-to-noise ratio S/N is

$$S/N = \frac{\left(\sum_{i=1}^{M} g_i V_i\right)^2}{N_b \sum_{i=1}^{M} g_i^2} \quad . \tag{4.7}$$

In equal gain diversity, all amplifier gains are same, i.e., $g_i=g$ for all i. The signal-to-noise ratio becomes

$$\text{Equal gain } S/N = \frac{\left(\sum_{i=1}^{M} V_i\right)^2}{MN_b} \quad . \tag{4.8}$$

Evidently, as long as all channels are not in a deep fade simultaneously, the signal-to-noise ratio is larger than that in which only one channel exists and is in deep fade.

b) Selection diversity

Selection diversity connects the branch with largest instantaneous S/N to the output. If this branch is the jth branch, the signal-to-noise ratio from (4.7) is

$$\text{Selection } S/N = \frac{V_j^2}{N_b} . \tag{4.9}$$

In this diversity method, so long as all channels are not in a deep fade simultaneously, the effect of fading is mitigated.

4.3 Summary

Indoor mobile radio channel is a fading multipath channel. The multipath effect degrades the performance of such a communication system. Diversity technique can be used to improve the system performance. By resolving the multiple path multipath diversity can be implemented. Antenna diversity is suitable for use in the base station receiver. Spread spectrum diversity is more practical for the mobile receiver.

Chapter 5

Bit Error Rate Performance

In preceding chapters, concepts and techniques such as direct-sequence spread-spectrum, multipath fading channel in an indoor environment, diversity, multiple access, and DMSK modulation method were introduced. In this chapter, the performance analysis of a system which incorporates these concepts and techniques is given. The system analyzed is a direct-sequence spread-spectrum multiple access (DS-SSMA) system with DMSK modulation. The channel is an indoor mobile radio channel and as discussed before a diversity technique is used to overcome fading.

5.1 System model, definitions and assumptions

An indoor communication system can be implemented using a cellular structure. Each cell in such a structure is a communication unit. Usually this basic unit is a star network configuration in which each user exercises average power control to determine the power transmitted for that user by the base station. In each cell, the star network configuration is employed to communicate with the base station which is also called a cell node. The cell nodes communicate with one another using a separate communication link. Each cell user communicates with users in other cells through base station. For SSMA system, the users in the same cell share same frequency band and each user has a unique spreading code. The adjacent cells operate in different frequency bands. The spreading codes can be reused in the adjacent cells.

A wireless PBX system may be considered as an example of the star network configuration. A simple block diagram of this system is depicted in Fig.5.1. The system

supports K simultaneous two-way users. Every active user is a transportable station and has a unique spread-spectrum code. The central station contains a bank of the spread-spectrum receivers, one for each active user. The central station transmits the K signals with equal power. All signals propagate via multiple paths to each of the receivers. The number and length of the paths varies from receiver to receiver.

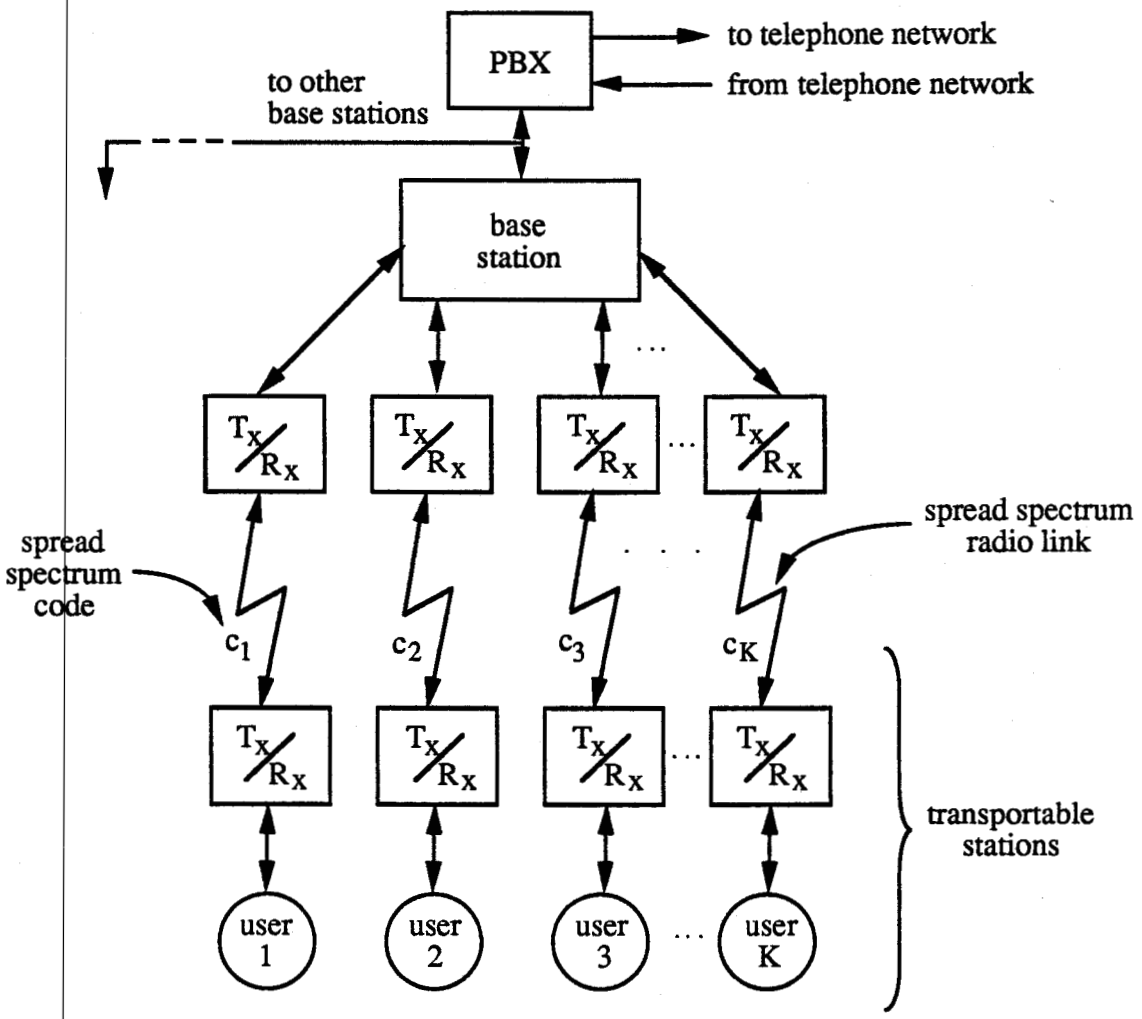

Fig.5.1 A star-connected indoor mobile radio system

For the system discussed above, an analysis of the average bit-error probability for the link between any active user and the corresponding receiver at the central station is presented.

To carry out the analysis, certain assumptions have to be made. The first one is that the channel between a user's transmitter and the corresponding receiver at the central station is a discrete multipath Rayleigh fading channel with slow fading. The second one is that the interference considered is only from other users in the same cell, and the interference caused by adjacent cells can be overcome by taking advantage of frequency band-selectivity of the receivers. It is also assumed that the interference power from each user is equal.

5.1.1 Transmitter model

There are K active users in the system. Every user transmits a differentially encoded binary data sequence at the same power, and employs a unique spreading code called psuedorandom code. The codes having a length N, i.e., N chips, are used to spread each data bit. For the kth user, the data sequence is denoted by d_k^j, j = . . ., -2, -1, 0, 1, 2, . . ., and the spreading code is a_k^i, i = . . ., -2, -1, 0, 1, 2, ... Also $a_k^{i+N} = a_k^i$ for all i. The bit and chip durations are denoted by T and T_c respectively, so that, $T=NT_c$. The data and chip waveforms denoted by $d_k(t)$ and $a_k(t)$ respectively may be written as

$$d_k(t) = \sum_j d_k^j P_T(t - jT) \quad , \tag{5.1}$$

$$a_k(t) = \sum_i a_k^i P_{T_c}(t - iT_c) \quad , \tag{5.2}$$

where $d_k^j = \pm 1$, $a_k^i = \pm 1$, and $a_k^{i+N} = a_k^i$. $P_T(t)$ is a rectangular waveform shape function which has a unit height and duration T.

Assuming that the modulation used is DMSK, the transmitter for such a modulation is shown in Fig.5.2.

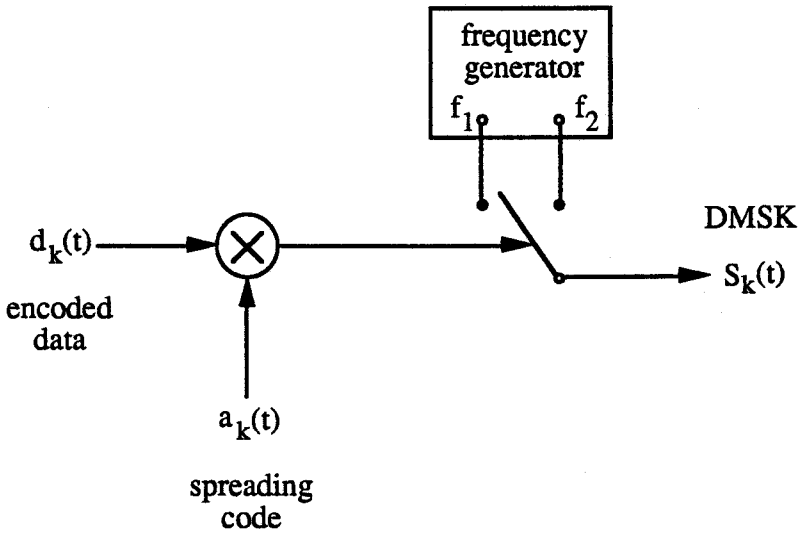

Fig.5.2 The block diagram of a DMSK modulator
with direct-sequence spread spectrum

In Fig.5.2, $f_1 = f_0 + \frac{1}{4T_c}$, $f_2 = f_0 - \frac{1}{4T_c}$, where f_0 is carrier frequency, and is same for all users. The carrier frequency f_0 is usually chosen as $f_0 = m\frac{1}{T_c} = mN\frac{1}{T}$ where m is an integer. Because the binary data sequence d_k^j and spreading code a_k^i take a value from $\{-1,1\}$, the product of $d_k(t)$ and $a_k(t)$ still takes a value from $\{-1,1\}$. When the product is positive the switch in Fig.5.2 contacts f_1, otherwise it contacts f_2. The transmitted signal for the kth user, $S_k(t)$ is given by

$$S_k(t) = A\cos\left\{ 2\pi\left[f_0 + d_k(t)a_k(t)\frac{1}{4T_c}\right]t + \theta_i \right\}$$

$$= A\cos\left\{ 2\pi\left[f_0 + D_k^i \frac{1}{4T_c}\right]t + \theta_i \right\}, \quad i = \cdots, -1, 0, 1, \cdots \qquad (5.3)$$

$$\theta_i = \left[\theta_{i-1} + \frac{1}{2}(D_k^i - D_k^{i-1})\pi i \right] \text{Mod } 2\pi, \quad i = \cdots, -1, 0, 1, \cdots \qquad (5.4)$$

Here, θ_i is a phase constant valid over the ith interval, and is selected to ensure a continuous phase in the output waveform. A is the carrier amplitude, and the energy per bit, E_b, is $\frac{1}{2}A^2T$.

A comparison of equation (5.3) with equation (3.5) shows that this equation expresses a DMSK waveform.

To carry out the analysis, signal $S_k(t)$ is expressed in a different form. Consider that the sequence $a_k(t)$ is demultiplexed into two branches, $a_{kI}(t)$ and $a_{kQ}(t)$. In each branch, the chip duration is $2T_c$, and the transitions of one branch are offset by T_c from the transitions of the other branch. So that $S_k(t)$ may be written as

$$S_k(t) = Ad_k(t)a_{kI}(t)\cos\frac{2\pi}{4T_c}t\cos 2\pi f_0 t - Ad_k(t)a_{kQ}(t)\sin\frac{2\pi}{4T_c}t\sin 2\pi f_0 t$$

$$= \text{Re}\left\{\left[S_k(t) = Ad_k(t)a_{kI}(t)\cos\frac{2\pi}{4T_c}t + j\,Ad_k(t)a_{kQ}(t)\sin\frac{2\pi}{4T_c}t \right] e^{j2\pi f_0 t}\right\}.$$

(5.5)

The lowpass equivalent signal $\tilde{S}_k(t)$ of $S_k(t)$ may be written as

$$\tilde{S}_k(t) = Ad_k(t)a_{kI}(t)\cos\frac{2\pi}{4T_c}t + j\,Ad_k(t)a_{kQ}(t)\sin\frac{2\pi}{4T_c}t. \qquad (5.6)$$

5.1.2 Channel model

As stated before, the channel between the kth transmitter and the corresponding receiver at the central station is a discrete multipath Rayleigh fading channel. Also in comparison with the data bit rate, the fading rate in an indoor environment is slow. This means that in two successive bit intervals the parameters associated with the channel do not vary significantly. The lowpass equivalent impulse response of this channel may be written as

$$\tilde{h}_k(t) = \sum_{j=1}^{L} \beta_{jk}\, \delta(t - \tau_{jk})\, e^{j\gamma_{jk}} \quad , \tag{5.7}$$

where β_{jk}, τ_{jk} and γ_{jk} are gain, time delay and phase of the lth path respectively. Random variables τ_{jk} and γ_{jk} have a uniform distribution in (0,T) and $(0,2\pi)$ respectively. β_{jk} has a Rayleigh distribution. The probability density function for β_{jk} is given by

$$f_{\beta_{jk}}(x) = \begin{cases} \dfrac{x}{\rho_{jk}}\, e^{-\dfrac{x^2}{2\rho_{jk}}} & x \geq 0 \\ 0 & x < 0 \end{cases} \tag{5.8}$$

where the parameter ρ_{jk} in the Rayleigh distribution for β_{jk} is equal to half the average path power, i.e., $\rho_{jk} = \frac{1}{2} E\{\beta_{jk}^2\}$. For each path, ρ_{jk} may be different. All of the three random variables β_{jk}, τ_{jk} and γ_{jk} are assumed to be independent.

The number of paths, L, is in general a random variable. To keep the analysis simple, L is assumed to be fixed and have a value equal to the maximum possible value. This is a worst case situation.

5.1.3 Receiver model

Two receiver models are considered in this thesis. The first model uses selection diversity, while the second model employs predetection combining as shown in Figs.5.3 and 5.4 respectively. For selection diversity receiver, the signal from the path that gives the largest peak is selected and demodulated. The diversity is obtained using multiple antennas and resolution of multiple paths. For the predetection combining receiver in Fig.5.4, the signals from every path are cophased and added prior to detection.

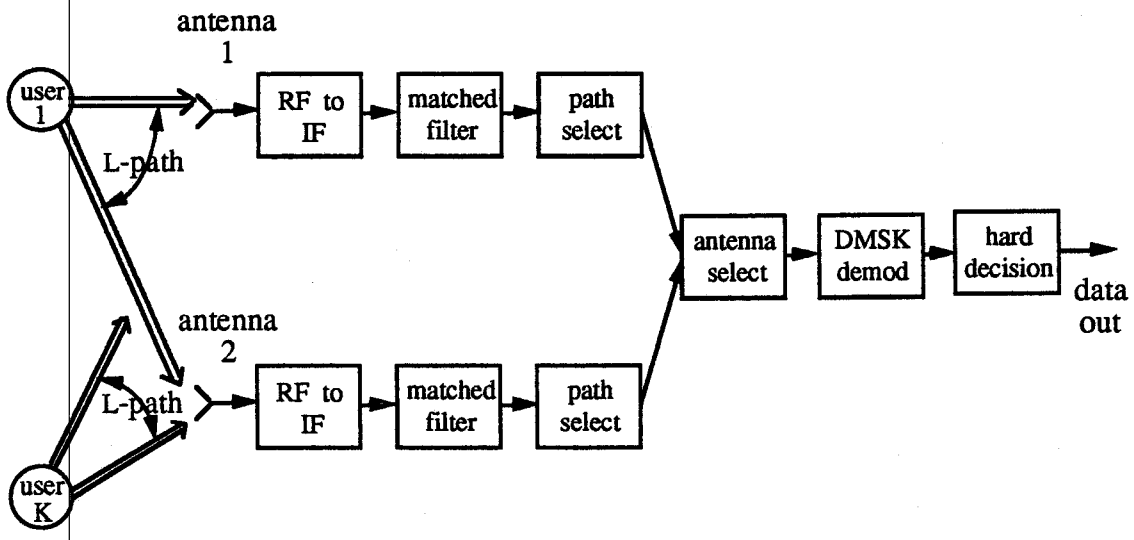

Fig.5.3 Base station receiver with direct-sequence spread-spectrum and selection diversity

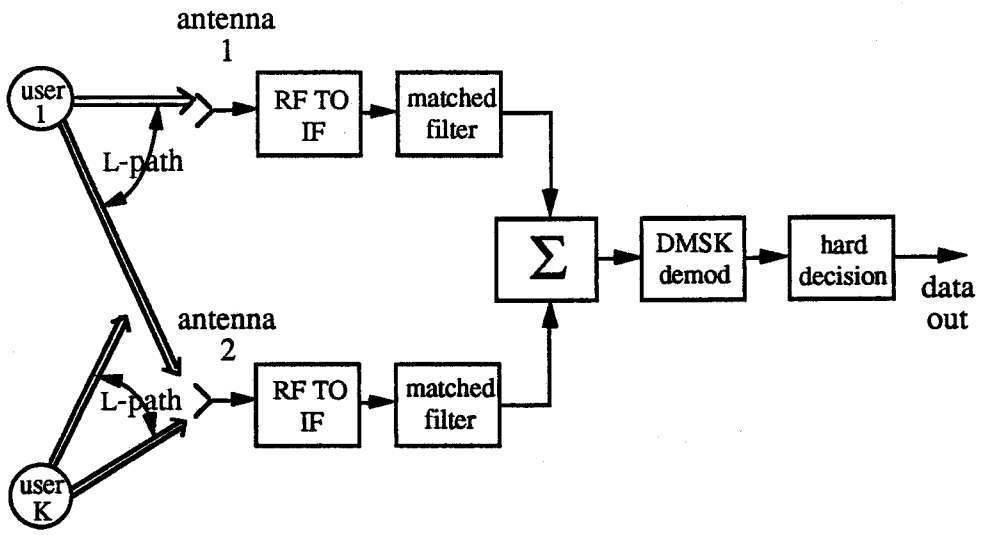

Fig.5.4 Base station receiver with direct-sequence spread-spectrum and predetection combining

The matched filters in the receivers match to the spreading codes of the reference user. It is assumed that the noise n(t) at the input of each receiver is band-limited white Gaussian noise with two-sided power spectral density of $\frac{N_0}{2}$. Therefore, the equivalent lowpass noise has a spectral density of N_0.

Therefore, the received signal at any input of the receiver is given by

$$r(t) = \mathrm{Re}\left\{ \sum_{k=1}^{K} S_k(t) * h_k(t) \right\} + n(t) \quad , \tag{5.9}$$

where '*' is a convolution operator, $S_k(t)$ is the kth user's signal given by equation (5.5), and $h_k(t)$ is the impulse response of the kth user's channel given by equation (5.7).

As stated in Chapter 3 the bandpass signal can be analyzed using equivalent lowpass signal. The complex envelope of the received lowpass signal may be written as

$$\tilde{r}(t) = \sum_{k=1}^{K} \tilde{S}_k(t) * \tilde{h}_k(t) + \tilde{n}(t) \quad , \tag{5.10}$$

where $\tilde{n}(t)$ is lowpass equivalent component of n(t), and $\tilde{n}(t)=n_c(t)+jn_s(t)$; $n_c(t)$ and $n_s(t)$ are independent quadrature Gaussian components [2].

Substituting for $\tilde{n}_k(t)$ from eq. (5.7) the lowpass equivalent components of the received signal can be written as:

$$\tilde{r}(t) = \sum_{k=1}^{K}\sum_{j=1}^{L}\beta_{jk}\,\tilde{S}_k(t-\tau_{jk})\,e^{j\gamma_{jk}} + \tilde{n}(t)$$

$$= \sum_{k=1}^{K}\sum_{j=1}^{L} A\beta_{jk}\Big[d_k(t-\tau_{jk})a_{kI}(t-\tau_{jk})\cos\gamma_{jk}\cos\frac{2\pi}{4T_c}(t-\tau_{jk})$$

$$- d_k(t-\tau_{jk})a_{kQ}(t-\tau_{jk})\sin\gamma_{jk}\sin\frac{2\pi}{4T_c}(t-\tau_{jk})\Big] + n_c(t)$$

$$+ j\left\{\sum_{k=1}^{K}\sum_{j=1}^{L} A\beta_{jk}\Big[d_k(t-\tau_{jk})a_{kI}(t-\tau_{jk})\,\sin\varphi_{jk}\,\cos\frac{2\pi}{4T_c}(t-\tau_{jk})\right.$$

$$\left. + d_k(t-\tau_{jk})a_{kQ}(t-\tau_{jk})\,\cos\gamma_{jk}\,\sin\frac{2\pi}{4T_c}(t-\tau_{jk})\Big] + n_s(t)\right\} \quad . \qquad (5.11)$$

Let x(t) and y(t) denote the real and imaginary parts of $\tilde{r}(t)$ so that

$$x(t) = \sum_{k=1}^{K}\sum_{j=1}^{L} A\beta_{jk}\Big[d_k(t-\tau_{jk})a_{kI}(t-\tau_{jk})\cos\gamma_{jk}\cos\frac{2\pi}{4T_c}(t-\tau_{jk})$$

$$- d_k(t-\tau_{jk})a_{kQ}(t-\tau_{jk})\sin\gamma_{jk}\sin\frac{2\pi}{4T_c}(t-\tau_{jk})\Big] + n_c(t) \quad ,$$

$$y(t) = \sum_{k=1}^{K}\sum_{j=1}^{L} A\beta_{jk}\Big[d_k(t-\tau_{jk})a_{kI}(t-\tau_{jk})\sin\gamma_{jk}\cos\frac{2\pi}{4T_c}(t-\tau_{jk})$$

$$+ d_k(t-\tau_{jk})a_{kQ}(t-\tau_{jk})\cos\gamma_{jk}\sin\frac{2\pi}{4T_c}(t-\tau_{jk})\Big] + n_s(t) \quad .$$

The carrier complex envelope r(t) is given by:

$$\tilde{r}(t) = x(t) + jy(t). \qquad (5.12)$$

5.2 System performance analysis

Presence of noise and interference results in bit errors. The bit error rate (BER) is most commonly used to characterize the system performance. The bit error rate depends on the channel, the modulation and detection method, the transmitted power as well as the interference and noise present in the system.

In this thesis, a BER analysis method is developed for an indoor mobile radio DSSS DMSK system. As in [8], the average probability of error, which is the error probability averaged over the ensemble of channels, is used to estimate the BER. The channel model used in the analysis was described in Chapter 4.

The block diagram of a receiver with differential detection is shown in Fig.5.5.

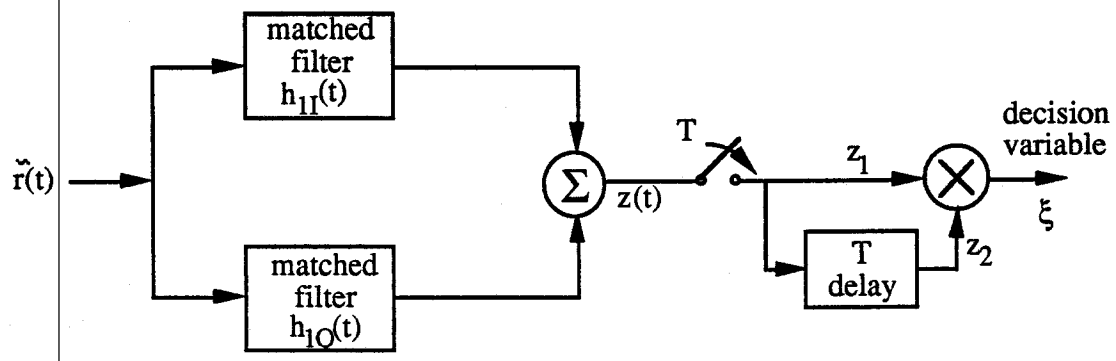

Fig.5.5 The receiver block diagram with differential detection

The first step in the BER analysis is computation of the decision variable ξ. This is done in the remainder of this section.

In Fig.5.5, $h_{1I}(t)$ and $h_{1Q}(t)$ are the impulse responses of the matched filters in the inphase and quadrature arms respectively. These are given by

$$h_{1I}(t) = a_{1I}(T-t)\cos\frac{2\pi}{4T_c}(T-t)$$

$$h_{1Q}(t) = a_{1Q}(T-t)\sin\frac{2\pi}{4T_c}(T-t) \qquad (5.13)$$

With input $\tilde{r}(t)$ given by eq. (5.12) the outputs for the inphase arm are

$$g_{Ix}(t) = x(t) * h_{1I}(t)$$

$$g_{Iy}(t) = y(t) * h_{1I}(t) \qquad (5.14.a)$$

The outputs of the matched filter in quadrature arm are

$$g_{Qx}(t) = x(t) * h_{1Q}(t)$$

$$g_{Qy}(t) = y(t) * h_{1Q}(t) \qquad (5.14.b)$$

The resultant output of the two matched filters is

$$z(t) = [g_{Ix}(t) + g_{Qx}(t)] + j[g_{Iy}(t) + g_{Qy}(t)] \qquad (5.15)$$

Substituting for x(t) and y(t) from (5.12) $g_{Ix}(t)$ is given by

$$g_{Ix}(t) = \sum_{k=1}^{K}\sum_{j=1}^{L} A\beta_{jk}\Bigg[\cos\gamma_{jk}\int_0^t d_k(s-\tau_{jk})a_{kI}(s-\tau_{jk})\cos\frac{2\pi}{4T_c}(s-\tau_{jk})$$

$$\times a_{1I}(T-t+s)\cos\frac{2\pi}{4T_c}(T-t+s)ds$$

$$-\sin\gamma_{jk}\int_0^t d_k(s-\tau_{jk})a_{kQ}(s-\tau_{jk})\sin\frac{2\pi}{4T_c}(s-\tau_{jk})a_{1I}(T-t+s)\cos\frac{2\pi}{4T_c}(T-t+s)ds\Big]$$

$$+\int_0^t n_c(s)a_{1I}(T-t+s)\cos\frac{2\pi}{4T_c}(T-t+s)ds$$

The sampled output $g_{Ix}(T)$ at t=T for the 0th bit is given by

$$g_{Ix}(T)=\sum_{k=1}^{K}\sum_{j=1}^{L}A\beta_{jk}\Big[\cos\gamma_{jk}\int_0^t d_k(s-\tau_{jk})a_{kI}(s-\tau_{jk})\cos\frac{2\pi}{4T_c}(s-\tau_{jk})$$

$$\times a_{1I}(s)\cos\frac{2\pi}{4T_c}(s)ds$$

$$-\sin\gamma_{jk}\int_0^t d_k(s-\tau_{jk})a_{kQ}(s-\tau_{jk})\sin\frac{2\pi}{4T_c}(s-\tau_{jk})a_{1I}(s)\cos\frac{2\pi}{4T_c}(s)ds\Big]$$

$$+\int_0^t n_c(s)a_{1I}(s)\cos\frac{2\pi}{4T_c}(s)ds$$

$$=\sum_{k=1}^{K}\sum_{j=1}^{L}A\beta_{jk}\{\cos\gamma_{jk}[d_k^{-1}R_{1kI}(\tau_{jk})+d_k^{0}\hat{R}_{1kI}(\tau_{jk})]$$

$$-\sin\gamma_{jk}[d_k^{-1}S_{1kI}(\tau_{jk})+d_k^{0}\hat{S}_{1kI}(\tau_{jk})]\}+\eta_I \quad . \qquad (5.16.a)$$

Similarly the other inphase and quadrature components of z(T) are given by

$$g_{Qx}(T)=\sum_{k=1}^{K}\sum_{j=1}^{L}A\beta_{jk}\{\cos\gamma_{jk}[d_k^{-1}S_{1kQ}(\tau_{jk})+d_k^{0}\hat{S}_{1kQ}(\tau_{jk})]$$

$$-\sin\gamma_{jk}[d_k^{-1}R_{1kQ}(\tau_{jk})+d_k^{0}\hat{R}_{1kQ}(\tau_{jk})]\}+\eta_Q \quad ,$$

$$g_{Iy}(T)=\sum_{k=1}^{K}\sum_{j=1}^{L}A\beta_{jk}\{\sin\gamma_{jk}[d_k^{-1}R_{1kI}(\tau_{jk})+d_k^{0}\hat{R}_{1kI}(\tau_{jk})]$$

$$-\cos\gamma_{jk}[d_k^{-1}S_{1kI}(\tau_{jk})+d_k^{0}\hat{S}_{1kI}(\tau_{jk})]\}+\upsilon_I \quad ,$$

$$g_{Qy}(T) = \sum_{k=1}^{K}\sum_{j=1}^{L} A\beta_{jk}\{\sin\gamma_{jk}[d_k^{-1}S_{1kQ}(\tau_{jk}) + d_k^{0}\hat{S}_{1kQ}(\tau_{jk})]$$

$$-\cos\gamma_{jk}[d_k^{-1}R_{1kQ}(\tau_{jk}) + d_k^{0}\hat{R}_{1kQ}(\tau_{jk})]\} + \upsilon_Q \quad , \qquad (5.16.b)$$

where

$$R_{1kI}(\tau_{jk}) = \int_0^{\tau_{jk}} a_{kI}(s-\tau_{jk})a_{1I}(s)\cos\frac{2\pi}{4T_c}(s-\tau_{jk})\cos\frac{2\pi}{4T_c}sds$$

$$\hat{R}_{1kI}(\tau_{jk}) = \int_{\tau_{jk}}^{T} a_{kI}(s-\tau_{jk})a_{1I}(s)\cos\frac{2\pi}{4T_c}(s-\tau_{jk})\cos\frac{2\pi}{4T_c}sds$$

$$S_{1kI}(\tau_{jk}) = \int_0^{\tau_{jk}} a_{kQ}(s-\tau_{jk})a_{1I}(s)\sin\frac{2\pi}{4T_c}(s-\tau_{jk})\cos\frac{2\pi}{4T_c}sds$$

$$\hat{S}_{1kI}(\tau_{jk}) = \int_{\tau_{jk}}^{T} a_{kQ}(s-\tau_{jk})a_{1I}(s)\sin\frac{2\pi}{4T_c}(s-\tau_{jk})\cos\frac{2\pi}{4T_c}sds$$

$$R_{1kQ}(\tau_{jk}) = \int_0^{\tau_{jk}} a_{kQ}(s-\tau_{jk})a_{1Q}(s)\sin\frac{2\pi}{4T_c}(s-\tau_{jk})\sin\frac{2\pi}{4T_c}sds$$

$$\hat{R}_{1kQ}(\tau_{jk}) = \int_{\tau_{jk}}^{T} a_{kQ}(s-\tau_{jk})a_{1Q}(s)\sin\frac{2\pi}{4T_c}(s-\tau_{jk})\sin\frac{2\pi}{4T_c}sds$$

$$S_{1kQ}(\tau_{jk}) = \int_0^{\tau_{jk}} a_{kI}(s-\tau_{jk})a_{1Q}(s)\cos\frac{2\pi}{4T_c}(s-\tau_{jk})\sin\frac{2\pi}{4T_c}sds$$

$$\hat{S}_{1kQ}(\tau_{jk}) = \int_{\tau_{jk}}^{T} a_{kI}(s-\tau_{jk})a_{1Q}(s)\cos\frac{2\pi}{4T_c}(s-\tau_{jk})\sin\frac{2\pi}{4T_c}sds$$

$$\eta_I = \int_0^T n_c(s) a_{1I}(s) \cos\frac{2\pi}{4T_c} s \, ds$$

$$\eta_Q = \int_0^T n_c(s) a_{1Q}(s) \sin\frac{2\pi}{4T_c} s \, ds$$

$$\upsilon_I = \int_0^T n_s(s) a_{1I}(s) \cos\frac{2\pi}{4T_c} s \, ds$$

$$\upsilon_Q = \int_0^T n_s(s) a_{1Q}(s) \sin\frac{2\pi}{4T_c} s \, ds$$

The real part of the sampled output is given by

$$g_x(T) = g_{Ix}(T) + g_{Qx}(T)$$

$$= \sum_{k=1}^{K} \sum_{j=1}^{L} A\beta_{jk} \{\cos\gamma_{jk} [d_k^{-1} R_{1kI}(\tau_{jk}) + d_k^0 \hat{R}_{1kI}(\tau_{jk}) + d_k^{-1} S_{1kQ}(\tau_{jk}) + d_k^0 \hat{S}_{1kQ}(\tau_{jk})]$$

$$-\sin\gamma_{jk} [d_k^{-1} R_{1kQ}(\tau_{jk}) + d_k^0 \hat{R}_{1kQ}(\tau_{jk}) + d_k^{-1} S_{1kI}(\tau_{jk}) + d_k^0 \hat{S}_{1kI}(\tau_{jk})]\} + \eta_I + \eta_Q \quad .$$

(5.17.a)

The imaginary part of the sampled output is given by

$$g_y(T) = g_{Iy}(T) + g_{Qy}(T)$$

$$= \sum_{k=1}^{K} \sum_{j=1}^{L} A\beta_{jk} \{\sin\gamma_{jk} [d_k^{-1} R_{1kI}(\tau_{jk}) + d_k^0 \hat{R}_{1kI}(\tau_{jk}) + d_k^{-1} S_{1kQ}(\tau_{jk}) + d_k^0 \hat{S}_{1kQ}(\tau_{jk})]$$

$$+\cos\gamma_{jk} [d_k^{-1} R_{1kQ}(\tau_{jk}) + d_k^0 \hat{R}_{1kQ}(\tau_{jk}) + d_k^{-1} S_{1kI}(\tau_{jk}) + d_k^0 \hat{S}_{1kI}(\tau_{jk})]\} + \upsilon_I + \upsilon_Q \quad .$$

(5.17.b)

It is assumed that path 1 is the direct path. Thus without any loss of generality, $\tau_{11}=0$ and $\gamma_{11} = -\frac{\pi}{4}$ can be assumed

$$R_{11I}(\tau_{11}) = R_{11Q}(\tau_{11}) = S_{11I}(\tau_{11}) = S_{11Q}(\tau_{11}) = \hat{S}_{11I}(\tau_{11}) = \hat{S}_{11Q}(\tau_{11}) = 0\,,$$

$$\hat{R}_{11I}(\tau_{11}) = \hat{R}_{11Q}(\tau_{11}) = \frac{T}{2}\,, \quad \sin\gamma_{11} = -\frac{\sqrt{2}}{2}\,, \quad \cos\gamma_{11} = \frac{\sqrt{2}}{2}\,.$$

$$z = g_x(T) + jg_y(T)$$

$$= \frac{\sqrt{2}}{2} A\beta_{11} T d_1^0 + \sum_{k=1}^{K} [d_k^{-1} X_{kI} + d_k^0 \hat{X}_{kI} - d_k^{-1} X_{kQ} - d_k^0 \hat{X}_{kQ} + d_k^{-1} U_{kQ}$$

$$+ d_k^0 \hat{U}_{kQ} - d_k^{-1} U_{kI} - d_k^0 \hat{U}_{kI}] + \eta + j \sum_{k=1}^{K} [d_k^{-1} Y_{kI} + d_k^0 \hat{Y}_{kI} + d_k^{-1} Y_{kQ}$$

$$+ d_k^0 \hat{Y}_{kQ} + d_k^{-1} W_{kQ} + d_k^0 \hat{W}_{kQ} + d_k^{-1} W_{kI} + d_k^0 \hat{W}_{kI}] + j\upsilon \qquad (5.18)$$

where the first term in the RHS is the required signal. The other terms are the unwanted noise and interference resulting from multipath effect and other users. For k=1

$$X_{1I} = \sum_{j=2}^{L} A\beta_{j1} R_{11I}(\tau_{j1}) \cos\gamma_{j1}, \quad \hat{X}_{1I} = \sum_{j=2}^{L} A\beta_{j1} \hat{R}_{11I}(\tau_{j1}) \cos\gamma_{j1},$$

$$X_{1Q} = \sum_{j=2}^{L} A\beta_{j1} R_{11Q}(\tau_{j1}) \sin\gamma_{j1}, \quad \hat{X}_{1Q} = \sum_{j=2}^{L} A\beta_{j1} \hat{R}_{11Q}(\tau_{j1}) \sin\gamma_{j1},$$

$$Y_{1I} = \sum_{j=2}^{L} A\beta_{j1} R_{11I}(\tau_{j1}) \sin\gamma_{j1}, \quad \hat{Y}_{1I} = \sum_{j=2}^{L} A\beta_{j1} \hat{R}_{11I}(\tau_{j1}) \sin\gamma_{j1},$$

$$Y_{1Q} = \sum_{j=2}^{L} A\beta_{j1} R_{11Q}(\tau_{j1}) \cos\gamma_{j1}, \quad \hat{Y}_{1Q} = \sum_{j=2}^{L} A\beta_{j1} \hat{R}_{11Q}(\tau_{j1}) \cos\gamma_{j1},$$

$$U_{1Q} = \sum_{j=2}^{L} A\beta_{j1} S_{11Q}(\tau_{j1}) \cos\gamma_{j1}, \quad \hat{U}_{1Q} = \sum_{j=2}^{L} A\beta_{j1} \hat{S}_{11Q}(\tau_{j1}) \cos\gamma_{j1},$$

$$U_{1I} = \sum_{j=2}^{L} A\beta_{j1} S_{11I}(\tau_{j1}) \sin\gamma_{j1}, \quad \hat{U}_{1I} = \sum_{j=2}^{L} A\beta_{j1} \hat{S}_{11I}(\tau_{j1}) \sin\gamma_{j1},$$

$$W_{1Q} = \sum_{j=2}^{L} A\beta_{j1} S_{11Q}(\tau_{j1}) \sin\gamma_{j1}, \quad \hat{W}_{1Q} = \sum_{j=2}^{L} A\beta_{j1} \hat{S}_{11Q}(\tau_{j1}) \sin\gamma_{j1},$$

$$W_{1I} = \sum_{j=2}^{L} A\beta_{j1} S_{11I}(\tau_{j1}) \cos\gamma_{j1}, \quad \hat{W}_{1I} = \sum_{j=2}^{L} A\beta_{j1} \hat{S}_{11I}(\tau_{j1}) \cos\gamma_{j1}.$$

for $k \geq 2$

$$X_{kI} = \sum_{j=1}^{L} A\beta_{jk} R_{1kI}(\tau_{jk}) \cos\gamma_{jk}, \quad \hat{X}_{kI} = \sum_{j=1}^{L} A\beta_{jk} \hat{R}_{1kI}(\tau_{jk}) \cos\gamma_{jk},$$

$$X_{kQ} = \sum_{j=1}^{L} A\beta_{jk} R_{1kQ}(\tau_{jk}) \sin\gamma_{jk}, \quad \hat{X}_{kQ} = \sum_{j=1}^{L} A\beta_{jk} \hat{R}_{1kQ}(\tau_{jk}) \sin\gamma_{jk},$$

$$Y_{kI} = \sum_{j=1}^{L} A\beta_{jk} R_{1kI}(\tau_{jk}) \sin\gamma_{jk}, \quad \hat{Y}_{kI} = \sum_{j=1}^{L} A\beta_{jk} \hat{R}_{1kI}(\tau_{jk}) \sin\gamma_{jk},$$

$$Y_{kQ} = \sum_{j=1}^{L} A\beta_{jk} R_{1kQ}(\tau_{jk}) \cos\gamma_{jk}, \quad \hat{Y}_{kQ} = \sum_{j=1}^{L} A\beta_{jk} \hat{R}_{1kQ}(\tau_{jk}) \cos\gamma_{jk},$$

$$U_{kQ} = \sum_{j=1}^{L} A\beta_{jk} S_{1kQ}(\tau_{jk}) \cos\gamma_{jk}, \quad \hat{U}_{kQ} = \sum_{j=1}^{L} A\beta_{jk} \hat{S}_{1kQ}(\tau_{jk}) \cos\gamma_{jk},$$

$$U_{kI} = \sum_{j=1}^{L} A\beta_{jk} S_{1kI}(\tau_{jk}) \sin\gamma_{jk}, \quad \hat{U}_{kI} = \sum_{j=1}^{L} A\beta_{jk} \hat{S}_{1kI}(\tau_{jk}) \sin\gamma_{jk},$$

$$W_{kQ} = \sum_{j=1}^{L} A\beta_{jk} S_{1kQ}(\tau_{jk}) \sin\gamma_{jk}, \quad \hat{W}_{kQ} = \sum_{j=1}^{L} A\beta_{jk} \hat{S}_{1kQ}(\tau_{jk}) \sin\gamma_{jk},$$

$$W_{kI} = \sum_{j=1}^{L} A\beta_{jk} S_{1kI}(\tau_{jk}) \cos\gamma_{jk}, \quad \hat{W}_{kI} = \sum_{j=1}^{L} A\beta_{jk} \hat{S}_{1kI}(\tau_{jk}) \cos\gamma_{jk}, \tag{5.19}$$

The fading is assumed to be slow compared to the data rate, so that the complex envelope and phase do not vary between the two sampling instants. Only data bits change

between the two sampling instants. The two sampled outputs z_1 and z_2 for the adjacent data bits d^0 and d^{-1} are given by

$$z_1 = \frac{\sqrt{2}}{2} A\beta_{11} T d_1^0 + \sum_{k=1}^{K} [d_k^{-1}(X_{kI} - X_{kQ} + U_{kQ} - U_{kI}) + d_k^0(\hat{X}_{kI} - \hat{X}_{kQ} + \hat{U}_{kQ} - \hat{U}_{kI})] + \eta$$

$$+ j \sum_{k=1}^{K} [d_k^{-1}(Y_{kI} + Y_{kQ} + W_{kQ} + W_{kI}) + d_k^0(\hat{Y}_{kI} + \hat{Y}_{kQ} + \hat{W}_{kQ} + \hat{W}_{kI})] + j\upsilon \tag{5.20}$$

$$z_2 = \frac{\sqrt{2}}{2} A\beta_{11} T d_1^{-1} + \sum_{k=1}^{K} [d_k^{-2}(X_{kI} - X_{kQ} + U_{kQ} - U_{kI}) + d_k^{-1}(\hat{X}_{kI} - \hat{X}_{kQ} + \hat{U}_{kQ} - \hat{U}_{kI})] + \eta$$

$$+ j \sum_{k=1}^{K} [d_k^{-2}(Y_{kI} + Y_{kQ} + W_{kQ} + W_{kI}) + d_k^{-1}(\hat{Y}_{kI} + \hat{Y}_{kQ} + \hat{W}_{kQ} + \hat{W}_{kI})] + j\upsilon \tag{5.21}$$

Finally with inputs z_1 and z_2, the differential detector output ξ is given by

$$\xi = \mathrm{Re}[\, z_1 z_2^* \,] = \frac{1}{2} [\, z_1 z_2^* + z_1^* z_2 \,] \tag{5.22}$$

This output is the decision variable used in statistical decision process. Assuming d_1^0 and d_1^{-1} to be 1, the error occurs when $\xi < 0$. So that the probability of error P_e is given by

$$P_e = P\{\xi < 0\} = \int_{-\infty}^{0} p(\xi)\, d\xi \tag{5.23}$$

where $p(\xi)$ is the probability density function of ξ.

For given values of delays $\{\tau_{jk}\}$, the random variables X_{kI}, $\hat{X}_{kI}$, X_{kQ}, $\hat{X}_{kQ}$, Y_{kI}, $\hat{Y}_{kI}$, Y_{kQ}, $\hat{Y}_{kQ}$, U_{kI}, $\hat{U}_{kI}$, U_{kQ}, $\hat{U}_{kQ}$, W_{kI}, $\hat{W}_{kI}$, W_{kQ},and $\hat{W}_{kQ}$ are zero-mean Gaussian for all k [15], and are all independent of one another, except pairs $(X_{kI}, \hat{X}_{kI})$, . . ., $(W_{kQ}, \hat{W}_{kQ})$. Finally, if X is a zero-mean Gaussian random variable and

d_k^j is a random variable that takes a value of +1 or -1 with equal probability, the random variable $d_k^j X$ is also zero-mean Gaussian with same variance as X [15]. So for a given delay, the white noise and interference terms in z_1 and z_2 are also Gaussian. In the next two sections diversity is incorporated and a final expression for the BER with diversity is obtained.

5.2.1 Selection diversity

The concept of selection diversity was mentioned in Chapter 4. Selection diversity implies selecting the maximum from M decision variables, i.e., $\xi_{max}^M = \max \xi_i$, where $\{\xi_i, i = 1,2, ..., M\}$.

In a selection diversity receiver M decision variables, $\xi_1,\xi_2,..., \xi_M$, can be obtained from M independent channels. As the noise and interference terms of the M demodulated signals have same mean values, ξ_{max}^M corresponds to the demodulated signal with the largest value of β_{11}, denoted by β_{max}. Thus, for various values of M, β_{max} is the only random variable whose density changes with M. As ξ is a function of β^2, ξ_{max}^M is a function of β_{max}^2. The probability density of β_{max}^2 is given by [15][16]

$$f_{\beta_{max}^2}(y) = \sum_{i=0}^{M-1} \binom{M-1}{i} \frac{(-1)^i}{2(i+1)\rho_i} e^{-\frac{y}{2\rho_i}} \qquad \text{for } y \geq 0 \tag{5.24}$$

where $\rho_i = \frac{\rho}{i+1}$, and $\rho = \frac{1}{2} E\{\beta^2\}$.

Delay $\{\tau_{jk}\}$, β_{max} and L are given by equations (5.20) and (5.21). From [16,Appendix 4B, eqs. (4B.1), (4B.6), (4B.21), and (4B.22)], the probability of error for a given $\{\tau_{jk}\}$, L and β_{max} is given by

$$P_{e|\beta_{max}, \{\tau_{jk}\}, L} = Q(a,b) - \frac{1}{2}\left(1 + \frac{\mu_{12}}{\sqrt{\mu_1\mu_2}}\right) I_0(ab) \exp\left(-\frac{a^2+b^2}{2}\right), \tag{5.25}$$

where Q(a,b) is the Marcum Q-function, $I_0(ab)$ is the Bessel function of the first kind [16], and

$$a = \frac{|m|}{\sqrt{2}}\left[\frac{1}{\sqrt{\mu_1}} - \frac{1}{\sqrt{\mu_2}}\right], \qquad b = \frac{|m|}{\sqrt{2}}\left[\frac{1}{\sqrt{\mu_1}} + \frac{1}{\sqrt{\mu_2}}\right]$$

$$|m| = |E\{z_1 | \beta_{max}, d_1^0\}| = |E\{z_2 | \beta_{max}, d_1^{-1}\}| = \frac{\sqrt{2}}{2} A \beta_{max} T ,$$

$$\mu_1 = \mathrm{Var}\{z_1 | \{\tau_{jk}\}, L\} = E\{|z_1 - m|^2 | \{\tau_{jk}\}, L\}$$

$$= E\left\{ \sum_{k=1}^{K} [X_{kI}^2 + X_{kQ}^2 + \hat{X}_{kI}^2 + \hat{X}_{kQ}^2 + U_{kI}^2 + U_{kQ}^2 + \hat{U}_{kI}^2 + \hat{U}_{kQ}^2 + Y_{kI}^2 + Y_{kQ}^2 + \hat{Y}_{kI}^2 + \hat{Y}_{kQ}^2 \right.$$

$$\left. + W_{kI}^2 + W_{kQ}^2 + \hat{W}_{kI}^2 + \hat{W}_{kQ}^2] | \{\tau_{jk}\}, L \right\} + 2\sigma_n^2 + E\{X_{1I}\hat{X}_{1I} + X_{1Q}\hat{X}_{1Q}$$

$$+ Y_{1I}\hat{Y}_{1I} + Y_{1Q}\hat{Y}_{1Q} + U_{1I}\hat{U}_{1I} + U_{1Q}\hat{U}_{1Q} + W_{1I}\hat{W}_{1I} + W_{1Q}\hat{W}_{1Q} | \{\tau_{jk}\}, L\} ,$$

$$\mu_2 = \mathrm{Var}\{z_2 | \{\tau_{jk}\}, L\} = E\{|z_2 - m|^2 | \{\tau_{jk}\}, L\}$$

$$= E\left\{ \sum_{k=1}^{K} [X_{kI}^2 + X_{kQ}^2 + \hat{X}_{kI}^2 + \hat{X}_{kQ}^2 + U_{kI}^2 + U_{kQ}^2 + \hat{U}_{kI}^2 + \hat{U}_{kQ}^2 + Y_{kI}^2 + Y_{kQ}^2 + \hat{Y}_{kI}^2 + \hat{Y}_{kQ}^2 \right.$$

$$\left. + W_{kI}^2 + W_{kQ}^2 + \hat{W}_{kI}^2 + \hat{W}_{kQ}^2] | \{\tau_{jk}\}, L \right\} + 2\sigma_n^2 ,$$

$$\mu_{12} = E\{(z_1 - m)(z_2 - m)^* | \{\tau_{jk}\}, L\}$$

$$= E\left\{ \sum_{k=1}^{K} [X_{kI}\hat{X}_{kI} + X_{kQ}\hat{X}_{kQ} + Y_{kI}\hat{Y}_{kI} + Y_{kQ}\hat{Y}_{kQ} + U_{kI}\hat{U}_{kI} + U_{kQ}\hat{U}_{kQ} + W_{kI}\hat{W}_{kI} \right.$$

$$\left. + W_{kQ}\hat{W}_{kQ}] + \hat{X}_{1I} + \hat{X}_{1Q} + \hat{Y}_{1I} + \hat{Y}_{1Q} + \hat{U}_{1I} + \hat{U}_{1Q} + \hat{W}_{1I} + \hat{W}_{1Q} | \{\tau_{jk}\}, L \right\} ,$$

$$E\{\hat{X}_{1I}^2 \mid \{\tau_{j1}\},L\} = E\{Y_{1I}^2 \mid \{\tau_{j1}\},L\} = \sum_{j=2}^{L} A^2 \hat{R}_{11I}^2(\tau_{j1})\rho_{j1} ,$$

$$E\{X_{1I}^2 \mid \{\tau_{j1}\},L\} = E\{Y_{1I}^2 \mid \{\tau_{j1}\},L\} = \sum_{j=2}^{L} A^2 R_{11I}^2(\tau_{j1})\rho_{j1} ,$$

$$E\{\hat{X}_{1Q}^2 \mid \{\tau_{j1}\},L\} = E\{Y_{1Q}^2 \mid \{\tau_{j1}\},L\} = \sum_{j=2}^{L} A^2 \hat{R}_{11Q}^2(\tau_{j1})\rho_{j1} ,$$

$$E\{X_{1Q}^2 \mid \{\tau_{j1}\},L\} = E\{Y_{1Q}^2 \mid \{\tau_{j1}\},L\} = \sum_{j=2}^{L} A^2 R_{11Q}^2(\tau_{j1})\rho_{j1} ,$$

$$E\{\hat{U}_{1I}^2 \mid \{\tau_{j1}\},L\} = E\{\hat{W}_{1I}^2 \mid \{\tau_{j1}\},L\} = \sum_{j=2}^{L} A^2 \hat{S}_{11I}^2(\tau_{j1})\rho_{j1} ,$$

$$E\{U_{1I}^2 \mid \{\tau_{j1}\},L\} = E\{W_{1I}^2 \mid \{\tau_{j1}\},L\} = \sum_{j=2}^{L} A^2 S_{11I}^2(\tau_{j1})\rho_{j1} ,$$

$$E\{\hat{U}_{1Q}^2 \mid \{\tau_{j1}\},L\} = E\{\hat{W}_{1Q}^2 \mid \{\tau_{j1}\},L\} = \sum_{j=2}^{L} A^2 \hat{S}_{11Q}^2(\tau_{j1})\rho_{j1} ,$$

$$E\{U_{1Q}^2 \mid \{\tau_{j1}\},L\} = E\{W_{1Q}^2 \mid \{\tau_{j1}\},L\} = \sum_{j=2}^{L} A^2 S_{11Q}^2(\tau_{j1})\rho_{j1} ,$$

$$E\{X_{kI}^2 \mid \{\tau_{jk}\},L\} = E\{Y_{kI}^2 \mid \{\tau_{jk}\},L\} = \sum_{j=1}^{L} A^2 R_{1kI}^2(\tau_{jk})\rho_{jk} ,$$

$$E\{X_{kQ}^2 \mid \{\tau_{jk}\},L\} = E\{Y_{kQ}^2 \mid \{\tau_{jk}\},L\} = \sum_{j=1}^{L} A^2 R_{1kQ}^2(\tau_{jk})\rho_{jk} ,$$

$$E\{\hat{X}_{kI}^2 \mid \{\tau_{jk}\},L\} = E\{\hat{Y}_{kI}^2 \mid \{\tau_{jk}\},L\} = \sum_{j=1}^{L} A^2 \hat{R}_{1kI}^2(\tau_{jk})\rho_{jk} ,$$

$$E\{\hat{X}_{kQ}^2 \mid \{\tau_{jk}\},L\} = E\{\hat{Y}_{kQ}^2 \mid \{\tau_{jk}\},L\} = \sum_{j=1}^{L} A^2 \hat{R}_{1kQ}^2(\tau_{jk})\rho_{jk} ,$$

$$E\{U_{kI}^2 \mid \{\tau_{jk}\},L\} = E\{W_{kI}^2 \mid \{\tau_{jk}\},L\} = \sum_{j=1}^{L} A^2 S_{1kI}^2(\tau_{jk})\rho_{jk} ,$$

$$E\{U_{kQ}^2 \mid \{\tau_{jk}\},L\} = E\{W_{kQ}^2 \mid \{\tau_{jk}\},L\} = \sum_{j=1}^{L} A^2 S_{1kQ}^2(\tau_{jk})\rho_{jk} ,$$

$$E\{\hat{U}_{kI}^2 \mid \{\tau_{jk}\},L\} = E\{\hat{W}_{kI}^2 \mid \{\tau_{jk}\},L\} = \sum_{j=1}^{L} A^2 \hat{S}_{1kI}^2(\tau_{jk})\rho_{jk} ,$$

$$E\{\hat{U}_{kQ}^2 \mid \{\tau_{jk}\},L\} = E\{\hat{W}_{kQ}^2 \mid \{\tau_{jk}\},L\} = \sum_{j=1}^{L} A^2 \hat{S}_{1kQ}^2(\tau_{jk})\rho_{jk} ,$$

$$E\{X_{kI}\hat{X}_{kI} \mid \{\tau_{jk}\},L\} = E\{Y_{kI}\hat{Y}_{kI} \mid \{\tau_{jk}\},L\} = \sum_{j=1}^{L} A^2 R_{1kI}\hat{R}_{1kI}(\tau_{jk})\rho_{jk} ,$$

$$E\{X_{kQ}\hat{X}_{kQ} \mid \{\tau_{jk}\},L\} = E\{Y_{kQ}\hat{Y}_{kQ} \mid \{\tau_{jk}\},L\} = \sum_{j=1}^{L} A^2 R_{1kQ}\hat{R}_{1kQ}(\tau_{jk})\rho_{jk} ,$$

$$E\{U_{kI}\hat{U}_{kI} \mid \{\tau_{jk}\},L\} = E\{W_{kI}\hat{W}_{kI} \mid \{\tau_{jk}\},L\} = \sum_{j=1}^{L} A^2 S_{1kI}\hat{S}_{1kI}(\tau_{jk})\rho_{jk} ,$$

$$E\{U_{kQ}\hat{U}_{kQ} \mid \{\tau_{jk}\},L\} = E\{W_{kQ}\hat{W}_{kQ} \mid \{\tau_{jk}\},L\} = \sum_{j=1}^{L} A^2 S_{1kQ}\hat{S}_{1kQ}(\tau_{jk})\rho_{jk} .$$

Generally, the third term in μ_1 is very small compared with the other terms. This term can be neglected, so that

$\mu_1=\mu_2$

$a=0$

$I_0(ab)=1$

$Q(a,b) = \exp(-\frac{b^2}{2})$

And the error probability in eq. (5.28) becomes

$$P_{e|\beta_{max},\{\tau_{jk}\},L} = \frac{1}{2}\left(1 - \frac{\mu_{12}}{\mu_2}\right)\exp\left(-\frac{m^2}{\mu_2}\right). \qquad (5.26)$$

For L=1, $X_{1I}=\hat{X}_{1I}=X_{1Q}=\hat{X}_{1Q}=Y_{1I}=\hat{Y}_{1I}=Y_{1Q}=\hat{Y}_{1Q}=U_{1I}=\hat{U}_{1I}=U_{1Q}=\hat{U}_{1Q}=W_{1I}=\hat{W}_{1I}=W_{1Q}=\hat{W}_{1Q}=0$. In this case eq. (5.26) is exact. When L>1, and K>2, eq.(5.26) is approximate as the last term was neglected.

This error rate is a function of β_{max}, $\{\tau_{jk}\}$, and L. Next the unconditional bit error probability is derived by removing the conditioning with respect to these parameters.

1) The first step in this process is the removal of conditioning on β_{max}

The conditional error probability $P_e \mid \beta_{max},\{\tau_{jk}\},L$ is a function of β_{max}^2, not β_{max}. The probability density function of β_{max}^2 is given by eq. (5.23). The bit error probability without conditioning on β_{max} is given by

$$P_{e|\{\tau_{jk}\},L} = \int_0^\infty P_{e|\beta_{jk},\{\tau_{jk}\},L}\; f_{\beta_{max}^2}(y)\,dy$$

$$= \frac{1}{2}\sum_{i=0}^{M-1}\binom{M-1}{i}\frac{(-1)^i}{(i+1)}\frac{\mu_2-\mu_{12}}{A^2T^2\rho_i+\mu_2}. \qquad (5.27)$$

For L=1, K=2

$$P_{e|\{\tau_{12}\}} = \frac{1}{2}\sum_{i=0}^{M-1}\binom{M-1}{i}\frac{(-1)^i}{(i+1)}\frac{\mu_2-\mu_{12}}{A^2T^2\rho_i+\mu_2} \qquad (5.28)$$

2) The second step is the removal of conditioning on τ_{jk}

For L>1, K>2, the error probability is a function of (LK-1) variables, τ_{12}, τ_{13}, ..., τ_{1k}, ..., τ_{L1}, τ_{L2}, ..., τ_{LK}. The removal of conditioning on $\{\tau_{jk}\}$ requires repeated integration over these (LK-1) variables. The computation can become very complex. Fortunately, the computation can be greatly simplified by using Monte Carlo

approximation. A brief discussion about this method is included in Section 5.3. To keep the analysis simple only the case L=1, K=2 is considered here. This is a non-multipath case, and there are only two users in a system. So only two time delays τ_{11} and τ_{12} are present. As τ_{11} was assumed to be zero; τ_{12} which is uniformly distributed over (0,T) need only be considered. The probability of error P_e in this case is given by

$$P_e = \int_0^T P_{e|\{\tau_{12}\}} f_{\tau_{12}}(\tau_{12})\, d\tau_{12}$$

$$= \frac{1}{2T} \sum_{i=0}^{M-1} \binom{M-1}{i} \frac{(-1)^i}{(i+1)} \int_0^T \frac{\mu_2 - \mu_{12}}{A^2T^2\rho_i + \mu_2} d\tau_{12} \qquad (5.29)$$

5.2.2 Predetection combining diversity

In Chapter 4, predetection combining diversity was introduced. This diversity combines different versions of the same signal before detection. Considering M independent channels, the decision variable in this case is given by

$$\xi_c = \frac{1}{2} \sum_{i=1}^{M} (z_{1i}\, z_{2i}^* + z_{1i}^*\, z_{2i}) = \mathrm{Re}\left[\sum_{i=1}^{M} (z_{1i}\, z_{2i}^*) \right] \qquad (5.30a)$$

where z_{1i} and z_{2i} are same as in selection diversity.

Further assume that the sum of interference and noise in z_{1i} is Gaussian and is denoted by N_{1i}, the sum of interference and noise in z_{2i} is Gaussian, and is denoted by N_{2i}. N_{1i} is independent of N_{2i} for each i, (N_{1i},N_{2i}) pair is independent of the pair (N_{1j},N_{2j}) for $i \neq j$ [8]. The decision variable under this assumption may be written as [8]

$$\xi_c = \mathrm{Re}\left[\sum_{i=1}^{M} \left(\frac{\sqrt{2}}{2} A\beta_i T d_1^0 + N_{1i} \right) \left(\frac{\sqrt{2}}{2} A\beta_i T d_1^{-1} + N_{2i} \right)^* \right] \qquad (5.30b)$$

The bit error probability in this case is given by [16, eq.(7.4.26)]

$$P_e = \frac{1}{2^{2M-1}(M-1)!\,(1+\lambda_c)^M} \sum_{i=0}^{M-1} C_i\,(M-1+i)! \left(\frac{\lambda_c}{1+\lambda_c}\right)^i \tag{5.31}$$

where $C_i = \frac{1}{i!} \sum_{n=0}^{M-1-i} \binom{2M-1}{n}$, λ_c is average channel signal-to-noise ratio is defined as

$$\lambda_c = \frac{\text{mean signal power}}{\text{interference power + noise power}}.$$

Mean signal power $= E^2\{z_1\} = E^2\{z_1\} = \frac{1}{2} A^2 \beta_i^2 T^2$, and

Interference power + noise power $= E\{|N_{1i}|^2\} = E\{|N_{2i}|^2\}$.

5.3 Monte Carlo approximation method

Monte Carlo method is a numerical computation method which is quite useful for computing integrals with non well behaved integrand. There are two simple techniques for computing one dimensional integrals. One is "the hit or miss Monte Carlo method", another is "the sample-mean Monte Carlo method". The latter method, which is more efficient than the former one [17], is used in this thesis. Only this method is discussed.

5.3.1 Sample-mean Monte Carlo method

In sample-mean method, a complex integral is obtained by computing the sample-mean of the integrand. Consider an integral expressed as

$$\Pi = \int_a^b g(x)\,dx \tag{5.32}$$

The integral is difficult to compute when g(x) is not well behaved. The integral is approximated by an expectation given by

$$\Pi = \int_a^b \frac{g(x)}{f_X(x)} f_X(x)\, dx = E\left\{ \frac{g(X)}{f_X(X)} \right\} \tag{5.33}$$

where $f_X(x)$ is probability density of X and $f_X(x)>0$ when $g(x)\neq 0$.

Assuming that X is a uniform random variable in (a,b), $f_X(x)$ is given by

$$f_X(x) = \begin{cases} \frac{1}{a-b} & a \le x \le b \\ 0 & \text{otherwise} \end{cases} \tag{5.34}$$

Then

$$\Pi = (b-a)\, E\{g(X_n)\} \tag{5.35}$$

To compute $E\{g(X)\}$, g(x) is sampled randomly in (a,b). An approximation for Π is given by

$$\Pi \approx (b-a) \frac{1}{N} \sum_{n=1}^{N} g(X_n) \tag{5.36}$$

where N is a number of the samples.

Computation of eq.(5.36) is much simpler than that of eq. (5.32) for non well behaved g(x).

5.3.2 Sample-mean method approximation for the system performance

In Section 5.2, the expressions of bit error rate were developed for both selection diversity and predetection diversity methods. The integral in eq.(5.29) for P_e is given by

$$I = \int_0^T \frac{\mu_2(\tau) - \mu_{12}(\tau)}{A^2T^2\rho_i + \mu_2(\tau)}\, d\tau$$

A comparison of this expression with eq.(5.32) yields a=0, b=T, $g(\tau)=\frac{\mu_2(\tau)-\mu_{12}(\tau)}{A^2T^2\rho_i+\mu_2(\tau)}$,

and the integral can be approximated by

$$I \approx T\,\frac{1}{N}\sum_{n=1}^{N} g(\tau_n)$$

Hence the bit error rate for L=1, K=2 is approximated by

$$P_e \approx \frac{1}{2N}\sum_{i=0}^{M-1}\binom{M-1}{i}\frac{(-1)^i}{(i+1)}\sum_{n=1}^{N} g(\tau_n) \qquad (5.37)$$

This simplifies the computation considerably. The accuracy achieved depends on the number of samples used. Equation (5.37) is used for computation of bit error rate results in the next chapter. Even though eq. (5.37) is an approximation the accuracy is sufficient [8]. The computed results are presented in the next chapter.

Chapter 6

Computed Bit-Error-Rate Performance

In this chapter, computed BER results for an indoor mobile radio channel are presented. Two kinds of spreading codes, namely Gold code and Kasami code are considered. Similarly two kinds of diversity techniques, selection diversity and predetection combining diversity are considered. The results for different codes and different diversity methods are compared. The performance of a system with DMSK is also compared with that for DPSK system reported before in literature [8].

6.1 Error performance with selection diversity

An analysis for P_e computation for this case was developed in the last chapter. Random variables L, β_{jk}, τ_{jk}, and γ_{jk}, are used to characterize the mobile channel.

As γ_{jk} is assumed to be uniformly distributed over $[0, 2\pi]$, $E\{\cos^2\gamma_{jk}\} = E\{\sin^2\gamma_{jk}\} = \frac{1}{2}$. This removes the need for considering γ_{jk} in the computation.

The time delay associated with each path was assumed to be uniformly distributed over [0,T]. The delays were also assumed to be independent of one another. In practice the delays are much smaller than the bit period and (0,T) distribution is not strictly right. However this assumption makes the computation simple and tractable, and a similar assumption was made in the DPSK system analysis [8].

In the error probability expression, path gain β_{jk} is replaced by ρ_{jk}, which is half of the mean square value of β_{jk}. It is assumed that ρ_{jk} is same for all paths and users, and can be thus denoted by ρ. This is a reasonable assumption because the variables in the set

$\{\beta_{jk}\}$ are independent and can be assumed to be identically distributed approximately. This parameter essentially determines the coverage area of each star-configured cell. The signals and interference are affected alike. A value of ρ=0.019 was assumed. Once again this is same as that used in [8] for DPSK system.

The number of paths L was assumed to be same between all transmitters and receivers.

For sake of convenience eq. (5.37) is reproduced here as eq. (6.1) and (6.2).

$$P_e \approx \frac{1}{2N} \sum_{i=0}^{M-1} \binom{M-1}{i} \frac{(-1)^i}{(i+1)} \sum_{n=1}^{N} g(\tau_n) \tag{6.1}$$

$$g(\tau_n) = \frac{\mu_2(\tau_n) - \mu_{12}(\tau_n)}{A^2T^2\rho_i + \mu_2(\tau_n)}$$

$$= \frac{2A^2\rho\,[\,R_{12I}^2(\tau_n) + \hat{R}_{12I}^2(\tau_n) + R_{12Q}^2(\tau_n) + \hat{R}_{12Q}^2(\tau_n) + S_{12I}^2(\tau_n) + \hat{S}_{12I}^2(\tau_n)}{A^2T^2\rho_i + 2A^2\rho\,[\,R_{12I}^2(\tau_n) + \hat{R}_{12I}^2(\tau_n)}$$

$$\frac{+\,S_{12Q}^2(\tau_n) + \hat{S}_{12Q}^2(\tau_n) - R_{12I}(\tau_n)\hat{R}_{12I}(\tau_n) - R_{12Q}(\tau_n)\hat{R}_{12Q}(\tau_n)}{+\,R_{12Q}^2(\tau_n) + \hat{R}_{12Q}^2(\tau_n) + S_{12I}^2(\tau_n) + \hat{S}_{12I}^2(\tau_n)}$$

$$\frac{-\,S_{12I}(\tau_n)\hat{S}_{12I}(\tau_n) - S_{12Q}(\tau_n)\hat{S}_{12Q}(\tau_n)\,] + 2\sigma_n^2}{+\,S_{12Q}^2(\tau_n) + \hat{S}_{12Q}^2(\tau_n)\,] + 2\sigma_n^2} \tag{6.2a}$$

Let $\rho_i = \frac{\rho}{1+i}$, $\frac{N_0}{T} = \sigma_n^2$, $E_b = \frac{A^2T}{2}$, $\alpha = \frac{E_b}{N_0} = \frac{A^2T}{2N_0}$.

Then

$$g(\tau_n) = \frac{\frac{2\alpha}{T^2}\rho\,[\qquad\qquad\qquad\qquad\qquad]+1}{\frac{2\alpha}{T^2}\rho\,[\qquad\qquad\qquad\qquad]+\alpha\frac{\rho}{1+i}+1} \tag{6.2b}$$

where the contents in [ ] in eq. (6.2b) are same as these in [ ] in eq. (6.2a).

Evidently, to calculate $g(\tau_n)$, $R_{12I}(\tau_n)$, $\hat{R}_{12I}(\tau_n)$, ..., $S_{12Q}(\tau_n)$, $\hat{S}_{12Q}(\tau_n)$ etc. have to be calculated. R and S represent correlation functions of two half-sinusoid sequences, and can be expressed in terms of the correlation functions of code sequences as.

$$R_{12I}(\tau) = C_{12I}\left(n - \frac{N}{2}\right) | A_2 | + C_{12I}\left(n - \frac{N}{2} + 1\right) | A_1 |$$

$$\hat{R}_{12I}(\tau) = C_{12I}(n) | A_2 | + C_{12I}(n+1) | A_1 | \tag{6.3a}$$

where

$$C_{12I}(m) = \begin{cases} \sum_{i=0}^{\frac{N}{2}-1-m} a_{2I}^{i}\, a_{1I}^{i+m} & 0 \le m \le \frac{N}{2}-1 \\ \sum_{i=0}^{\frac{N}{2}-1+m} a_{2I}^{i-m}\, a_{1I}^{i} & -(\frac{N}{2}-1) \le m < 0 \\ 0 & \text{otherwise} \end{cases}$$

Similarly for the Q correlation functions

$$R_{12Q}(\tau) = C_{12Q}\left(n - \frac{N}{2}\right) | A_2 | + C_{12Q}\left(n - \frac{N}{2} + 1\right) | A_1 |$$

$$\hat{R}_{12Q}(\tau) = C_{12Q}(n) | A_2 | + C_{12Q}(n+1) | A_1 | \tag{6.3b}$$

where

$$C_{12Q}(m) = \begin{cases} \sum_{i=0}^{\frac{N}{2}-1-m} a_{2Q}^{i}\, a_{1Q}^{i+m} & 0 \le m \le \frac{N}{2}-1 \\ \sum_{i=0}^{\frac{N}{2}-1+m} a_{2Q}^{i-m}\, a_{1Q}^{i} & -(\frac{N}{2}-1) \le m < 0 \\ 0 & \text{otherwise} \end{cases}$$

Similarly 'S' terms may be expressed as

$$S_{12I}(\tau) = S_{12Q}(\tau) = C_{12IQ}\left(n - \frac{N}{2}\right) |A_4| + C_{12IQ}\left(n - \frac{N}{2} + 1\right) |A_3|$$

$$\hat{S}_{12I}(\tau) = \hat{S}_{12Q}(\tau) = C_{12IQ}(n) |A_4| + C_{12IQ}(n+1) |A_3| \qquad (6.3c)$$

where

$$C_{12IQ}(m) = \begin{cases} \sum_{i=0}^{\frac{N}{2}-1-m} a_{2I}^{i}\, a_{1Q}^{i+m} & 0 \le m \le \frac{N}{2}-1 \\ \sum_{i=0}^{\frac{N}{2}-1+m} a_{2I}^{i-m}\, a_{1Q}^{i} & -(\frac{N}{2}-1) \le m < 0 \\ 0 & \text{otherwise} \end{cases}$$

Where $|A_1|$, $|A_2|$, $|A_3|$, and $|A_4|$ are calculated in Appendix A. Functions $C_{12I}(m)$, $C_{12Q}(m)$, and $C_{12IQ}(m)$ are the discrete aperiodic correlation function of the chip sequences $\{a_{1I}^{i}\}$ and $\{a_{2I}^{j}\}$, $\{a_{1Q}^{i}\}$ and $\{a_{2Q}^{j}\}$, and $\{a_{1I}^{i}\}$ and $\{a_{2Q}^{j}\}$ for $j \neq i$ respectively.

To facilitate a comparison with the BER the results reported in [8] for DPSK, the data rate and code length were assumed to be 25 KHz, and 255 respectively which are same as in [8].

The computed BER results for both Gold and Kasami codes are presented in the next section.

6.1.1 Gold code as the spreading code

BER results for this case are shown in Fig.6.1 as a function of the bit energy to noise spectral density ratio, E_b/N_0. The number of paths L is equal to 1 and the number of users K=2. The results are shown for no diversity (M=1) and dual selection diversity M=2.

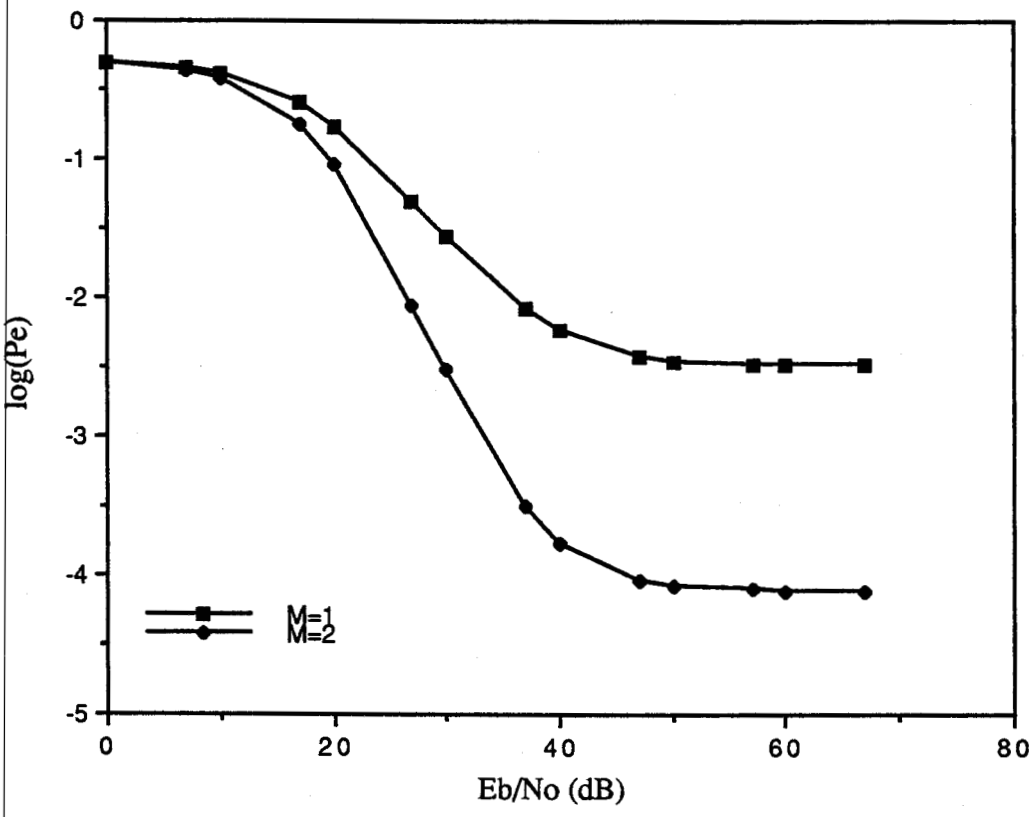

Fig.6.1 The performance of DMSK with selection diversity for K=2, L=1

In Fig.6.2 Gold code BER performance is presented for K=15, and L=4 for four values of M.

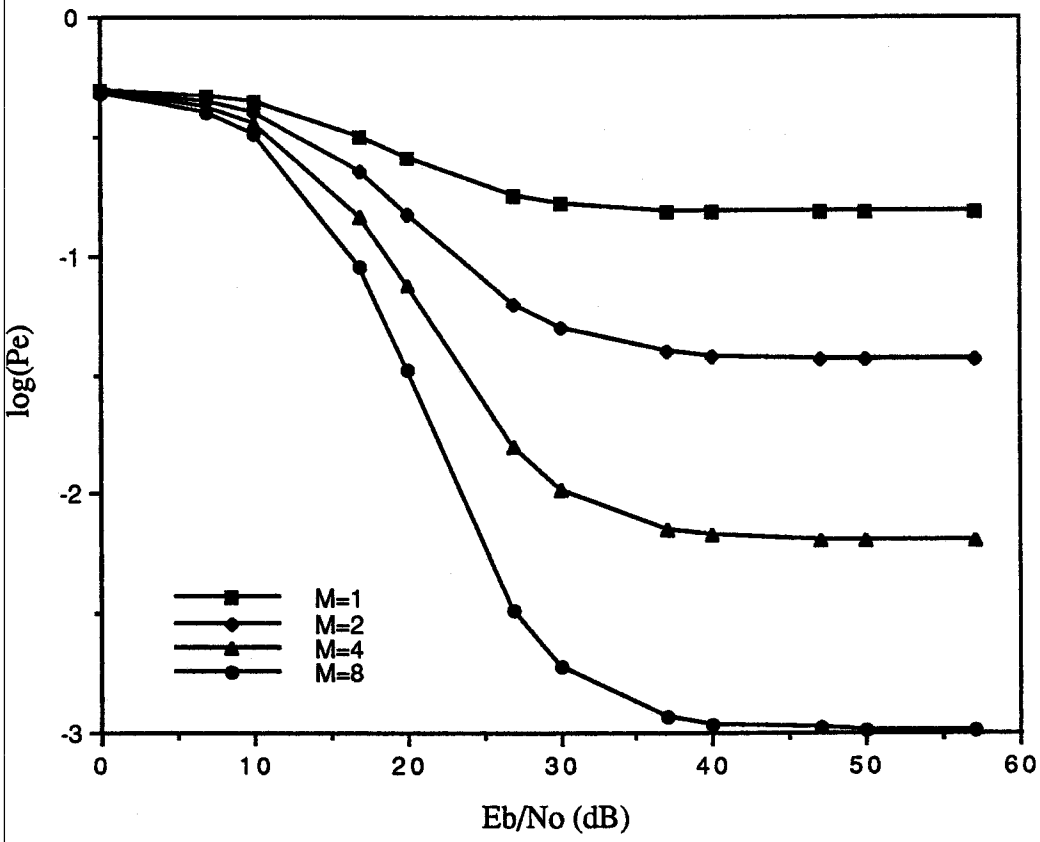

Fig.6.2 The performance of DMSK with selection diversity for K=15, L=4, N=255 and Gold code

From Fig.6.1 and Fig.6.2 it may be seen that BER increases as K and L increase. This is expected as the interference from multipath effect and mutiple users effect becomes large when K and L increase. Also the performance is better for higher order of diversity. Note that a fourth-order diversity can be achieved with just a single antenna when L=4. The eighth-order diversity is achieved with two antennas and L=4. The gap in the irreducible error probability, (i.e. the flat part of the error probability curves), increases slightly as the diversity order, M is doubled. The improvement in irreducible error is by a factor of 4.2 when M is increased from M=1 to M=2. This factor is 6.1 when M is increased from 4 to 8.

6.1.2 Kasami code as the spreading code

The spreading code sequence is separated into I and Q streams in a quadrature-multiplexing signalling schemes. For sequence length of 255, the lengths of I stream and Q stream are 127 and 128 respectively. In the Gold code system, two Gold sequences with lengths 2^7-1=127 are required for each user. Hence thirty spreading code sequences are needed when K=15. For Kasami codes this can not be achieved as these codes have a length 2^n-1 and n has to be odd. In Kasami code system the I and Q streams are obtained

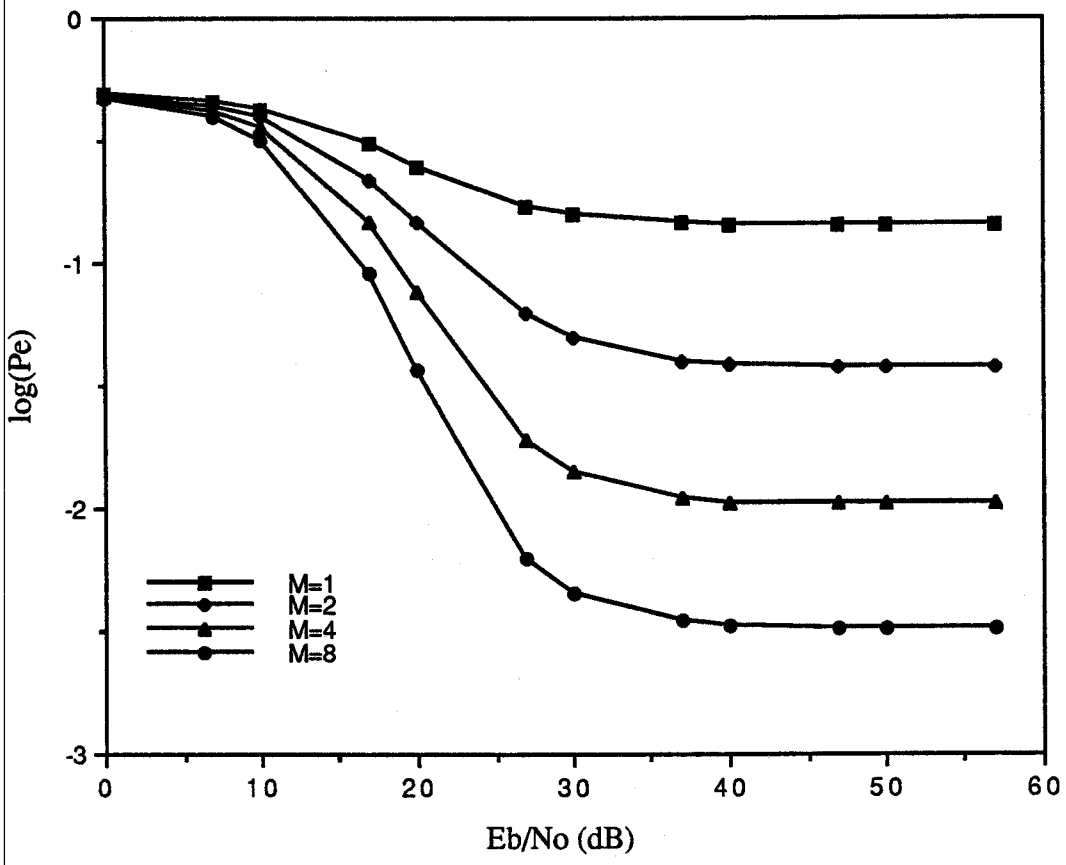

Fig.6.3 The performance of DMSK with selection diversity
for K=15, L=4, N=255 and Kasimi code

by sampling and staggering a Kasami code sequence of length 2^8-1=255. In this case I and Q streams are not real Kasami code and the advantage of correlation property is lost. This translates to poorer performance than Gold codes as shown in Fig.6.3.

6.1.3 Comparison of results with Gold code and Kasami code

In Fig.6.4, BER results with Gold code and Kasami code are plotted together. As seen from this figure the performance with the Gold code is better. If a true Kasami code was used in I and Q channels, the results for this code would have been better than the

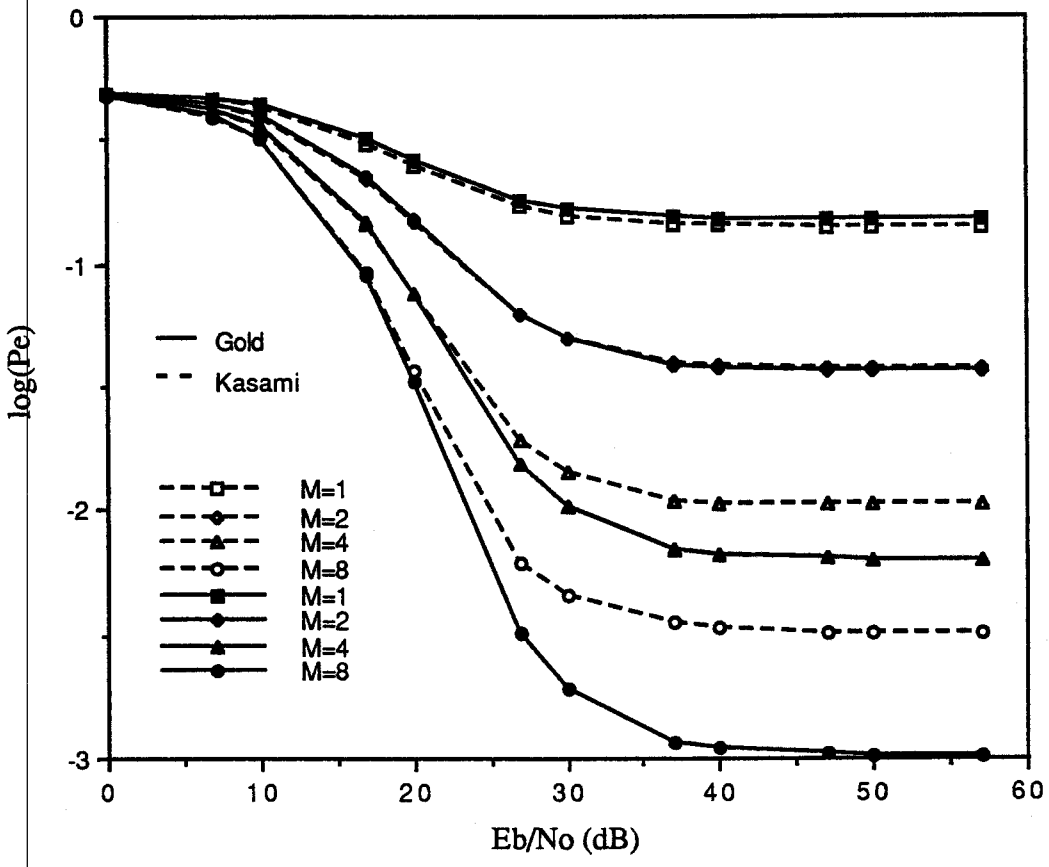

Fig.6.4 The comparision of the performance of DMSK with selection diversity for Kasami and Gold codes

Gold code due to better cross correlation properties. Arbitrary division of Kasami code into I and Q channel codes was responsible for the poorer performance.

6.2 BER with predetection combining diversity

The theoretical analysis required for the computation of BER in this case was developed in the last chapter. Equation (5.31) from that chapter is reproduced below as equation (6.4).

$$P_e = \frac{1}{2^{2M-1}(M-1)!\,(1+\lambda_c)^M} \sum_{i=0}^{M-1} C_i\,(M-1+i)! \left(\frac{\lambda_c}{1+\lambda_c}\right)^i \tag{6.4}$$

where $C_i = \frac{1}{i!} \sum_{n=0}^{M-1-i} \binom{2M-1}{n}$, $\lambda_c = \frac{E^2\{z_1\}}{E\{|N_{1i}|^2\}} = \frac{\alpha\rho}{1+\frac{4}{3N}\alpha\rho KL}$ [13]. Constants α and ρ are same as in the previous section. As before K is the number of users, L is the number of multipath, N is the length of spreading code, and M is the order of diversity.

The performance of DMSK system with predetection combining diversity is shown in Fig.6.5. In this figure the error probability, P_e is plotted as a function of E_b/N_0 for K=15, L=4, and N=255. The improvement in the irreducible error probability with M is more pronounced than that for selection diversity.

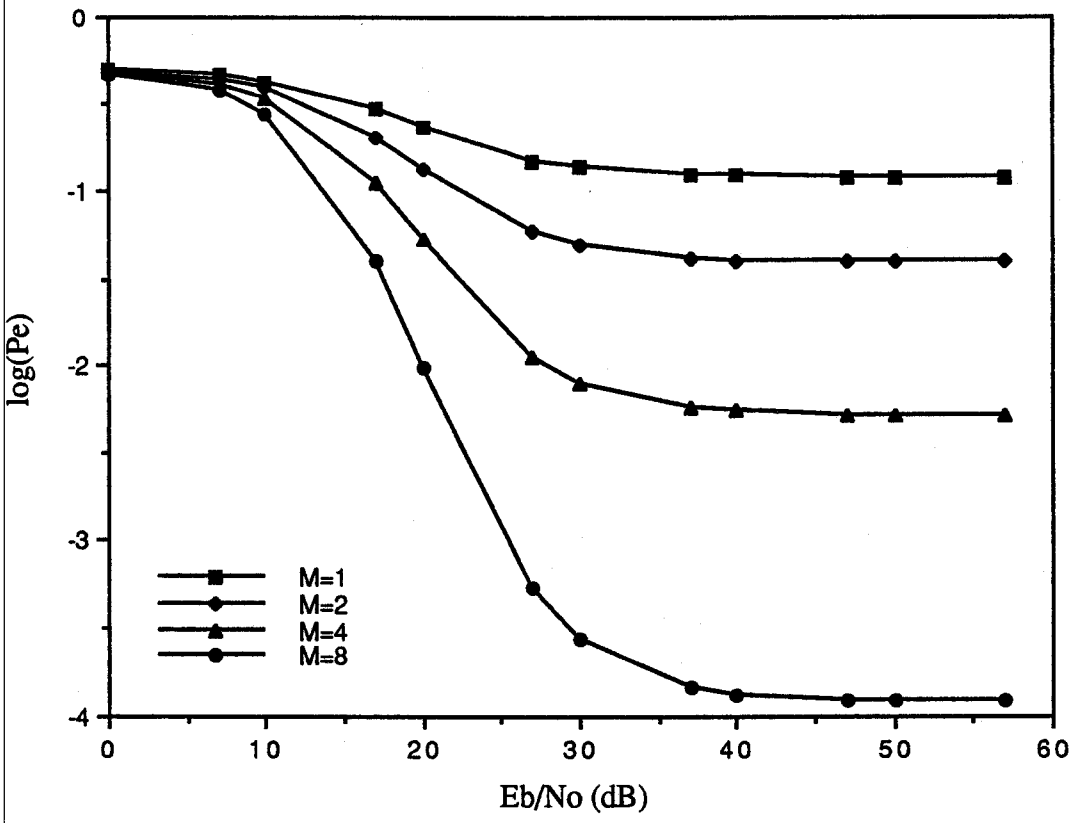

Fig6.5 The performance of DMSK with predetection combining diversity for K=15, L=4, and N=255

6.3 Comparison between selection diversity and predetection combining diversity

In the last two sections the computed BER results for the two types of diversity were presented. The performance is further compared in this section. In Fig.6.6 $\log P_e$ is plotted for the two diversity cases for different orders of diversity. For an M value lower than 4, Pe is quite close for the two cases. However for M=8 the predetection diversity outperforms the selection diversity.

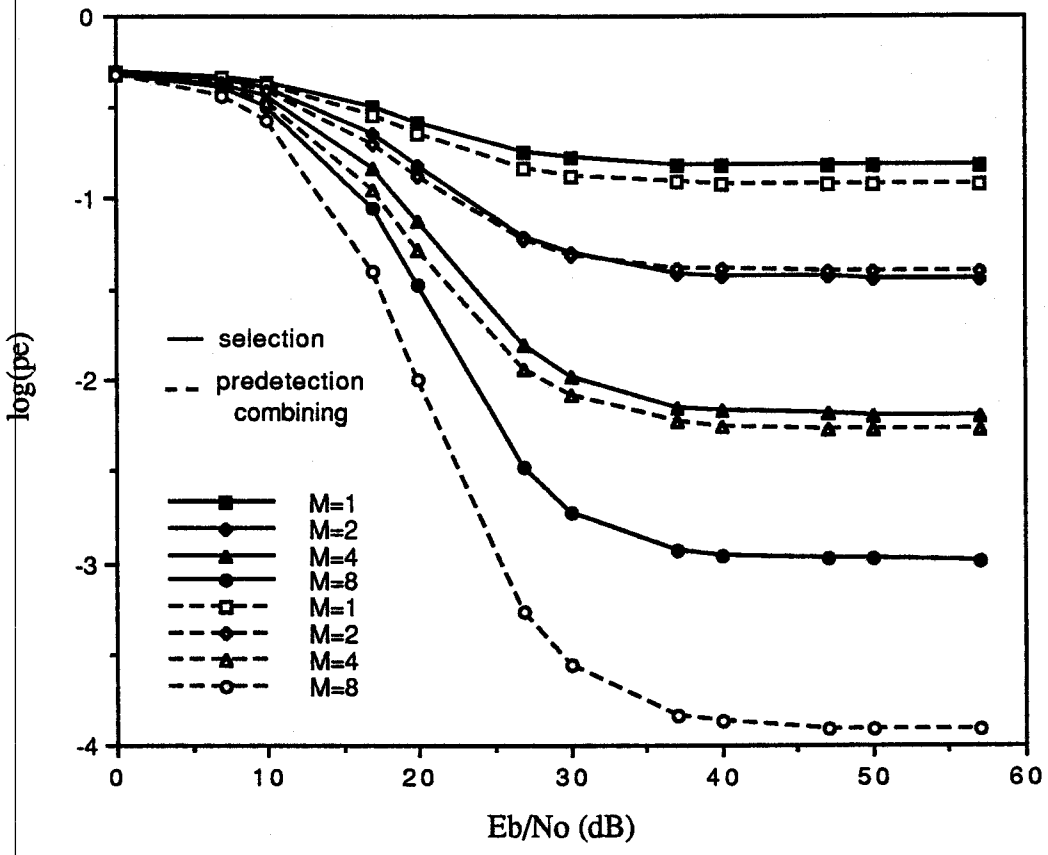

Fig.6.6 Comparison of selection and predetection combining diversity for DMSK (K=15, L=4, and N=255)

6.4 Performance comparison between DMSK and DPSK modulations

In this section the performance of DS-SSMA system with selection diversity and predetection combining diversity is compared for two types of modulations. The performance with DMSK modulation was presented in the previous two sections. Similar results for DPSK were reported in [8].

In Fig. 6.7, the BER with selection diversity is plotted for DPSK and DMSK. The DMSK system performance is worse than that of DPSK system with the same diversity order. The DPSK BER is better by a factor of 2 for all values of M. For non flat part of the error probability curves, i.e., for $10 \leq E_b/N_0(dB) \leq 25$, the power penalty for the same Pe and same diversity order in the DMSK and DPSK is another measure of comparison. The power penalty is the part of the power needed by DMSK system higher than that by DPSK system for same P_e. The power penalty decreases from around 7dB to around 4dB when the diversity order increases from 1 to 8. This indicates that the DMSK system would require higher power than the DPSK system for same P_e. The degradation for DMSK can be attributed to higher interference due to the presence of I and Q channels.

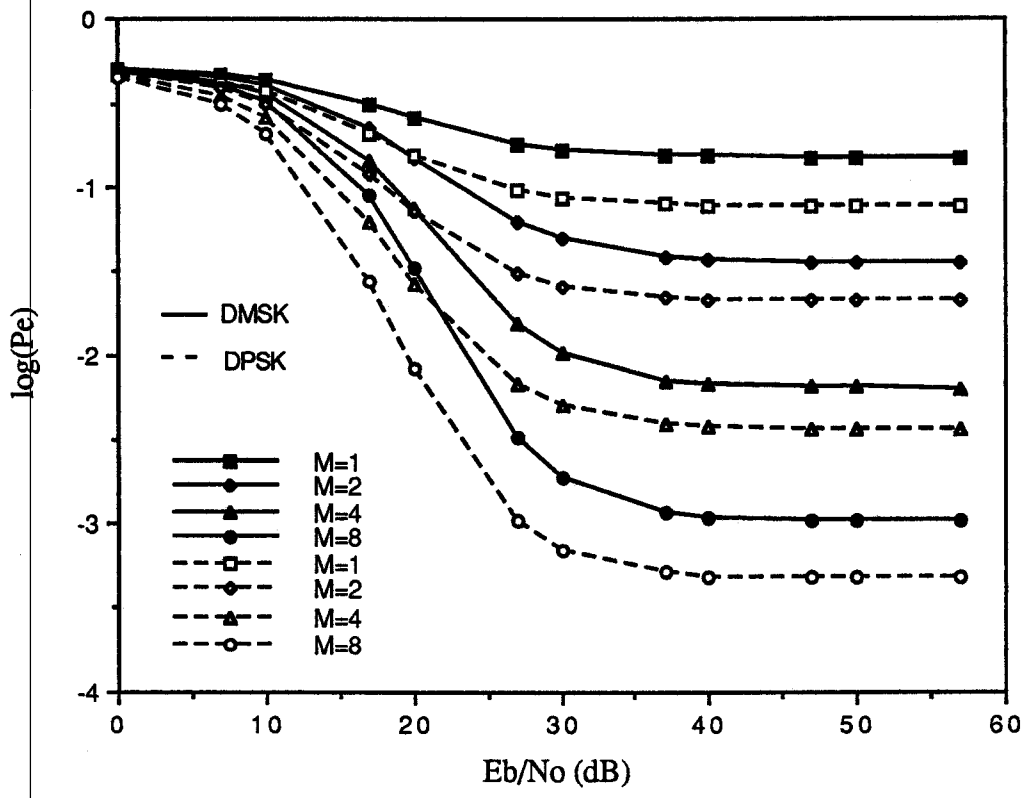

Fig.6.7 The comparison of the performance of DMSK and DPSK with selection diversity for K=15, L=4, and N=255

The results for DMSK and DPSK with predetection combining diversity are shown in Fig.6.8. As in the case of selection diversity, DPSK outperforms DMSK.

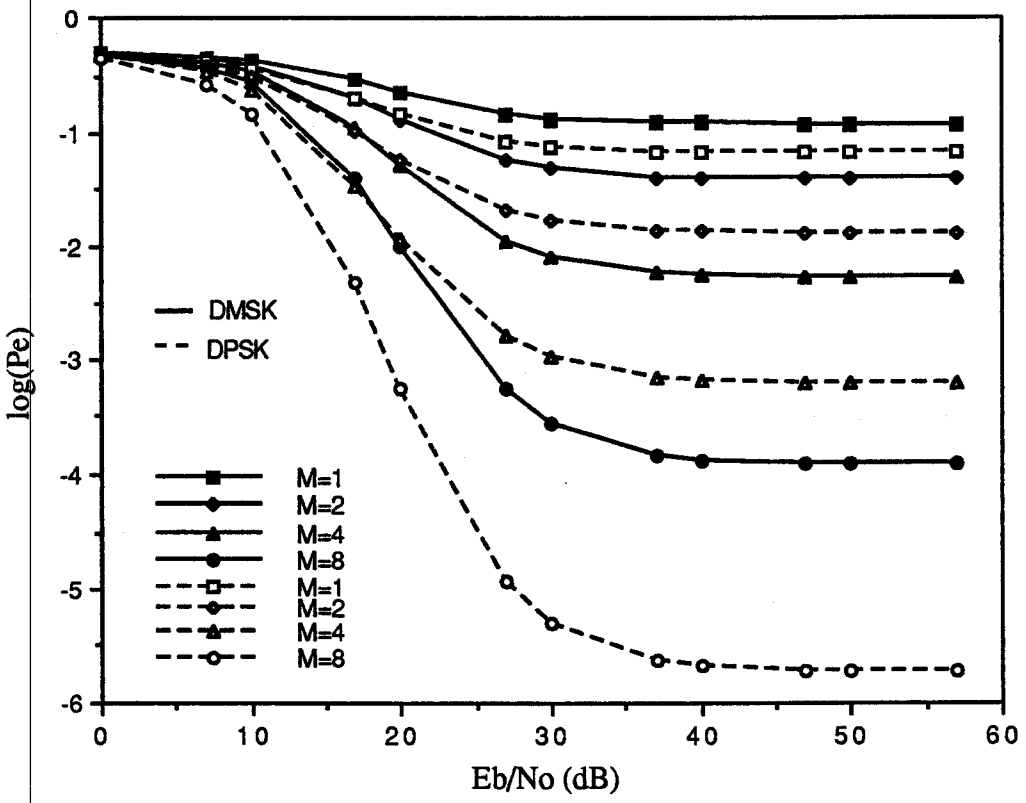

Fig.6.8 Comparison of the performance of DMSK and DPSK with predetection combining diversity for K=15, L=4, N=255

Although both the gap in irreducible error probability and the power penalty indicate that DMSK performance is worse than that of DPSK, the performance degradation of DMSK may be tolerable, because of other benefits such as frequency efficiency and transmitter simplicity. In Chapter 3, it was mentioned that DMSK is a bandwidth efficient modulation. For same information data rate, the bandwidth of DMSK signal is only 75% of

that for DPSK. When many users have to share the limited frequency spectrum, this is a significant advantage.

In addition to bandwidth efficiency, DMSK modulation can be generated using a high power oscillator with a single RF power device [18]. This makes the transmitter in a DMSK system simpler in construction, lower in cost, and smaller in size than that for DPSK system. The transmitter circuits for both DMSK and DPSK are shown in Fig.6.9. These advantages make DMSK system very attractive for mobile radio indoor communication system, in spite of its poorer BER performance.

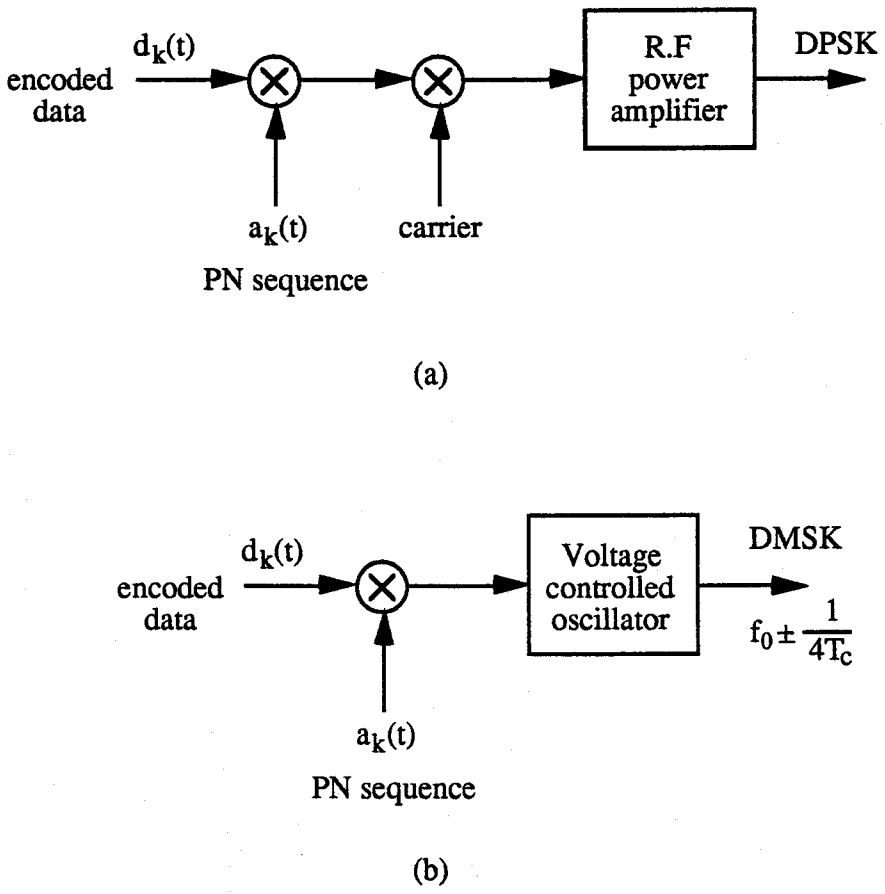

Fig.6.9 Block diagram of transmitters for (a) DPSK (b) DMSK

6.4 Summary

The results described in this chapter may be summarized as

1) The selection of spreading code can affect the system performance. The small cross-correlation property of the spreading code is desirable, this results in lower interference in a multiuser environment.

2) Under the assumptions made in the analysis, predetection combining diversity outperforms selection diversity.

3) The BER for DMSK is worse than that for DPSK. For selection diversity the ratio between the two BER is 2 : 1. For predetection diversity this factor increases with the order of diversity. However DMSK requires three fourth of the bandwidth and has a simpler transmitter circuit. These advantages may outweigh poorer BER performance.

Chapter 7

Conclusions

Indoor digital mobile radio communication systems are currently being designed and planned for commercial use in the near future. An indoor mobile radio channel presents a challenging environment. Use of direct sequence spread spectrum multiple accessing with differential minimum shift keying modulation has been proposed and analyzed in this thesis.

The development of bit-error-rate analysis as well as computation and comparison of this performance with DPSK were laid out to be the two objectives in Chapter 1. The work reported in this thesis shows that both these objectives were realized.

Closed form expressions for computation of the BER for the proposed system were developed. Computations and comparison with DPSK revealed that BER performance of DMSK is poorer than DPSK. The performance degradation can be obtained by using the results reported in Chapter 6. DMSK modulation does offer a number of other advantages and the work reported in this thesis should provide a useful tool to carry out the system trade-off study.

References

[1] R. L. PICKHOLTZ, D. L.SCHILLING and L. B. MILSTEIN, " Theory of Spread-spectrum Communication - A Tutorial ", IEEE Trans. on Comm. vol. com-30, No. 5, May 1982.

[2] R. E. ZIEMER and R. L. PETERSON, " Digital Communications and Spread Spectrum Systems ", Macmillan Publishing Company , New York , 1985.

[3] S. LIN and D. J. COSTELLO, " Error Control Coding: Fundamentals and Applications ", Englewood Cliffs, N. J. , Prentice-Hall, 1983.

[4] G. BIRKHOFF and S. MACLANE, " A Survey of Modern Algebra ", New York: Macmillan, 1965.

[5] D. V. SARVATE and M. B. PURSLEY, " Cross-correlation Properties of Pseudorandom and Related Sequences ", IEEE, Proc. , vol. com-68 No. 5, pp. 593-619, May 1980.

[6] R. GOLD, " Optimal Binary Sequences for Spread Spectrum Multiplexing ", IEEE Trans. Inform. Theory, vol. IT-13, No. 4, pp. 619-621,1967.

[7] R. GOLD, " Maximal Recursive Sequences with 3-Valued Recursive Cross-correlation Functions ", IEEE Trans. Inform. Theory, vol. IT-14, No. 1, pp. 154-156, 1968.

[8] M. KAVEHRAD, and B. RAMAMURTHI " Direct-sequence Spread Spectrum with DPSK Modulation and Diversity for Indoor Wireless Communications ", IEEE, Trans. Comm. vol. com-35, No. 2, Feb. 1987.

[9] B. SKLAR, " Digital Communications Fundamentals and Applications ", Englewood Cliffs, New Jersey 07632, Prentice-Hill, 1988.

[10] K. PAHLAVAN and M. CHASE, " Spread-Spectrum Multiple-Access Performance of Orthogonal Codes for Indoor Radio Communications", IEEE, Trans, on Comm. Vol. 38, No. 5, May 1990.

[11] G. L. TURIN, " Introduction to Spread-spectrum Antimultipath Technique and Their Applications to Urban Digital Radio ", IEEE, Proc. vol. 68, No. 3, March 1980.

[12] D. C. COX, " Universal Digital Portable Radio Communications ", IEEE, Porc. vol. 75, No. 4, April 1987.

[13] M. KAVEHRAD and P. J. McLANE, " Performance of Low-complexity Channel Coding and Diversity for Spread Spectrum in Indoor Wireless Communication ", AT & T Technique Journal vol. 64, No. 8, Oct. 1985.

[14] S. E. ALEXANDER, " Radio Propagation within Buildings at 900 MHz ", Electron. Lett. , vol. 18, pp. 913-914, Oct. 1982.

[15] A. PAPOULIS, "Probability, Random Variables, and Stochastic Processes" McGraw-Hill Book Company, 1984.

[16] J. G. PROAKIS, "Digital Communication" New York McGraw-Hill, 1983.

[17] R. Y. RUBINSTEIN, "Simulation and the Monte Carlo Method ", John Wiley & Sons, 1981.

[18] S. KUMAR, "Directly Modulated Vsat Transmitters", Microwave Journal, pp. 255-264, April 1990.

[19] T. KASAMI, "Weight Distribution Formula for Some Class of Cyclic Codes", Coordinated Science Lab. Univ. Illinois, Urbana, Tech. Rept. R-285 (AP 632574), 1966.

[20] T. KASAMI, "Weight Distribution of Bose-Chaudhuri-Hocquenghem Codes", Coordinated Science Lab. Univ. Illinois, Urbana, Tech. Rept. R-317, 1966.

[21] D. C. COX, "Antenna Diversity Performance in Mitigating the Effects of Portable Radiotelephone Orientation and Multipath Propagation", IEEE Trans. on Comm. Vol. COM-31, No. 5, May 1983.

Appendix A

Computation of A_1 ... A_4 in eq. (6.3)

The A_1 and A_2 are the parameters in the correlation between two inphase sinusodial waveforms. And A_3 and A_4 are the parameters in the correlation between two quadrature half-sinusodial waveforms. In Fig.A.1, the correlation of the half-sinusodial sequences is presented.

From this figure the A_1, A_2, A_3 and A_4 are presented as

$$A_1 = \int_{2nT_c}^{2nT_c+\tau} \sin\frac{2\pi}{4T_c}t \sin\frac{2\pi}{4T_c}(t-2nT_c-\tau)\,dt = -\frac{\tau}{2}\cos\frac{2\pi}{4T_c}\tau + \frac{T_c}{\pi}\sin\frac{2\pi}{4T_c}\tau$$

$$A_2 = \int_{2nT_c+\tau}^{(2n+2)T_c+\tau} \sin\frac{2\pi}{4T_c}t \sin\frac{2\pi}{4T_c}(t-2nT_c-\tau)\,dt = \frac{2T_c-\tau}{2}\cos\frac{\pi}{2T_c}\tau + \frac{T_c}{\pi}\sin\frac{\pi}{2T_c}\tau$$

If $2nT_c < \tau' < (2n+1)T_c$, then

$$A_3 = \int_{0}^{T_c+\tau} \sin\frac{2\pi}{4T_c}t \cos\frac{2\pi}{4T_c}(t-\tau)\,dt = \frac{T_c+\tau}{2}\sin\frac{\pi}{2T_c}\tau + \frac{T_c}{\pi}\cos\frac{\pi}{2T_c}\tau$$

$$A_4 = \int_{T_c+\tau}^{2T_c} \sin\frac{2\pi}{4T_c}t \cos\frac{2\pi}{4T_c}(t-\tau)\,dt = \frac{T_c-\tau}{2}\sin\frac{\pi}{2T_c}\tau - \frac{T_c}{\pi}\cos\frac{\pi}{2T_c}\tau$$

If $(2n+1)T_c < \tau' < (2n+2)T_c$, then

$$A_3 = \int_{0}^{\tau-T_c} \sin\frac{2\pi}{4T_c}t \cos\frac{2\pi}{4T_c}(t-\tau)\,dt = \frac{T_c-\tau}{2}\sin\frac{\pi}{2T_c}\tau + \frac{T_c}{\pi}\cos\frac{\pi}{2T_c}\tau$$

$$A_4 = \int_{\tau-T_c}^{2T_c} \sin\frac{2\pi}{4T_c}t \cos\frac{2\pi}{4T_c}(t-\tau)\,dt = \frac{3T_c-\tau}{2}\sin\frac{\pi}{2T_c}\tau - \frac{T_c}{\pi}\cos\frac{\pi}{2T_c}\tau$$

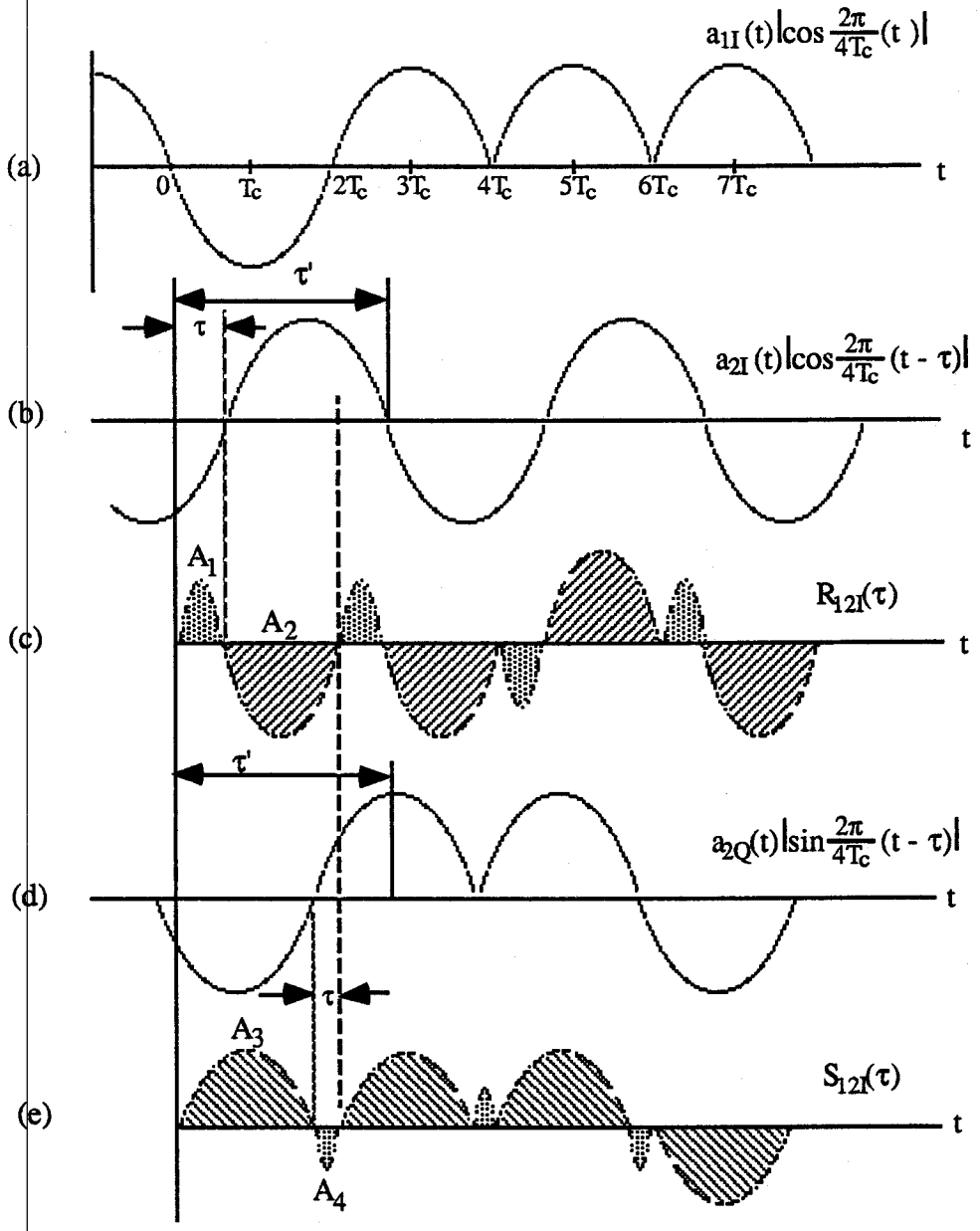

Fig.A.1 The diagram for computing the correlation coefficient

Appendix B

THIS PROGRAM IS USED TO CALCULATE THE BER OF DMSK SYSTEM
FOR N=254, L=4, K=15 IN MONTE CARLO INTEGRATION METHOD
(GOLD CODE)

```
      PROGRAM  BER    !(TAPE5=INPUT,TAPE16=OUTPUT)
      INTEGER      MY(127),AI1(127),AQ1(127),AI(127,15),AQ(127,15)
      INTEGER    M,NC,NNS,n,NF,FM,FB,Y1(127),MMY(127)
      INTEGER    X1,X2,X3,X4,X5,X6,X7,Z1,Z2,Z3,Z4,Z5,Z6,Z7
      REAL   T,LAW,P,PINT,P1,TC,TAU,PI,S1,S2,S3,S4,S5,S6
      REAL    PE(13),LPE(13),LALF
      COMMON  TC,PI,T,LAW,NC,n,AI1,AQ1,AI,AQ
      OPEN  (UNIT=12,FILE='GDOGS.DAT',STATUS='NEW')
      OPEN  (UNIT=10,FILE='MTL.DAT',ACCESS='SEQUENTIAL',
     1  STATUS='OLD',FORM='FORMATTED')
      DATA  IN,IO,PI  /10,12,3.14159/
!     '2NC' IS THE LENGTH OF THE PNC, 'NNS' IS THE LENGTH OF THE SEQUENCE.
      NC=127
      NNS=100
      DO 1 I=1,NC
1     MY(I)=0
      DATA  X1,X2,X3,X4,X5,X6,X7/1,0,0,0,0,0,0/
      DO 5 I=0,126
         MY(I)=X1
         Z1=X2
         Z2=X3
         Z3=MOD((X1+X4),2)
         Z4=X5
         Z5=X6
         Z6=X7
         Z7=X1
         X1=Z1
         X2=Z2
         X3=Z3
         X4=Z4
         X5=Z5
         X6=Z6
         X7=Z7
         AI1(I)=MY(I)
5     CONTINUE
      DO 10 I=0,126
         IF (AI1(I) .EQ. 0)THEN
         AI1(I)=-1
         ELSE
         AI1(I)=AI1(I)
         ENDIF
10    CONTINUE
      DO 15 I=0,126*17
         IF(MOD(I,17) .EQ. 0)THEN
         J=I/17.0
         NF=IFIX(I/127.0)
```

```
          MMY(J)=MY(I-NF*127)
          ELSE
          GOTO 15
          ENDIF
          AQ1(J)=MMY(J)
15        CONTINUE
          DO 17 I=0,126
          IF (AQ1(I) .EQ. 0)THEN
          AQ1(I)=-1
          ELSE
          AQ1(I)=AQ1(I)
          ENDIF
17        CONTINUE
          DO 25 K=2,15
          DO 20 I=0,126
          IF((I+K) .LT. 127)THEN
          Y1(I)=MOD((MY(I)+MMY(I+K)),2)
          ELSE
          Y1(I)=MOD((MY(I)+MMY(I+K-127)),2)
          ENDIF
          IF(Y1(I) .EQ. 0)THEN
          Y1(I)=-1
          ELSE
          Y1(I)=Y1(I)
          ENDIF
          AI(I,K)=Y1(I)
20        CONTINUE
25        CONTINUE
          DO 30 J=17,30
          K=J-15
          DO 26 I=0,126
          IF((I+J) .LT. 127)THEN
          Y1(I)=MOD((MY(I)+MMY(I+J)),2)
          ELSE
          Y1(I)=MOD((MY(I)+MMY(I+J-127)),2)
          ENDIF
          IF(Y1(I) .EQ. 0)THEN
          Y1(I)=-1
          ELSE
          Y1(I)=Y1(I)
          ENDIF
          AQ(I,K)=Y1(I)
26        CONTINUE
30        CONTINUE
          DO 32 I=0,126
          AI(I,1)=AI1(I)
          AQ(I,1)=AQ1(I)
32        CONTINUE

!         'M' IS THE INDEX OF THE SUM FOR Pe
          READ(IN,35)M,T,LAW
          PRINT *,'M=',M,T,LAW
35        FORMAT(I2,2X,F8.2,2X,F6.2)
          ALF=0.5
```

```
      DO 90 L=2,13
         IF (MOD(L,2) .EQ. 1)THEN
         ALF=5.0*ALF
         ELSE
         ALF=2*ALF
         ENDIF
         TC=T/(2*NC)
         FM=1
         P=0
         P1=0
         PE(L)=0
         FB=1
         DO 36 J=0,M-1
            IF(J .EQ. 0)THEN
            FM=FM*1
            ELSE
            FM=FM*J
            ENDIF
36       CONTINUE
         DO 70 I=1,M
            I1=I-1
            FB=1
            CALL INTEG(I1,ALF,PINT)
            IF(I1 .EQ. 0) THEN
            FB=FM
            GOTO 60
            ELSE
            DO 40 I2=1,I1
40          FB=FB*I2
            DO 50 I3=0,M-1-I1
               IF(I3 .EQ. 0)THEN
               FB=FB*1
               ELSE
               FB=FB*I3
               ENDIF
50          CONTINUE
            ENDIF
60          P1=FM*PINT/FB/(I1+1)
            IF((I1 .EQ. 1) .OR. (MOD(I1,2) .EQ. 1)) THEN
            P=P-P1
            GOTO 70
            ELSE
            P=P+P1
            ENDIF
70       CONTINUE
         PE(L)=P/(2*NNS)
         LPE(L)=ALOG10(PE(L))
         LALF=10*ALOG10(ALF)
         WRITE(IO,80)LALF,LPE(L)
80       FORMAT(1X,F8.0,2X,E12.4)
90    CONTINUE
      END

      FUNCTION S1(X1)
```

```
REAL X1,XX1,LAW
COMMON TC,PI,T,LAW,NC,n
XX1=X1-n*TC
S1   =(XX1/2)*COS(PI*(1-XX1/(2*TC)))
+    +(TC/PI)*SIN(PI*XX1/(2*TC))
RETURN
END

FUNCTION S2(X2)
REAL X2,XX2,LAW
COMMON TC,PI,T,LAW,NC,n
XX2=X2-n*TC
S2   =((2*TC-XX2)/2)*COS(PI*XX2/(2*TC))
+    +(TC/PI)*SIN(PI*XX2/(2*TC))
RETURN
END

FUNCTION S3(X3)
REAL X3,XX3,LAW
COMMON TC,PI,T,LAW,NC,n
XX3=X3-n*TC
S3   =((XX3+TC)/2)*SIN((PI*XX3)/(2*TC))
+    +(TC/PI)*COS((PI*XX3)/(2*TC))
RETURN
END

FUNCTION S4(X4)
REAL X4,XX4,LAW
COMMON TC,PI,T,LAW,NC,n
XX4=X4-n*TC
S4   =((TC-XX4)/2)*SIN((PI*XX4)/(2*TC))
+    -(TC/PI)*COS((PI*XX4)/(2*TC))
RETURN
END

FUNCTION S5(X5)
REAL X5,XX5,LAW
COMMON TC,PI,T,LAW,NC,n
XX5=X5-n*TC
S5   =((XX5-TC)/2)*SIN((PI*XX5)/(2*TC))
+    +(TC/PI)*COS((PI*XX5)/(2*TC))
RETURN
END

FUNCTION S6(X6)
REAL X6,XX6,LAW
COMMON TC,PI,T,LAW,NC,n
XX6=X6-n*TC
S6   =((3*TC-XX6)/2)*SIN((PI*XX6)/(2*TC))
+    -(TC/PI)*COS((PI*XX6)/(2*TC))
RETURN
END
```

```
!     FOR THE INTEGRATION COMPUTATION IN THE MONTE CARLA METHOD.
      SUBROUTINE INTEG(IND1,ALF,FINT)
      INTEGER  IND1,ANS,AI1(127),AQ1(127),AI(127,15),AQ(127,15)
      INTEGER  AII(127),AQQ(127)
      REAL RI,RIC,RQ,RQC,SI,SIC,SQ,SQC,SUM1,SUM2,FI,XJ(4,15)
      REAL  TAU,FINT,RR1,SS1,RR2,SS2,RR11,RR12,RR21,RR22
      REAL SS11,SS12,SS21,SS22,LAW
      COMMON TC,PI,T,LAW,NC,n,AI1,AQ1,AI,AQ
      SUM1=0
      SUM2=0
      FI=0
      FINT=0
      RI=0
      RIC=0
      RQ=0
      RQC=0
      SI=0
      SIC=0
      SQ=0
      SQC=0
      ANS=60
      INV=53
      DO 150 J=1,5
         RR1=0
         RR2=0
         SS1=0
         SS2=0
         INV=INV+4
         CALL RSEQ(ANS,INV,XJ)
         K=1
         DO 100 I=1,127
            AII(I)=AI(I,K)
100      CONTINUE
         DO 110 I=1,127
            AQQ(I)=AQ(I,K)
110      CONTINUE
         DO 120 L=2,4
            n=0
            n=IFIX(XJ(L,1)*NC*2)
            TAU=XJ(L,1)*T
            CALL RALC(TAU,1,AII,RI)
            CALL RALC(TAU,2,AII,RIC)
            CALL RALC(TAU,3,AQQ,RQ)
            CALL RALC(TAU,4,AQQ,RQC)
            CALL RALC(TAU,5,AQQ,SI)
            CALL RALC(TAU,6,AQQ,SIC)
            CALL RALC(TAU,7,AII,SQ)
            CALL RALC(TAU,8,AII,SQC)
            RR11=RI**2+RQ**2-RI*RIC-RQ*RQC
            RR1=RR1+RR11
            SS11=SI**2+SQ**2-SI*SIC-SQ*SQC
            SS1=SS1+SS11
            RR21=RI**2+RIC**2+RQ**2+RQC**2
            RR2=RR2+RR21
```

```
            SS21=SI**2+SIC**2+SQ**2+SQC**2
            SS2=SS2+SS21
120       CONTINUE
          DO 140 L=1,4
             DO 130 K=2,15
                DO 125 I=1,127
125             AII(I)=AI(I,K)
                DO 126 I=1,127
126             AQQ(I)=AQ(I,K)
                n=0
                n=IFIX(XJ(L,K)*NC*2)
                TAU=XJ(L,K)*T
                CALL RALC(TAU,1,AII,RI)
                CALL RALC(TAU,2,AII,RIC)
                CALL RALC(TAU,3,AQQ,RQ)
                CALL RALC(TAU,4,AQQ,RQC)
                CALL RALC(TAU,5,AQQ,SI)
                CALL RALC(TAU,6,AQQ,SIC)
                CALL RALC(TAU,7,AII,SQ)
                CALL RALC(TAU,8,AII,SQC)
                RR12=RI**2+RQ**2+RIC**2+RQC**2-RI*RIC-RQ*RQC
                RR1=RR1+RR12
                SS12=SI**2+SQ**2+SIC**2+SQC**2-SI*SIC-SQ*SQC
                SS1=SS1+SS12
                RR22=RR11+RI*RIC+RQ*RQC
                RR2=RR2+RR22
                SS22=SS11+SI*SIC+SQ*SQC
                SS2=SS2+SS22
130          CONTINUE
140       CONTINUE
          SUM1=1+2*ALF*LAW*(RR1+SS1)/(T**2)
          SUM2=2*ALF*LAW*(RR2+SS2)/(T**2)
          FI=1+ALF*LAW/(IND1+1)
          GI=SUM1/(SUM2+FI)
          FINT=FINT+GI
150     CONTINUE
        RETURN
        END

!       TO WORK ALL R AND S OUT
        SUBROUTINE RALC(TU,IND,AIQ,R)
        REAL TU,R,LAW
        INTEGER IND,CN1,C1,C2,AIQ(127)
        INTEGER AI1(127),AQ1(127)
        COMMON TC,PI,T,LAW,NC,n,AI1,AQ1
        R=0
        C1=0
        C2=0
        CN1=0
200     GOTO(210,220,230,240,250,260,270,280),IND
210     CN1=n-NC
        CALL SIGNC(CN1,AIQ,AI1,C1)
        CN1=CN1+1
        CALL SIGNC(CN1,AIQ,AI1,C2)
```

```
      R=C1*ABS(S2(TU))+C2*ABS(S1(TU))
      GOTO 300
220   CN1=n
      CALL SIGNC(CN1,AIQ,AI1,C1)
      CN1=CN1+1
      CALL SIGNC(CN1,AIQ,AI1,C2)
      R=C1*ABS(S2(TU))+C2*ABS(S1(TU))
      GOTO 300
230   CN1=n-NC
      CALL SIGNC(CN1,AIQ,AQ1,C1)
      CN1=CN1+1
      CALL SIGNC(CN1,AIQ,AQ1,C2)
      R=C1*ABS(S2(TU))+C2*ABS(S1(TU))
      GOTO 300
240   CN1=n
      CALL SIGNC(CN1,AIQ,AQ1,C1)
      CN1=CN1+1
      CALL SIGNC(CN1,AIQ,AQ1,C2)
      R=C1*ABS(S2(TU))+C2*ABS(S1(TU))
      GOTO 300
250   CN1=n-NC
      CALL SIGNC(CN1,AIQ,AI1,C1)
      CN1=CN1+1
      CALL SIGNC(CN1,AIQ,AI1,C2)
      IF(MOD(n,2) .EQ. 0) THEN
      R=C1*ABS(S4(TU))+C2*ABS(S3(TU))
      ELSE
      R=C1*ABS(S6(TU))+C2*ABS(S5(TU))
      GOTO 300
      ENDIF
260   CN1=n
      CALL SIGNC(CN1,AIQ,AI1,C1)
      CN1=CN1+1
      CALL SIGNC(CN1,AIQ,AI1,C2)
      IF(MOD(n,2) .EQ. 0) THEN
      R=C1*ABS(S4(TU))+C2*ABS(S3(TU))
      ELSE
      R=C1*ABS(S6(TU))+C2*ABS(S5(TU))
      ENDIF
      GOTO 300
270   CN1=n-NC
      CALL SIGNC(CN1,AIQ,AQ1,C1)
      CN1=CN1+1
      CALL SIGNC(CN1,AIQ,AQ1,C2)
      IF(MOD(n,2) .EQ. 0) THEN
      R=C1*ABS(S4(TU))+C2*ABS(S3(TU))
      ELSE
      R=C1*ABS(S6(TU))+C2*ABS(S5(TU))
      ENDIF
      GOTO 300
280   CN1=n
      CALL SIGNC(CN1,AIQ,AQ1,C1)
      CN1=CN1+1
      CALL SIGNC(CN1,AIQ,AQ1,C2)
```

```
      IF(MOD(n,2) .EQ. 0) THEN
      R=C1*ABS(S4(TU))+C2*ABS(S3(TU))
      ELSE
      R=C1*ABS(S6(TU))+C2*ABS(S5(TU))
      ENDIF
      GOTO 300
300   CONTINUE
      RETURN
      END

!     TO GENERATE A SEQUENCE OF RANDOM NUMBERS
      SUBROUTINE RSEQ(EN,INV,RN)
      INTEGER EN,SEED
      REAL RN(EN)
      SEED=INV
      DO 305 J=1,EN
         RN(J)=RAN(SEED)
305   CONTINUE
      RETURN
      END

!     TO COMPUTE C'S
      SUBROUTINE SIGNC(cn,KA,KB,CS)
      INTEGER  CS,cn,KA(127),KB(127),MD
      COMMON TC,PI,T,LAW,NC,n
      CS=0
      MD=NC-1
      IF((cn .GE. 0) .AND. (cn .LE. MD)) THEN
      DO  310  I=1,MD-cn+1
310   CS=CS+KA(I)*KB(I+cn)
      GOTO 320
      ELSE
      IF((cn .GE. -MD) .AND. (cn .LT. 0)) THEN
      DO  315  J=1,MD+cn+1
315   CS=CS+KA(J-cn)*KB(J)
      GOTO 320
      ELSE
      CS=0
      ENDIF
      ENDIF
320   CONTINUE
      RETURN
      END
```